The Dissertation Committee for Yerim Yeon Certifies that this is the approved version of the following dissertation:

Calix[4]arene-Based Ion or Ion-pair Receptors

Committee:

Jonathan L. Sessler, Supervisor

Hung-wen Liu

Adrian T. Keatinge-Clay

Guangbin Dong

Sean M. Kerwin

Calix[4]arene-Based Ion and Ion-pair Receptors

by

Yerim Yeon, B.S.; M.S.; M.A.

Dissertation

Presented to the Faculty of the Graduate School of

The University of Texas at Austin

in Partial Fulfillment

of the Requirements

for the Degree of

Doctor of Philosophy

The University of Texas at Austin

May 2016

Calix[4]arene-Based Ion and Ion-pair Receptors

Yerim Yeon, Ph. D.

The University of Texas at Austin, 2016

Supervisor: Jonathan, L. Sessler

Calix[4]arene derivatives are one of the most important supramolecular scaffolds. They have been extensively exploited to build more elaborate systems. Calix[4]arene derivatives can stabilize host-guest complexes with various ions and neutral molecular guests through non-covalent interactions (e.g., hydrogen bonding, electrostatic interactions and cation-π interactions). This dissertation describes efforts to develop more efficient calix[4]arene-based ion and ion-pair receptors.

Chapter 1 describes an overview of sensitive ion selective chromogenic and fluoregenic sensors based on calix[4]arene derivatives. Chapter 2 details a chromogenic calix[4]arene-calix[4]pyrrole sensor system formed by appending an indane substituent to the β-pyrrole position of the calix[4]pyrrole portion of the hybrid and its use in detecting cesium salts. The indane substituted calix[4]arene-calix[4]pyrrole system gives rise to a colorimetric response when only exposed to simple ion pairs containing the cesium cation. Chapter 3 describes amido-indole incorporated calix[4]arene anion receptors. An amido-indole moieties appended calix[4]arene provides multiple hydrogen bond donors for the interaction with anions. In Chapter 4, graphene field-effect transistors (GFETs) are introduced for cesium ion sensing based on electrostatic measurements. In this work, a crown-6-ether strapped calix[4]arene derivative that adopts a cesium ion selective conformation was prepared. Then, it was attached to various graphene field-

effect transistors (GFETs) via π–π interactions. The co-complexation of Cs^+ ion and calix[4]arene receptor on the GFETs alters the electronic behavior of the system in an ion and concentration dependent manner. This work serves to extend the fundamental chemistry of calix[4]arene-based cesium ion recognition to new research areas. Lastly, an experimental section and characterization data are provided in Chapter 5.

Table of Contents

List of Schemes ix

List of Figures x

List of Tables xx

Chapter 1: Chromogenic and Fluoregenic Receptors Based Upon Calix[4]arene ..1

1.1 Introduction 1

1.2 Colorimetric sensors 2

1.3 Fluorescent sensors of calix[4]arene derivatives 13

1.3.1 Photo-Induced Electron Transfer Fluorescent Sensors 15

1.3.2 Photo-Induced Charge Transfer Fluorescent Sensors 28

1.3.3 Fluorescence Resonance Electron Transfer Fluorescent Sensors 31

1.3.4 Excimer Sensors 37

1.4 Crown ether strapped calix[4]arene-based fluorescent cesium ion sensors 50

1.5 Conclusion 57

1.6 Reference 59

Chapter 2: 3-(Dicyanomethylidene)indan-1-one-Appended Calix[4]arene-Calix[4]pyrrole System: 63

Colorimetric Ion-Pair Sensor for Cesium Salts 63

2.1 Introduction 63

2.2 Results and discussions 65

2.2.1 Synthesis and NMR and UV-Vis Spectroscopic Studies 65

2.3 Conclusions 77

2.4 Future directions 78

2.5 Reference 81

Chapter 3: Tetra-Amidoindole Substituted Calix[4]arene 82

for Anion and Ion Pair Recognition 82

3.1 Introduction 82

3.2 Results and discussions 85
3.3 Conclusion 107
3.3 Future Directions 108
3.4 Reference 111

Chapter 4: Crown-6-ether Strapped Calix[4]arene 112

Bearing Pyrenyl Moieties Towards the Detection of the Cs^+ Ion 112

Using Graphene Field-Effect Transistors 112
4.1 Introduction 112
4.2 Results and discussions 114
4.2.1 Synthesis and Spectroscopic Studies of Receptor 4.1 114
4.2.2 Preparation of Graphene Field-Effect Transistors 117
4.2.3 Raman Spectroscopy and I-V Measurements 118
4.3 Conclusion 121
4.4 Future directions 122
4.5 Reference 123

Chapter 5: Experimental Procedures 124
5.1 General procedures 124
5.2 Experimental details for chapter 2 124
5.2.1 Synthetic Procedures and Characterization Data 124
5.2.2 Single Crystal X-ray Crystallographic Data 126
5.2.3 Studies by UV-Vis spectroscopy 129
5.3 Experimental details for chapter 3 132
5.3.1 Synthetic Procedures and Characterization Data 132
5.3.2 ^{1}H NMR Spectroscopic Studies 134
5.4 Experimental details for chapter 4 141
5.5 Reference 142

Reference 143
1.6 Reference 143
2.5 Reference 145

3.4 Reference 146
4.5 Reference 147
5.5 Reference 148

Vita 149

List of Schemes

Scheme 2.1: Synthetic pathway used to prepare compound **2.1**. 65

Scheme 3.1: Syntheses of compounds **3.3** and **3.4**. i) 5-Nitroindole-2-carboxylic acid, EDCI, HOBt, DMAP, DMF at room temperature for 6 h; ii) indole-2-carboxylic acid, HOBt, DMAP, DCM/THF (2:1, v/v) at room temperature for 4h.....86

Scheme 3.2: Target **3.7** and its synthesis.....109

Scheme 4.1: Synthesis of the pyrene-fuctionalized crown-6-ether strapped calix[4]arene receptor **4.1**. 114

List of Figures

Figure 1.1: Generalized structure of calix[4]arene structure and its four limiting conformers. 2

Figure 1.2: Calix[4]arene compounds used to detect alkali cations. 3

Figure 1.3: Calix[4]arene compound **1.3** developed for Ca^{2+} ion recognition.....4

Figure 1.4: Triazole- and azophenol-coupled calix[4]arene **1.4** and UV-Vis spectra of compound **1.4** (10 μM) before and after adding 100 μM concentration of various metal perchlorates in MeCN/$CHCl_3$ (1000:4, v/v). Originally published in *Tetrahedron Lett*. **2007**, *48*, 7274-7278. Reproduced by permission. Copyright ELSEVIER. 6

Figure 1.5: Two compounds bearing phenylazo- or allyl- group at the upper rim that were developed by Chung for Hg^{2+} recognition. 7

Figure 1.6: Schiff-base calix[4]arene for lanthanide ions (Dr^{3+} and Er^{3+}) detection. Color changes of compound **1.7** after 24 h in the dark (from left to right: La^{3+}, Pr^{3+}, Eu^{3+}, Gd^{3+}, Dy^{3+}, Er^{3+} and Yb^{3+}). Originally published in *Tetr. Lett*. **2007**, *48*, 3587-3590. Reproduced by permission. Copyright ELSEVIER.....8

Figure 1.7: A monoindoaniline modified calix[6]arene developed for UO^{2+} ion recognition and sensing.....9

Figure 1.8: Amido-urea substituted calix[4]arene derivatives **1.9** and **1.10** generated as sensors for F^- and $H_2PO_4^-$.....11

Figure 1.9: a) 1,1'-Binaphthyl subunit and two indophenol chromophores that are appended to a calix[4]arene case to produce sensor **1.11**. b) Possible structure for the complex formed between **1.11** and (R)-phenylglycinol. 12

Figure 1.10: Mechanism of a classic photo-induced electron transfer process. ...14

Figure 1.11: Compound **1.12**, A) its X-ray crystal structure of **1.12**•KSCN•MeOH complex, B) Absorption spectrum of **1.12** (dash dot) and excitation spectrum of [Tb•**1.12**]$^{3+}$ (line) in methanol. Figure 1.11 A) was originally published in *J. Chem. Soc. Chem. Commun.* **1987**, 344-346. Copyright The Royal Society of Chemistry. Figure 1.11 B) was originally published in *J. Chem. Soc. Chem. Commun.* **1990**, 878-879. Copyright The Royal Society of Chemistry.....16

Figure 1.12: Compound **1.13** and proposed metal complexation chemistry. 18

Figure 1.13: Fluorescence emission properties of compound **1.14** observed in ethanol upon the addition of Ag^+ and Cs^+, respectively. 18

Figure 1.14: Fluorescence emission of compound **1.15** observed upon the addition of Cs^+ and Cu^{2+}, respectively in ethanol/dichloromethane (9/1, v/v). ...20

Figure 1.15: Line drawings of compounds **1.16a** and **1.16b**. These two receptors contain the same fluorophore but give rise to different fluorescence response when treated with the cesium ion.....21

Figure 1.16: 1,3-Alternative two iminoquinoline substituted calix[4]arenes, **1.17a** and **1.17b**. Fluorescent intensity of compound **1.17b** (10^{-5} M) recorded in acetonitrile after the addition of 11.0 equiv. of various metal ions (M^{n+} denotes Li^{+}, Na^{+}, K^{+}, Mg^{2+}, Ca^{2+}, and Ba^{2+}). All cations were studied as the perchlorate salts. This result was originally published in *Chem. Commun*. **2008**, 1774-1776. Reproduced with permission. Copyright The Royal Society of Chemistry.....23

Figure 1.17: pH-dependent on/off molecular switching seen in the case of compound **1.18**.....24

Figure 1.18: A calix[4]arene extractant **1.19** that relies on dansyl moieties for the sensing Hg^{2+}. 25

Figure 1.19: Structure of fluorescence chemosensors **1.20** and the response produced upon complexation of Pb^{2+} and F^{-}. 26

Figure 1.20: Structure of the fluorescence chemosensors **1.21a** and **b** and the proposed interactions with Pb^{2+}. 27

Figure 1.21: Tetrakis-(4-carbamoylphenyl)-substituted calix[4]arene, **1.22**, and its proposed interactions with the acetate anion. 28

Figure 1.22: *p*-Tert-butyl calix[4]aren receptors **1.23** and **1.24** containing one and four methoxynaphthylene subunits respectively.....29

Figure 1.23: Two coumarin units attached calix[4]arene, **1.25** and its proposed interaction with the F- anion. 30

Figure 1.24: Schematic representation of the FRET OFF-On approach to Cu^{2+} sensing developed by Kim, et al. Also shown are the color changes seen upon irradiation at 420 nm. This figure was originally published in *Chem. Soc. Rev.* **2008**, 1465-1472 and reproduced with permission. Copyright The Royal Society of Chemistry.....32

Figure 1.25: Compounds **1.27** and **1.28**.....34

Figure 1.26: Differing complexation pathways for compound **1.29** proposed to be operational in the case of Hg^{2+} and Al^{3+}.....36

Figure 1.27: Compound **1.30**.....38

Figure 1.28: Compound **1.31**.....39

Figure 1.29: Compounds **1.32** and **1.33**.....40

Figure 1.30: Compounds **1.34** and **1.35**.....41

Figure 1.31: X-ray crystal structure of compound **1.34** with hydrogen bonds represented by dotted bonds. This figure was originally published in *Inorg. Chem.* **2005**, 7866-7875. Reproduced with permission. Copyright American Chemical Society.....42

Figure 1.32: Compounds **1.36** and **1.37**. Job plot of **1.36** with Pb^{2+} in $CHCl_3/CH_3CN$ (1:3, v/v). $\Delta A = A_{obs}-A_h$, where A_{obs} and A_h denote the absorbance at 375 nm upon metal ion and **1.36**, respectively. This figure was originally published in *Org. Lett.* **2006**, 1601-1604. Reproduced with permission. Copyright American Chemical Society.....43

Figure 1.33: Calculated geometries for (a) **1.37•**Ca^{2+} and **(b) 1.37•**Pb^{2+}**.** Hydrogen atoms are omitted for clarity, except the hydrogen involved in NH•••OC bonding interaction. In the **1.37•**Ca^{2+} complex, the hydrogen bonding interaction between the amides in shown in the dotted line. Oxygen atoms are shown in red; nitrogen atoms are in blue. This figure was originally published in *Org. Lett.* **2006**, 1601-1604. Reproduced with permission. Copyright American Chemical Society.....45

Figure 1.34: Compound **1.38** and binding of Cl^- ions by **1.38**. Quenching of excimer emission (452 nm) caused by perturbation of the pyrene π–π interaction by the conformational 'unstacking' of pyrene moieties. This was published originally in *J. Am. Chem. Soc.* **2006**, 8607-8614. Reproduced with permission. Copyright American Chemical Society.....46

Figure 1.35: Structure of the pyrene- and (4-nitrophenyl)azo appended calix[4]arene **1.39**.....47

Figure 1.36: Guanidium ion selective calix[4]arene derivatives **1.40** and **1.41**....49

Figure 1.37: Schematic representation of 1,3-alternate crown-6-ether strapped calix[4]arene derivatives, **1.42a-d**. 50

Figure 1.38: Crystal structure of the complex **1.42d•**CsPic in the 1,3-alternate conformation (the picrate counter ion has been omitted for clarity). This figure was originally published in *J. Am. Chem. Soc.* **1995**, *117*, 2767-2777. Reproduced with permission. Copyright American Chemical Society.....52

Figure 1.39: Molecular structures of **1.43** and **1.43**-H^+ and schematic representation of how they can function via pH modulation.....53

Figure 1.40: Molecular structures of **1.44a** and **1.44b**$^-$ 55

Figure 1.41: Cesium ion complexation mechanism believed to be operative in the case of the calix[4]arene derivative, **1.45**. beaing 2,3-naphtocrown-6-ether and two coumarin amide fluorophores. 56

Figure 2.1: Two different views of the single crystal X-ray diffraction structures of **2.1**. Solvent molecules and hydrogen atoms have been omitted for clarity. 66

Figure 2.2: (Left) solutions of receptor **2.1** (150 μM) in MeOH/$CHCl_3$ (1/9, v/v) photographed in the absence and presence of excess ions (100 equiv), (Right) UV-Vis absorption spectra of receptor **2.1** (50 μM) in MeOH/$CHCl_3$ (1/9, v/v) in the absence (A) and presence of 100 equiv of (B) $CsClO_4$ (C) TBACl, (D TBAF, (E) CsF, (F) CsCl and (G) $CsNO_3$. 67

Figure 2.3: Partial ^{1}H NMR spectra of (a) **2.1** only, (b) **2.1** + 5 equiv of TBAF, (c) **2.1** + 5 equiv of TBACl, (d) **2.1** + 5 equiv of $CsClO_4$, (e) **2.1** + 5 equiv of $CsNO_3$, (f) **2.1** + 5 equiv of CsF and (g) **2.1** + 5 equiv of CsCl in $CD_3OD/CDCl_3$ (1:9, v/v).....68

Figure 2.4: **Upper**: (Left) solution of receptor **2.1** (50 μM) in MeOH/$CHCl_3$ (1/9, v/v) in the presence of excess ions, (Right) UV-Vis absorption spectra of receptor **2.1** (50 μM) in MeOH/$CHCl_3$ (1/9, v/v) (A) and in the presence of 100 equiv of (B) TBAF + $CsClO_4$ (5 equiv, respectively), and (C) 5 equiv. of CsF, **Below**: Partial ^{1}H NMR spectra of (a) **2.1** only, (b) **2.1** + 5 equiv of TBAF and 5 equiv of $CsClO_4$, and (c) **2.1** + 5 equiv of CsF, in $CD_3OD/CDCl_3$ (1:9, v/v). The purple arrows indicate the NH-pyrrole resonances. 70

Figure 2.5: Titration of receptor **2.1** (50 μM) with CsF in 10% of CH_3OH in $CHCl_3$. 71

Figure 2.6: UV-Vis absorption spectra of receptor **2.1** (50 μM) in MeOH/$CHCl_3$ (1/9, v/v) recorded in the absence and presence of 100 equiv of excess of various salts, namely LiCl, NaCl, KCl, and CsCl.....73

Figure 2.7: Partial ^{1}H NMR spectra of (a) **2.1** only, (b) **2.1** + 5 equiv of LiCl, (c) **2.1** + 5 equiv of NaCl, (d) **2.1** + 5 equiv of KCl, and (e) **2.1** + 5 equiv of CsCl recorded in $CD_3OD/CDCl_3$ (1:9, v/v). 74

Figure 2.8: Liquid-Liquid extraction, UV-Vis absorption spectra of compound **2.1** (50 μM) in nitrobenzene recorded before and after contacting with 100 equiv of $CsClO_4$, CsF, CsCl, CsBr and $CsNO_3$ dissolved in H_2O. The spectra were recorded after roughly 30 min. of sonication.....75

Figure 2.9: Partial ^{1}H NMR spectra of (a) **2.1** only, (b) **2.1**+10 equiv. of CsF, (c) **2.1**+10 equiv. of CsBr, (d) **2.1**+10 equiv. of CsCl, (e) **2.1**+10 equiv. of $CsNO_3$ and (f) **2.1**+10 equiv. of $CsClO_4$ in nitrobenzene-d_5. The spectra were recorded after roughly 30 min. of sonication. 76

Figure 2.10: Proposed AND logic gate binding behavior of **2.1** towards Cs salts ion pair in $CD_3OD/CDCl_3$. 77

Figure 2.11: A) Structures of **2.4a-d**. B) Absorption spectra of **2.4a** (black line), **2.4b** (blue line), **2.4c** (orange line) and **2.4d** (pink line) in CH_2Cl_2 (50 μM). C) The solution of sensors **2.4 a-d** (50 mM in CH_2Cl_2) in the presence of anions (10 equiv. excess). This figure was originally published in *Org. Lett.* **2006**, *8*, 359-362. Reproduction was permitted. Copyright American Chemical Society. 79

Figure 2.12: Candidates proposed as ion pair sensors that may prove more effective than **2.1** as colorimetric Cs^+ ion pair sensors. 80

Figure 3.1: Urea-based calix[4]arene anion receptors **3.1a-e** and **3.2**. 84

Figure 3.2: Solutions of receptor **3.3** (1 mM) in DMSO/$CHCl_3$ (1/9, v/v) photographed in the absence and in the presence of 5 equiv of various TBA anion salts. From left to right: **3.3** only, F^-, Cl^-, Br^-, I^-, $H_2PO_4^-$, $HP_2O_7^{3-}$, HSO_4^- and SO_4^{2-}. 87

Figure 3.3: Partial ^1H NMR spectra of **3.3** (3 mM) recorded in DMSO-d_6/$CDCl_3$ (1:9, v/v) in the absence and in presence of excess ions (as their TBA^+ salts) (a) **3.3** only, (b) **3.3** + HCO_3^-, (c) **3.3** + HSO_4^-, (d) **3.3** + SO_4^{2-}, (e) **3.3** + $H_2PO_4^-$, (f) **3.3** + $HP_2O_7^{3-}$, (g) **3.3** + NO_3^- (h) **3.3** + I^- (i) **3.3** + Br^- (j) **3.3** + Cl^-, and (k) **3.3** + F^-. 89

Figure 3.4: Partial ^1H NMR spectra of **3.4** (3 mM) recorded in DMSO-d_6/$CDCl_3$ (1:9, v/v) in the absence and in presence of excess ions (as their TBA salts) (a) **3.4** only, (b) **3.4** + HCO_3^-, (c) **3.4** + HSO_4^-, (d) **3.4** + SO_4^{2-}, (e) **3.4** + $H_2PO_4^-$, (f) **3.4** + $HP_2O_7^{3-}$, (g) **3.4** + NO_3^- (h) **3.4** + I^- (i) **3.4** + Br^- (j) **3.4** + Cl^-, and (k) **3.4** + F^-. 90

Figure 3.5: Partial UV-Vis spectra of compound **3.3** (10 μM) recorded in DMSO/$CHCl_3$ (5/95, v/v) upon the addition of various TBA^+ salts (A) Cl^-, (B) $H_2PO_4^-$, (C) $HP_2O_7^-$. 92

Figure 3.6: Association constants K_a (M^-) obtained from UV-Vis spectroscopic titration of compound **3.3** (10 μM) of (A) TBACl, (B) $TBAH_2PO_4$, (C) $(TBA)_3HP_2O_7$ in DMSO/$CHCl_3$ (5/95, v/v). 93

Figure 3.7: Association constants (M^{-1}) obtained from UV-Vis spectroscopic titration of **3.3** (10 μM) with various TBA anion salts in DMSO/$CHCl_3$ (5/95, v/v). 94

Figure 3.8: Partial UV-Vis spectra of compound **3.4** (10 μM) recorded in DMSO/$CHCl_3$ (5/95) upon addition of various TBA^+ salts (a) F^-, (b) Br^-, (c) Cl^-, (d) $H_2PO_4^-$, (e) $HP_2O_7^-$, and (f) HSO_4^-, ...95

Figure 3.9: Partial ^1H NMR spectra recorded during the titration of compound **3.3** (3 mM) with $H_2PO_4^-$ (as TBA^+ salt) in 10% DMSO-d_6 in $CHCl_3$. Its association constant (K_a) is 4.6×10^3 M^{-1}. 96

Figure 3.10: Job plots corresponding to the interaction of compound **3.3** (0.15 mM) with the TBA^+ salts of (A) $HP_2O_7^{3-}$, (B) $H_2PO_4^-$ and (c) Cl^- as recorded using UV-Vis spectroscopy in DMSO/ $CHCl_3$ (5/95, v/v). 97

Figure 3.11: Partial ^1H NMR spectra of (a) **3.3** only, (b) **3.3** after exposure to an excess of NaCl, (c) **3.3** after exposure to an excess of LiCl in DMSO-d_6/$CDCl_3$ (1/9, v/v). The spectra were recorded after subjecting to sonication for roughly 30 min.....99

Figure 3.12: Partial ^1H NMR spectra of (a) **3.3** only, (b) **3.3** after exposure to an excess of $LiClO_4$, (c) **3.3** after exposure to an excess of TBACl, (d) **3.3** with excess of TBACl + $LiClO_4$, (e) **3.3** with excess of $LiClO_4$ + TBACl, (f) **3.3** with excess of LiCl in DMSO-d_6/$CDCl_3$ (1/9, v/v). The spectra were recorded after subjecting to sonication for roughly 30 min. 100

Figure 3.13: Partial ^{1}H NMR spectra of (a) **3.4** only, (b) **3.4** after exposure to an excess of NaCl, (c) **3.4** after exposure to an excess of LiCl in DMSO-d_6/$CDCl_3$ (1/9, v/v). The spectra were recorded after subjecting to sonication for roughly 30 min.....101

Figure 3.14: Partial ^{1}H NMR spectra of (a) **3.4** only, (b) **3.4** after exposure to an $LiClO_4$, (c) **3.4** after exposure to an TBACl, (d) **3.4** with excess of $LiClO_4$ + TBACl, (e) **3.4** with excess of TBACl + $LiClO_4$, (f) **3.4** with excess of LiCl in DMSO-d_6/$CDCl_3$ (1/9, v/v). The spectra were recorded after roughly 30 min. of sonication.....102

Figure 3.15: HRMS of Li^+ ion complexced compound **3.4** 103

Figure 3.16: Partial ^{1}H NMR spectra recorded during the titration of compound **3.4** (3 mM) with Cl^- (TBA^+ salt) in presence of excess $LiClO_4$ in 10% DMSO-d_6 in $CDCl_3$. Its association constant (K_a) is 6.3×10^2 M^{-1}.104

Figure 3.17: Binding isotherm (red line) and data points (black) used to calculate the binding constant (K_a; 6.3×10^2 M^{-1}) corresponding to the interaction of Cl^- (TBA salt) to the preformed complex **3.4**•Li^+ as obtained from a ^{1}H NMR spectroscopic titration carried out in DMSO-d_6/$CDCl_3$ (1/9, v/v). 105

Figure 3.18: Partial ^{1}H NMR spectra recorded during the titration of compound **3.4** with Cl^- (TBA^+ salt) in 10% DMSO-d_6 in $CHCl_3$. 106

Figure 3.19: HRMS of compound **3.3**. 107

Figure 3.20: ^{1}H NMR spectroscopy of compound **3.7** recorded in DMSO-d_6....110

Figure 4.1: Partial ^{1}H NMR spectra of **4.1**, (a) **4.1** with 10 equiv of Na^+, (b) **4.1** with 10 equiv of K^+ (c) **4.1** with 10 equiv of Cs^+ and (d) **4.1** only in $CDCl_3$. The Picrate (2,4,6-trinitrophenolate) anion was used as the counterion. 115

Figure 4.2: Fluorescence spectra of receptor **4.1** (10.0 μM) recorded before and after the addition of excess of Cs^+, K^+, and Na^+ (all as their perchlorate) in chloroform with excitation at 344 nm.....116

Figure 4.3: Fabrication of graphene field-effect transistors (GFETs). 117

Figure 4.4: Raman spectra of GFETs: A) pristine graphene, B) GFETs functionalized with receptor **4.1** (0.5 mM), C) after exposure of the system in B) to Cs^+ picrate salt (100 μM) in acetonitrile. 119

Figure 4.5: Current *versus* voltage (I-V) traces for graphene on gold electrodes; A) pristine graphene, B) GFETs functionalized with receptor **4.1** (0.5 mM), C) after exposure of the system in B) to Cs^+ picrate salt (100 μM) in acetonitrile). 120

Figure 4.6: I-V response expected before and after complexation of the cesium ion for GFETs functionalized with receptor **4.1** 121

Figure 5.1: View of **2.1**. Displacement ellipsoids are scaled to the 50% probability level. Most hydrogen atoms have been omitted for clarity.....129

List of Tables

Table 1.1: Association constants (M^{-1}) of compound **1.3** with various metal cations in 99 % ethanol at room temperature. SCN^- used as a counterion for Na^+, K^+ and Ca^{2+} and ClO_4^- used for Mg^{2+}. 5

Table 1.2: Association constants (log K_a) of compounds **1.42a,c** and **d** for cesium and sodium picrate salts in chloroform.....51

Table 3.1: Associate constants, K_a (M^{-1}) of urea-derived *p*-tert-butylcalix[4]arenes in $CHCl_3$. All counter ions are TBA^+ salts.....84

Table 5.1: Raw data used to obtain the binding constant of Figure 2.5. This corresponds to the interaction of CsF to the preformed **2.1** as obtained from a UV-Vis spectroscopic titration carried out in $CD_3OD/CDCl_3$ (1/9, v/v).....131

Table 5.2: Raw data used to obtain the binding constant of Figure 3.9. This corresponds to the interaction of $H_2PO_4^-$ (TBA^+ salt) with the preformed receptor **3.3** as obtained from a ^1H NMR spectroscopic titration carried out in DMSO-d_6/$CDCl_3$ (1/9, v/v).....136

Table 5.3: Raw data of used to obtain the binding constant of Figure 3.17. This corresponds to the interaction of Cl^- (TBA+ salt) with the preformed receptor complex **3.4**•Li^+ as obtained from a ^1H NMR spectroscopic titration carried out in DMSO-d_6/$CDCl_3$ (1/9, v/v).....137

Table 5.4: Job plot method-2: Excel formula sheet used to obtain a binding affinity values from the raw data obtained from UV-Vis spectral titrations. 139

Table 5.5: Raw data used to create the Job plot shown in Figure 3.10 corresponding to the interaction of compound **3.3** with the TBA^+ salts of $H_2PO_4^-$ as recorded using UV-Vis spectroscopy in DMSO/ $CHCl_3$ (5/95, v/v). These data were treated according to Job Plot method-2 (Table 5.4). 139

Table 5.6: Raw data of used to construct the Job plot, show in Figure 3.10. This corresponds to the interaction of compound **3.3** with the TBA^+ salts of $HP_2O_7^{3-}$ and Cl^-, respectively, as obtained from UV-Vis spectral titrations carried out in DMSO/ $CHCl_3$ (5/95, v/v). These plots were constructed using the Job plot method-1. 140

Chapter 1: Chromogenic and Fluoregenic Receptors Based Upon Calix[4]arene

1.1 INTRODUCTION

The separation of any species from a chemical or biological molecular environment is dependent upon its selective interaction with a particular molecular receptor. This interaction can be determined by the size, charge and shape complementarity of the target species and the receptor. This recognition event between a molecular receptor and a target molecule is often driven by non-covalent forces. In favorable cases, the molecular recognition event can be detected by observing changes in the color, electronic, photonic or redox potential properties of the receptor or system as a whole.

Calix[n]arenes, first synthesized by von Baeyer in 1872, are key members of the metacyclophane class of macrocycles.[1] This series of molecules can be subject to functionalization of the so-called upper and lower rims. This allows the incorporation of binding groups for selective extraction, as well as substituents to tether the macrocycles to a solid support or to signal the binding event through a change in optical or electrical properties. The central cavity or annulus plays key role in most calix[n]arene-mediated events via π-cation or π-π stacking interactions.[2] The diversity of functional groups, that may be attached to calix[n]arenes has enabled the development of procedures for obtaining cone, partial cone, 1,2-alternate or 1,3-alternate conformations in the case of calix[4]arenes. This, in turn, has allowed for the preparation of receptors capable of recognizing numerous ions and molecules selectively or sensitively.[3]

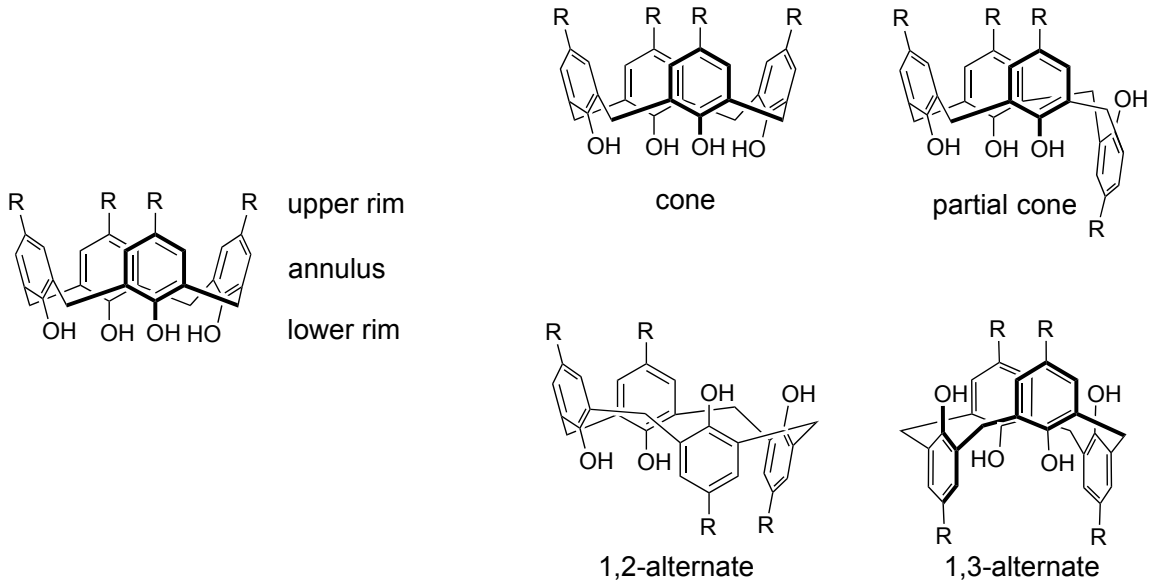

Figure 1.1: Generalized structure of calix[4]arene structure and its four limiting conformers.

1.2 COLORIMETRIC SENSORS

Color changes induced in response to metal ions is one of the most characteristic molecules detection methods exploited in the case of calix[4]arene derivatives. Although other detection techniques, such as fluorescence or oxidation-reduction potential changes, can provide greater sensitivity, a simple color change detectable by the unaided eye has the advantage of allowing easy observation. One of the earliest successful examples where a calix[4]arene was functionalized with a chromogenic moiety with the intention of sensing metal ions was reported by McKervey.[4] He and his coworkers reported a Li^+ responsive *p*-t-butylcalix[4]arene (**1.1**) with three ethyl esters and a hydroxynitrobenzylacetate at the lower rim (Figure 1.1). The ring formed by the phenolic oxygens of calix[4]arene (2 Å) matches well with the diameter of lithium ion (1.36 Å),

Nevertheless, the lithium ion binds at the lower rim instead of inside the cavity due to its strong hydration, The interaction of Li^+ ion to Mckervey's system could be visualized by monitoring the color change from colorless to yellow. However, some interference from Na^+ was observed.[5] New separate from Mckervey, There are many successful reports of Na^+ recognition using calix[4]arene. For instance, in calix[4]arenes bearing carboxylethoxy groups, such as compound **1.2** developed by Shinkai, the carbonyl and phenolic oxygens combine to form a cavity that is suitable size for Na^+recognition. A 42 nm bathochromic shift was observed in the case of **1.2**, which bears an indoaniline moiety at the upper rim. In this system, a conformational change in the calix[4]arene is seen upon exposure to sodium ion salts in ethanol.[6]

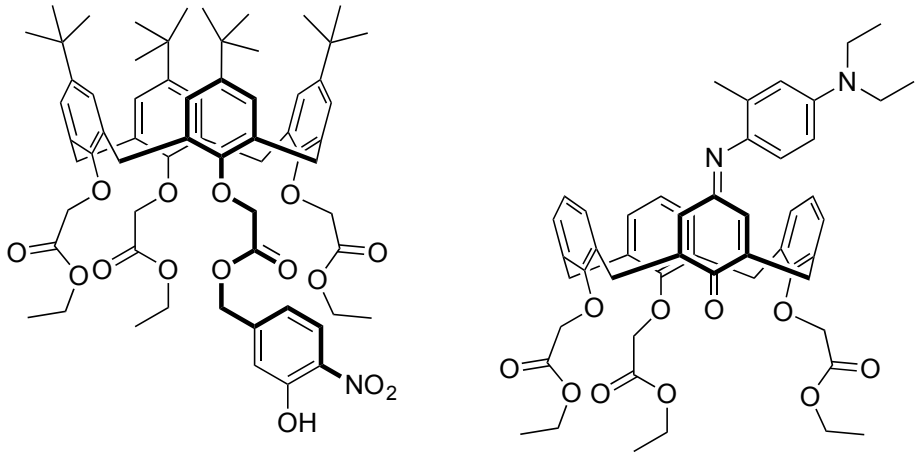

1.1 **1.2**

Figure 1.2: Calix[4]arene compounds used to detect alkali cations.

In the case of Ca^{2+} binding, it was assumed that a partial cone conformation, especially a 1,3-alternate conformation was adopted rather than the cone conformation. Changing the conformation to partial cone or an alternative conformation establishes a

better pre-organized structure for larger size ions than Li^+. In fact, compound **1.2** showed a great selectivity toward the Na^+ ion, than the Li^+ ion. In 1993, Kubo reported compound **1.3** (Figure 1.3), a 1,3-alternate calix[4]arene that incorporates lower rim ethyl esters and upper rim indoaniline chromophores. This system showed the greatest response to Ca^{2+}. Table 1.1 lists the association constants for Na^+, K^+, Mg^{2+} and Ca^{2+} as determined from UV-Vis titrations carried out in 99 % ethanol. Under these conditions, the highest binding affinity was seen for Ca^{2+} (as the SCN- salt), with remarkable λ_{max} change from 609 nm to 719 nm was seen in the UV-Vis spectrum. Weaker responses were observed for Mg^{2+} and K^+; however, the wavelength shift and the intensity of the signals were relatively insignificant.[7]

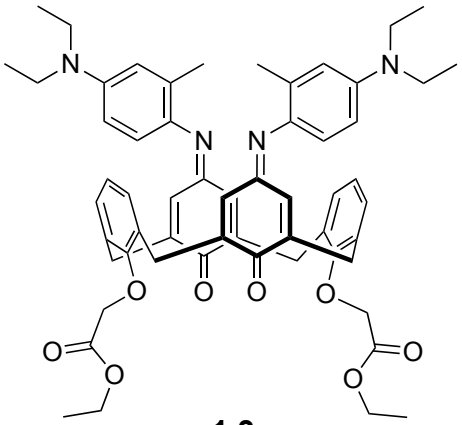

1.3

Figure 1.3: Calix[4]arene compound **1.3** developed for Ca^{2+} ion recognition.

Host	Na^+	K^+	Mg^{2+}	Ca^{2+}
1.3	3.7×10^4	3.2×10^5	100	7.6×10^6

Table 1.1: Association constants (M^{-1}) of compound **1.3** with various metal cations in 99 % ethanol at room temperature. SCN^- used as a counterion for Na^+, K^+ and Ca^{2+} and ClO_4^- used for Mg^{2+}.

Another Ca^{2+} selective receptor, the triazole- and azo-functionalized calix[4]arene **1.4,** was developed by Chung.[8] Here, the two triazole moieties were expected to provide efficient Ca^{2+} binding site. Bathochromic shifts were seen upon exposure to Ca^{2+} ions (perchlorate salts, studied in CH_3CN/ $CHCl_3$ 1000:4, v/v), an effect ascribed to the electrostatic interaction of metal cations with the two azophenol moieties, as well as the ion-dipole interactions with the metal ions. However, as can be seen from Figure 1.4, the interference in terms of sensing is ascribed to the similar sizes of the two ions concerned, namely Ca^{2+} and Pb^{2+} in the UV-Vis absorption spectrum.

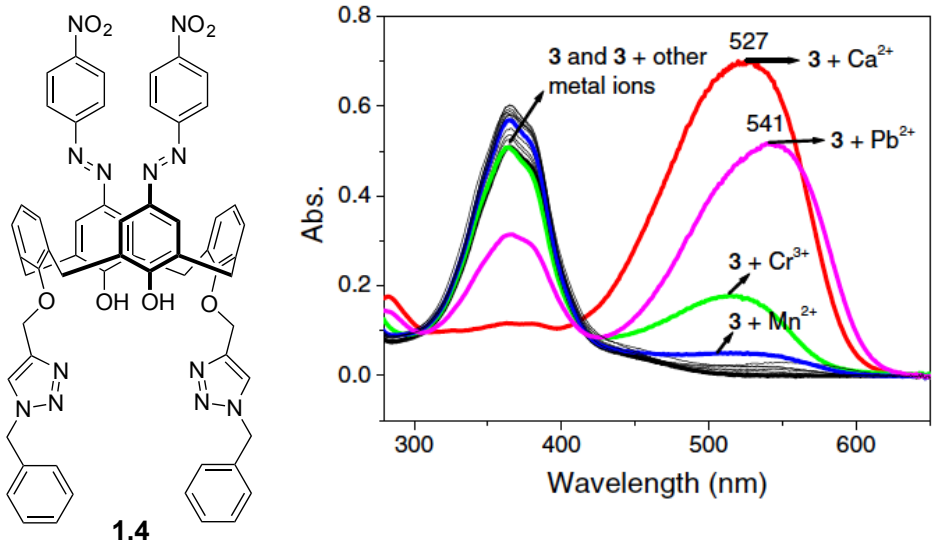

Figure 1.4: Triazole- and azophenol-coupled calix[4]arene **1.4** and UV-Vis spectra of compound **1.4** (10 μM) before and after adding 100 μM concentration of various metal perchlorates in MeCN/$CHCl_3$ (1000:4, v/v). Originally published in *Tetrahedron Lett*. **2007**, *48*, 7274-7278. Reproduced by permission. Copyright ELSEVIER.

Chung and his coworkers also successively developed very strong Hg^{2+} sensitive and selective receptors **1.5** and **1.6** that bear *p*-methoxyphenylazo and *p*-allyl groups (Figure 1.5).[9,10] The absorbance of the free ligand **1.5** in a methanol/chloroform mixture (1/399, v/v) at 355 nm was seen to disappear upon the complexation with the mercury (II) ion (perchlorate salts). Concurrently, a more intense peak at 484 nm appeared. Such spectral changes are in accord with the observed color changes from pale green to pink. However, it turned out that the *p*-allyl groups present in the receptor **1.5** do not participate in the metal binding. Very little interference was seen for alkali, alkaline earth or other p- and d-block metal cations. System 1.6, reported later by Chung et al., involves another combination of *p*-methoxyphenylazo and *p*-allyl substitutents. In this case, two *p*-methoxyphenylazo groups bind the Hg^{2+} cation in a distal orientation rather than a

proximal one. The third flanking *p*-methoxyphenylazo group plays a major role in disturbing the binding interactions involving the other two diazo groups. In this case, Chung and coworkers proposed that, in contrast to what was true for **1.5**, the allyl groups do participate in metal binding.

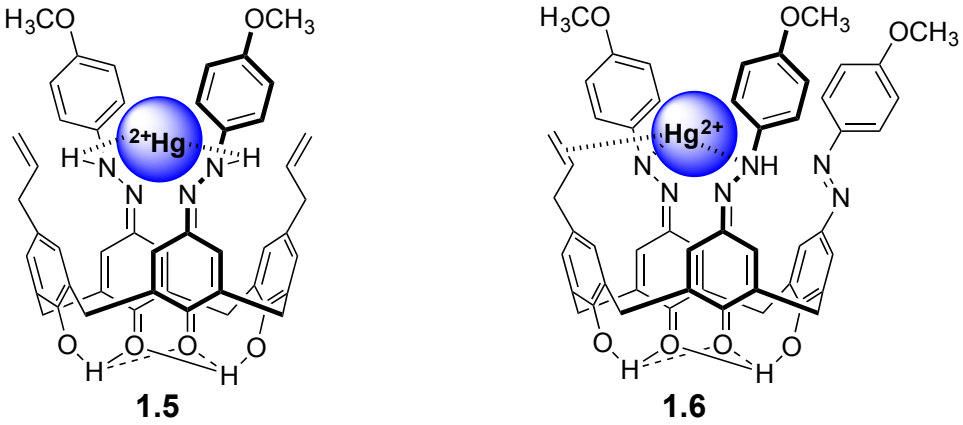

Figure 1.5: Two compounds bearing phenylazo- or allyl- group at the upper rim that were developed by Chung for Hg^{2+} recognition.

Gao and Kubo carried out pioneering studies involving the interaction of lanthanide and actinide ions with modified calixarenes. First, Gao and his coworkers incorprated imine groups into the upper rim of calix[4]arene leading to the Schiff base-calix[4]arene, **1.7** (Figure 1.6). Receptor **1.7** was able to recognize selectively lanthanide ions, with Dy^{3+} and Er^{3+} showing different color changes from colorless to pale pink and to pale yellow, respectively. However, when alkali metal ions, alkaline earth metal ions, transition metal ions or other lanthanide ions (such as La^{3+}, Pr^{3+}, Eu^{3+}, Gd^{3+} or Yb^{3+}) were

added as their cation salts to the dichloromethane solutions of **1.7**, visible changes in color were not observed. Although the author did not provide a rationalization, the positive effect seen for Dy^{3+} and Er^{3+} might be explained by their similar size (ionic radii: Dy^{3+}=178 pm, Er^{3+}=176 pm).[11]

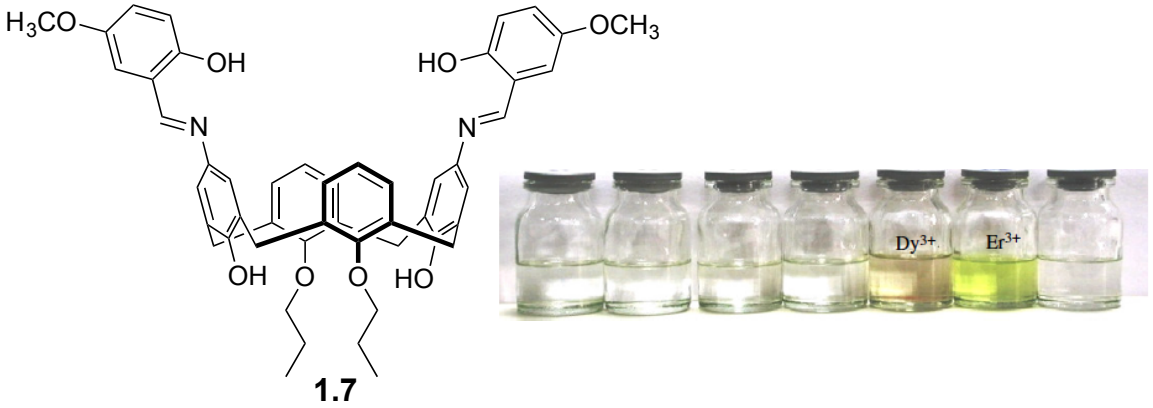

Figure 1.6: Schiff-base calix[4]arene for lanthanide ions (Dr^{3+} and Er^{3+}) detection. Color changes of compound **1.7** after 24 h in the dark (from left to right: La^{3+}, Pr^{3+}, Eu^{3+}, Gd^{3+}, Dy^{3+}, Er^{3+} and Yb^{3+}). Originally published in *Tetr. Lett.* **2007**, *48*, 3587-3590. Reproduced by permission. Copyright ELSEVIER.

In 1994, Kubo synthesized an optically active calix[6]arene receptor for the UO^{2+} ion. He and his coworkers did this by incorporating one indoaniline chromophore at the upper rim. It was speculated that the indoaniline chromophore provided a key benefit, because its optical properties could be perturbed significantly by chemical stimuli, including specifically binding a metal ion. The quinone carbonyl group of indoaniline-type ligands strongly interacts with divalent metal ions, resulting in color changes.[12] In his paper, Kubo, et al. explained that compound **1.8** has a visible absorption band with λ = 665 nm in ethanol solution. However, upon addition of DBU (1,8-diazabicyclo [5.4.0]undec-7-ene), a hypsochromic shift of 37 nm was observed with lower absorbance

intensity than the original band. These changes were attributed to the removal of intramolecular hydrogen bonding interaction between the quinone carbonyl of the indoaniline subunit and the adjacent phenolic hydroxyl groups. In contrast, upon complexation with the UO^{2+} ion, there was a significant bathochromic shift from 628 nm to 687 nm accompanied by a 90% increase in absorbance intensity. A small degree of interferences from both the Sr^{2+} and Cs^{+} ions were observed during the UV-Vis spectral studies. However, this was considered to be only a minor drawback in the content of sensing compared to the UO^{2+}. The apparent association constant for UO^{2+} was calculated to be 8×10^{4} M^{-1} based on a Benesi-Hildebrand plot. On the basis of UV-Vis spectra studies, showing selectivity toward UO^{2+}, it was concluded that receptor **1.8**, supports can a specific coordination mode of the UO^{2+}. In particular, the authors suggested that the UO^{2+} cation is complexed in a 6-coordinate manner with the calix[6]arene adopting a pseudoplanar structure.

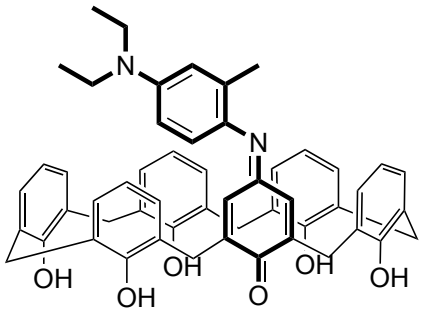

1.8

Figure 1.7: A monoindoaniline modified calix[6]arene developed for UO^{2+} ion recognition and sensing.

So far, we have discussed colorimetric cation sensors based on calixarenes. Next, calixarene derivatives that function as anion sensors will be discussed. Selective detection or extraction of anions is of interest because anions are ubiquitous in biological milieus. It has also been suggested that the transport of anions or ion pair across cell membranes could have medicinal value. However, anion sensing using calix[4]arene is difficult to achieve because of a general incompatibility between the geometry, size, and polarizability of the target anion and the receptor. Nonetheless, recently some excellent examples of chromogenic anion sensings using calixarenes have been reported. Mostly, sensors for the F^- and $H_2PO_4^-$ anions have been prepared to date. Gunnlaugsson is one of the prolific researchers who have contributed significantly to the field of calixarene-based anion sensing.[13,14] For instance, Gunnlaugsson and his coworkers appended two amido-urea substituents at the lower rim of a 1,3-alternative calix[4]arene to produce compound **1.9,** which can donate hydrogen bonding to anions like acetate and phosphate. The incorporation of a 4-nitrobenzene subunit into the receptor allowed anion binding to be monitored using absorption spectroscopy. It was found that receptor **1.9** binds F^- with a 1:1 stoichiometric. Colorimetric changes are observed. This finding was ascribed to binding events that occur through hydrogen bonding. No evidence of NH deprotonation was observed prior to the addition of high relative quantities of F^-. Strong 1:1 interactions with binding for both $H_2PO_4^-$ and hydrogenpyrophosphate were seen. The latter anion is bound in a bridging manner across the lower rim cavity of the compound **1.9**. In 2007, the Gunnlaugsson group reported the tetra-amidourea calix[4]arene **1.10**. This receptor responded very well to F^- and $H_2PO_4^-$. In dimethyl sulfoxide (DMSO) solution, color changes from colorless to dark red were seen upon exposure to salts of these anions. Gunnlaugsson and coworkers suggested that $H_2PO_4^-$ binds to a network of urea protons

and that this causes the spectral changes. In contrast, the response to F^- was ascribed to the almost certain formation of HF_2^- resulting from deprotonation of the urea protons.

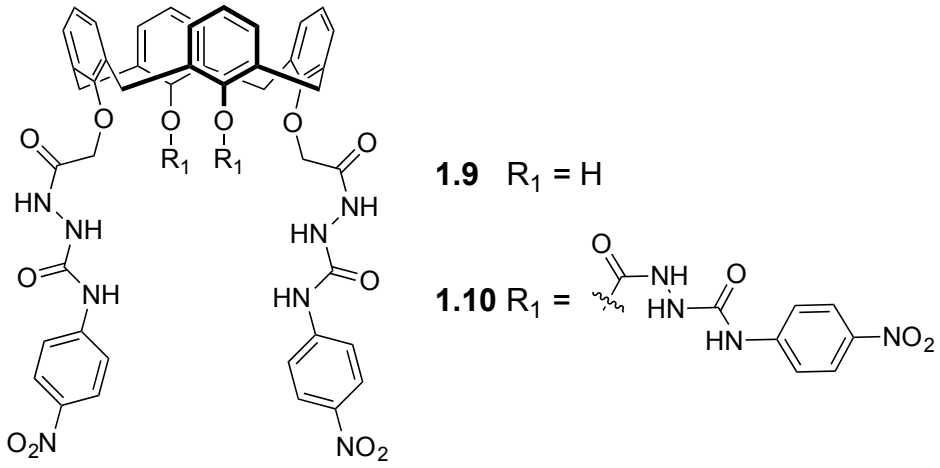

Figure 1.8: Amido-urea substituted calix[4]arene derivatives **1.9** and **1.10** generated as sensors for F^- and $H_2PO_4^-$.

Calixarenes have also been used as scaffolds to produce colorimetric sensors for neutral molecules. Trimethylamine and chiral amines have received particular attention as analytes. In 1996, Kubo et al. designed calix[4]arene derivatives that were expected to be selective for chiral amines. They did this by appending a 1,1'-binaphthyl bridge as well as installing two indophenol chromophores on the calixarene framework.[15] (R)-phenylglycinol and (R)-phenylalaninol were detected by monitoring the change in color from red to blue violet upon complexation. In accord with design expectations, the (S)-enantiomers did not bind to the calixarenes and did not induce binding to a significant change in color. These findings were taken to indicate that during the amine complexation process, binding to compound **1.11** takes place within a cavity consisting of the ether oxygens of the macrocycle and phenolate moiety of the indophenol. Figure 1.9

b) illustrates the complex structure that is proposed to form when a chiral amine guest binds to **1.11**. In other words, three recognition motifs (di-ethylene glycol, indophenol O^-, and a binaphthly group) are proposed to contribute to the enantioselective binding. The di-ethylene glycol and the indophenol O^- stabilize the host-guest complex and restrict the rotation of the guest along the C^*-NH^{3+} axis via ion-dipole and hydrogen bonding interactions. The third recognition group, the binaphthyl group, acts as a minor steric-repulsive site for the (R) isomer, and as a major steric-repulsive site for the (S)-isomer. Consequently, the treatment of **1.11** with the (S)-phenylglycinol did not produce a distinguishable color change. Kubo hypothesized that the binding of the (R) amine substrate may have transformed the position of the binaphthyl unit in a way that is not seen in the case of (S)-phenylglycinol.

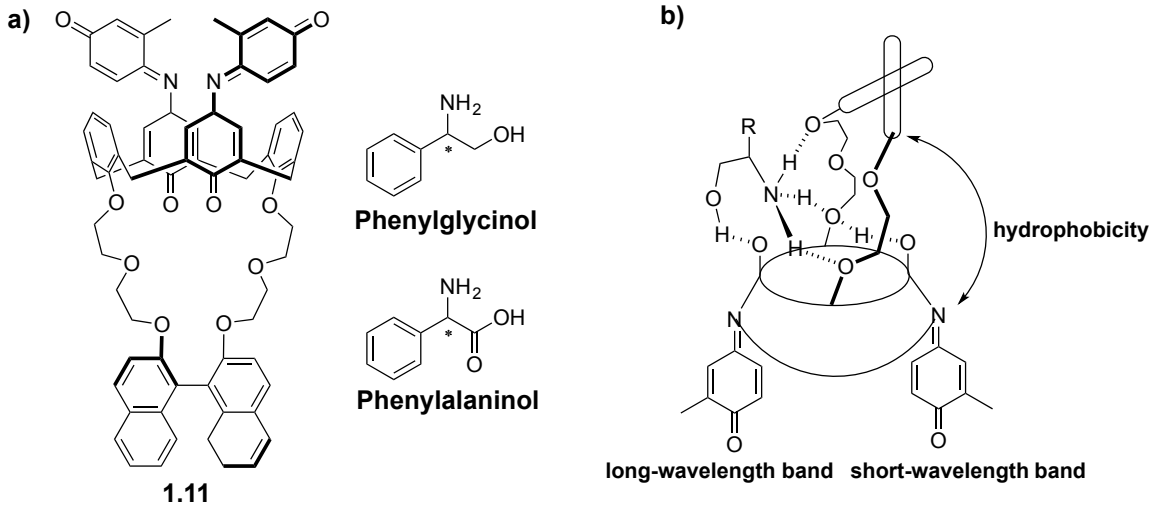

Figure 1.9: a) 1,1'-Binaphthyl subunit and two indophenol chromophores that are appended to a calix[4]arene case to produce sensor **1.11**. b) Possible structure for the complex formed between **1.11** and (R)-phenylglycinol.

1.3 FLUORESCENT SENSORS OF CALIX[4]ARENE DERIVATIVES

As noted above, the development of colorimetric sensors for the detection of specific analytes is an increasing research area because of their potential utilities in the fields of chemistry, biology and medicine.[18] Among various sensing methods, detection by fluorescent techniques present some distinct advantages in terms of sensitivity, selectivity, response time, etc.[19]. In fact, the monitoring of recognition process by luminescent spectral changes is widespread. Fluorescent molecular sensors can be designed by combining an ionophore, constructed for the binding of particular guests, with a fluoregenic unit whose photophysical properties perturbed during the recognition process. In general, these perturbations are reflected in the photophysical properties, such as excimer formation or emission spectroscopy. Often fluoregenic receptors are synthesized that have two aromatic fluorophores in close proximity so as to support π–π interactions. Pyrene and naphthyl substituents are frequently utilized because they exhibit a strong intramolecular excimer band that can be modulated in the presence of guest ions.[20] Ionophore is one of the key components of an effective ion sensing receptor. The conformation, size, ion accepting ability and steric hindrance of the core receptor are critical factors that determine ion selectivity. Because they may be modified,[21] relatively rigid calixarene derivatives as very attractive frameworks for the construction of ion sensing receptors.

Three principle effects are usually observed when there is a binding event between fluoregenic calixarene receptors and ions depending on the manner of response. Photo-induced electron transfer (PET) is a key property of appropriately functionalized calixarenes and one that may be used to follow a binding event. PET proceeds by transformation of an excited electron from a donor to an acceptor. This results in fluorescence quenching (Figure **1.10**). Photo-induced charge transfer (PCT) occurs when

the properties of the fluorophore are affected by electron donation from, or accepting by, the analyte. The resulting change in fluorophore dipole moment is often manifesting in a change in the molar absorptivity and in the λ_{max} of emission. Fluorescence resonance energy transfer (FRET) takes place when the calixarene contains two fluorophores. Upon addition of guest molecules, one fluorophore works as an excited state energy donor for the other fluorophore, which then fluorescences. Excimer formation or its decomposition represents another widely used method to generate a signal diagnostic of analyte binding. The binding event and the induced change in FRET and excimer structure may result from analyte induced changes in calixarene comformation.

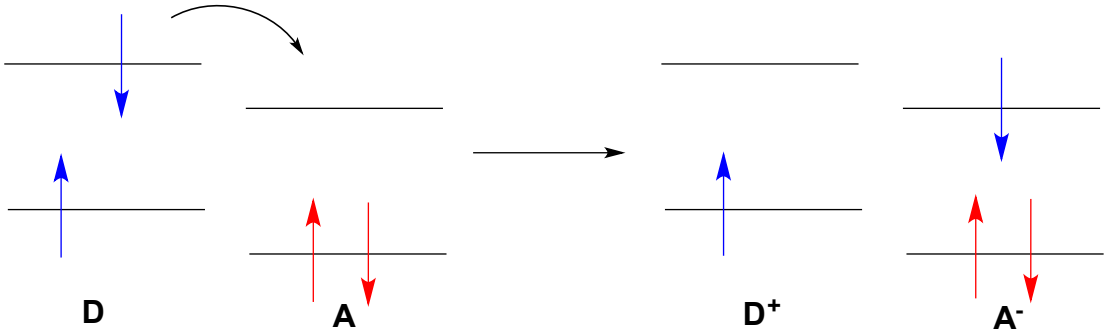

Figure 1.10: Mechanism of a classic photo-induced electron transfer process.

1.3.1 Photo-Induced Electron Transfer Fluorescent Sensors

Most examples of calixarene-based fluorogenic sensors reported to date were constructed with a view to detecting cations via PET modulation. The resulting sensor systems typically contain electron transfer pathways that allows for deactivation of the excited state. Binding to metal cations can block this deactivation route, which allows the fluorophores to emit strongly. This approach has been tested with various alkali metal, alkaline earth metals, heavy metal or radioactive metal cations. In this section, selective ion detection with fluorogenic calix[4]arene derivatives using a PET method will be discussed. One of the first reports of a fluorescence response involving calix[4]arenes did not rely on the use of traditional fluorophores.[22] This report, published by Ungaro, in 1987, relied on compound **1.12.** This system was found to bind alkali metal cations effectively. A few years later, Ungaro and coworkers realized that this compound could coordinate Tb^{3+} selectively in water and to produce a complex with high luminescent intensity in aqueous solution as shown in Figure 1.11. Two rationales were put forward to account for this phenomenon: efficient ligand-to-metal energy transfer and excellent shielding of the encapsulated metal ion from the interaction with water molecules. Figure 1.11 shows the chemical formula of compound **1.12** and its X-ray diffraction structure of its complexation with K^+.

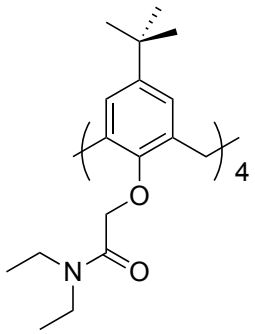

1.12

A)

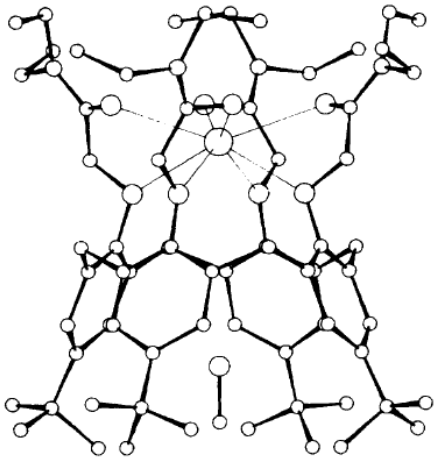

B)

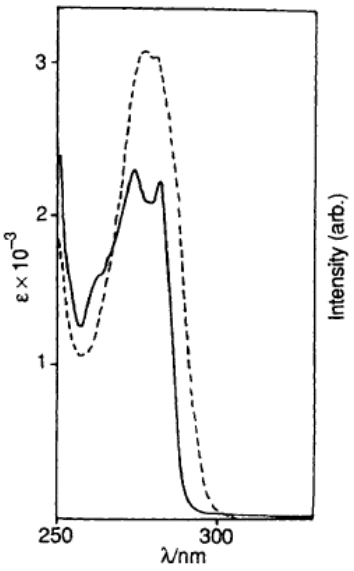

Figure 1.11: Compound **1.12**, A) its X-ray crystal structure of **1.12**•KSCN•MeOH complex, B) Absorption spectrum of **1.12** (dash dot) and excitation spectrum of [Tb•**1.12**]$^{3+}$ (line) in methanol. Figure 1.11 A) was originally published in *J. Chem. Soc. Chem. Commun.* **1987**, 344-346. Copyright The Royal Society of Chemistry. Figure 1.11 B) was originally published in *J. Chem. Soc. Chem. Commun.* **1990**, 878-879. Copyright The Royal Society of Chemistry.

Crown-6-ether strapped calix[4]arene locked in the 1,3-alternative have been widely studied.[23] Many of these systems bind the cesium ion with remarkable strength and selectivity. Efforts to extend this work to obtain visually-active, cesium selective

receptors by appending a fluoresecent moiety have been made. In 1996, Dabestani developed a 9-cyanoanthracene modified crown-6-ethered calix[4]arene, compound **1.13**.[24] In the absence of cesium ions, the fluorescence of the **1.13** is partially quenched as the result of photo-induced transfer (PET) from the dialkoxybenzene moiety of the crown ring to the excited singlet state of the 9-cyanoanthracene subunit. However, upon complexationof Cs^+, the oxygen lone pairs of crown ether will no longer participate in PET, causing the emission of the 9-cyanoanthracene fluorophore to increase. Kim also reported a calix[4]arene possessing both 18-crown-6-ether and *N*-(pyrenemethyl)aza-15-crown-5-ether binding sites a few years later.[25] This system , compound **1.14,** was found to fluoresce strongly when Ag^+ was bound. Here, the nitrogen lone pairs of the azacrown ring not only participate in the selective binding to Ag^+, but also serve to reduce the PET. The net result is a cation-induced increase in the emission intensity. This phenomenon is referred to as a chelation-enhanced fluorescence (CHEF) effect. The enhanced fluorescence was largely quenched upon the addition of Cs^+, which served to discharge the Ag^+. No effect was seen upon the addition of K^+. This difference was ascribed to the cavity size of the crown-6 loop being too large to capture the K^+ ion. On the other hand, the cesium ion fits well with the crown-6 cavity, displacing the silver ion from the azacrown-5 loop as a result of metal-metal ion repulsion.

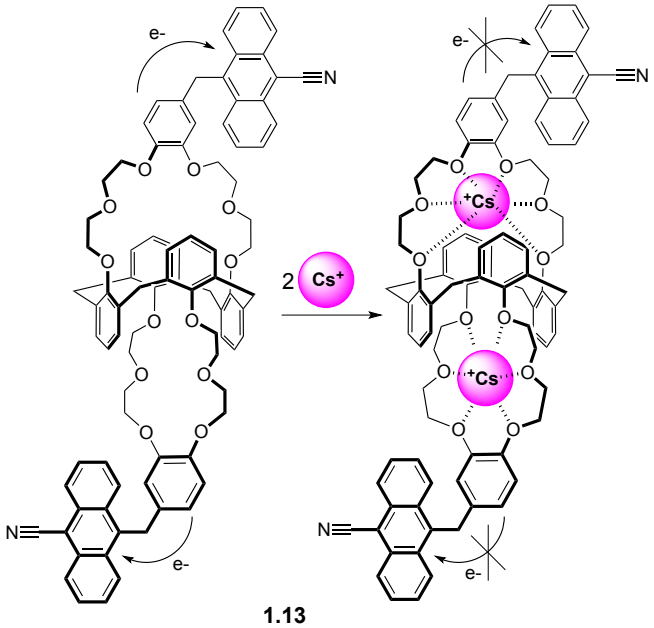

Figure 1.12: Compound **1.13** and proposed metal complexation chemistry.

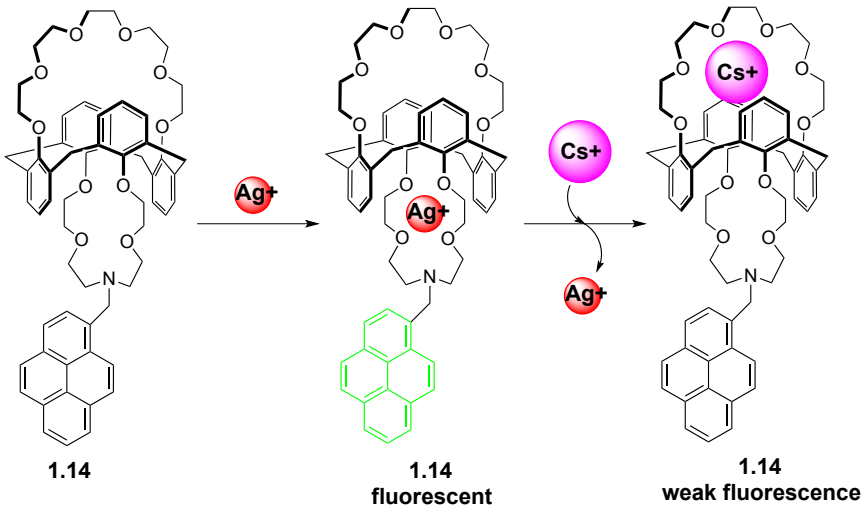

Figure 1.13: Fluorescence emission properties of compound **1.14** observed in ethanol upon the addition of Ag^{+} and Cs^{+}, respectively.

Kim and his colleagues also synthesized a cesium selective crown-ether calix[4]arene receptor bearing a 9-cyanoanthracene subunit as shown in Figure 1.14.[26] In this system (**1.15**), a 9-cyanoanthracene subunit was appended to the upper crown-ether of compound **1.15** while azacrown was attached to the lower rim of calix[4]arene. In this system, the selective binding of metal ion pairs, Cs^+-Cu^{2+} and Cs^+-Ag^+, were investigated by monitoring the fluorescence changes. Upon the addition of Cs^+ to **1.15**, a CHEF effect was observed due to the inhibition of the PET mechanism, in analogy to what was seen in the case of **1.14**. This CHEF effect is consistent with the Cs^+ being bound within the crown ether site. When Cu^{2+} was added to a solution of **1.15** and Cs^+, a fluorescence quenching effect was observed that proved dependent on the Cu^{2+}. This was taken as evidence that the complexation of Cu^{2+} occurs within the azacrown ether site. This binding, in turn, induces decomplexation of the Cs^+ from the crown ether site. Similar behavior was seen in the case of the Cs^+ and Ag^+.

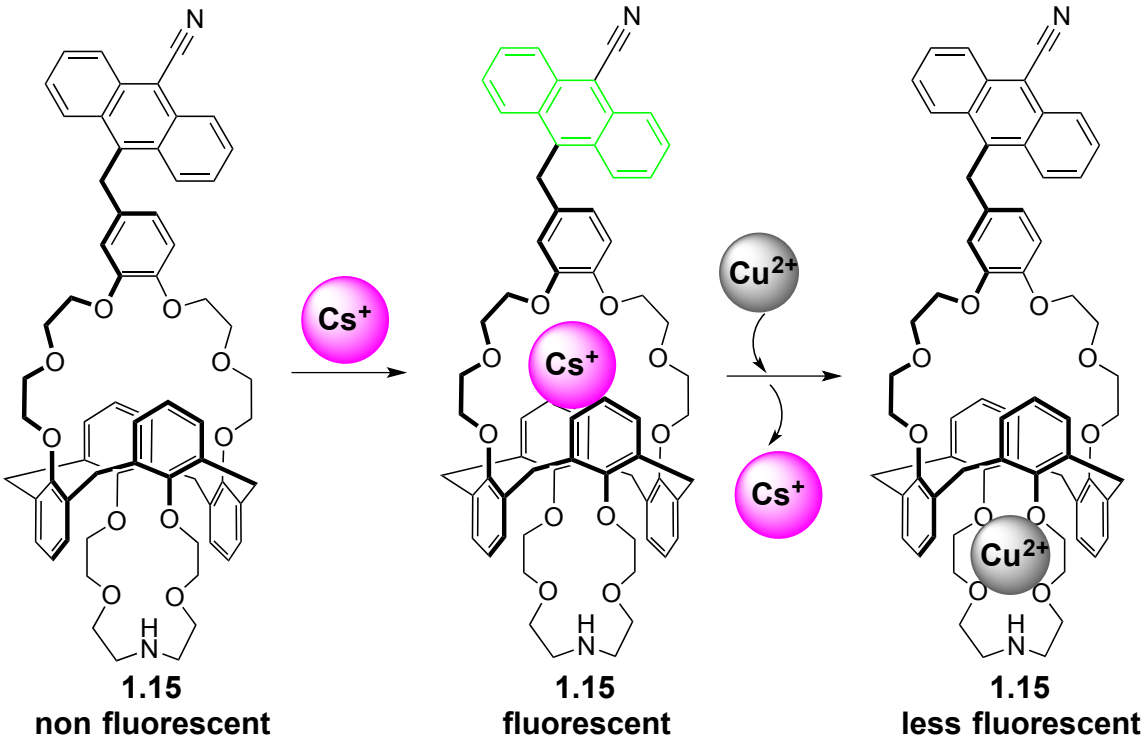

Figure 1.14: Fluorescence emission of compound **1.15** observed upon the addition of Cs^+ and Cu^{2+}, respectively in ethanol/dichloromethane (9/1, v/v).

Several other fluorogenic cesium sensors, specifically the crown-6-ether calix[4]arene derivatives **1.16a** and **1.16b** were synthesized by Sachleben.[27] Interestingly, although these two compounds are based on the same fluorophore, they gave rise to significantly different fluorescence enhancements upon complexation of the cesium cation and this observation was ascribed to the stabilization of a slightly different conformations.

In particular, the more sensitive response of **1.16b** to cesium complexation was interpreted in terms of a stronger interaction between the cesium cation and the ether oxygens of the benzo group present in this receptor. This, in turn, results in a greater

charge dispersion onto the oxygen atoms of the crown ethers and results in stronger interactions with the bound cesium cation.

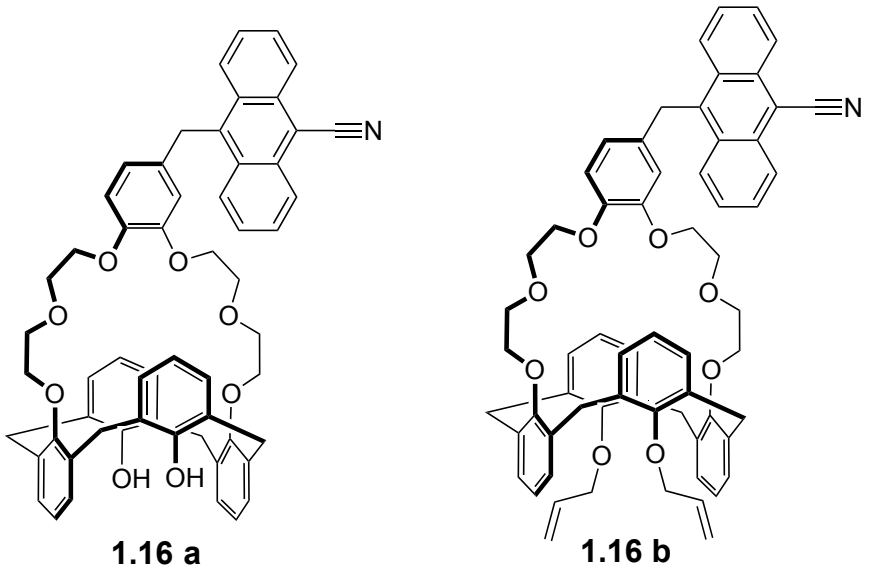

Figure 1.15: Line drawings of compounds **1.16a** and **1.16b**. These two receptors contain the same fluorophore but give rise to different fluorescence response when treated with the cesium ion.

A large number of fluorescence-responsive calix[4]arene receptors for transition metal ions, such as Hg^{2+}, Cu^{2+}, Pb^{2+} or Cd^{2+}, have been reported. Most paramagnetic transition metal ions are efficient fluorescence quenchers. Not surprisingly, therefore early cation sensors relied on fluorescence quenching to signal the presence of metal ions. The quenching was the result of an electron or energy transfer process. In general a full review of this work is not possible here. However a few of representative examples will be discussed for the sake of illustration. Because the Cu^{2+} ion is of importance in the environment and in biology, considerable attraction has been devoted to the development

of fluorescent Cu^{2+} chemosensors. In 2008, Chen and Huang reported a highly efficient and selective turn-on fluorescent sensors for the Cu^{2+} ion based on a calix[4]arene bearing iminoquinoline subunits on the upper rim. The compound; involved **1.17a** and **1.17b,** were designed such that a fluorescence unit interacts directly with the metal ions. Furthermore, these systems contain the two or four fluorophore ion recognition units instead of the single-ion recognition subunits typically seen in Cu^{2+} sensors.[28] These systems displayed a remarkable Cu^{2+} selectivity in contrast to other sensors, many of which should interference from Pb^{2+} and Fe^{3+}. In fact, compound **1.17b** shows a dramatically enhanced fluorescent intensity (about 1200-fold) in the presence of the Cu^{2+} ion as the perchlorate salts and high selectivity towards the Cu^{2+} ion over a wide range of metal ions in acetonitrile (Figure 1.16). As a comparing system, the di-iminoquinoline derived compound **1.17a** was synthesized and studied. In analogy to **1.17b**, fluorescence enhancement was seen for **1.17a** in the presence of the Cu^{2+} ion. However, the response was significantly lower than that of **1.17a**. Association constants (K_a) of 3.7×10^5 M^{-1} and 3.7×10^7 M^{-1} were calculated for **1.17a** and **1.17b**, respectively. The results led the authors to suggest that the tetraiminoquinoline derived compound, **1.17b,** might have a preorganized structure and thus provide multiple complexation sites for the Cu^{2+} ion.

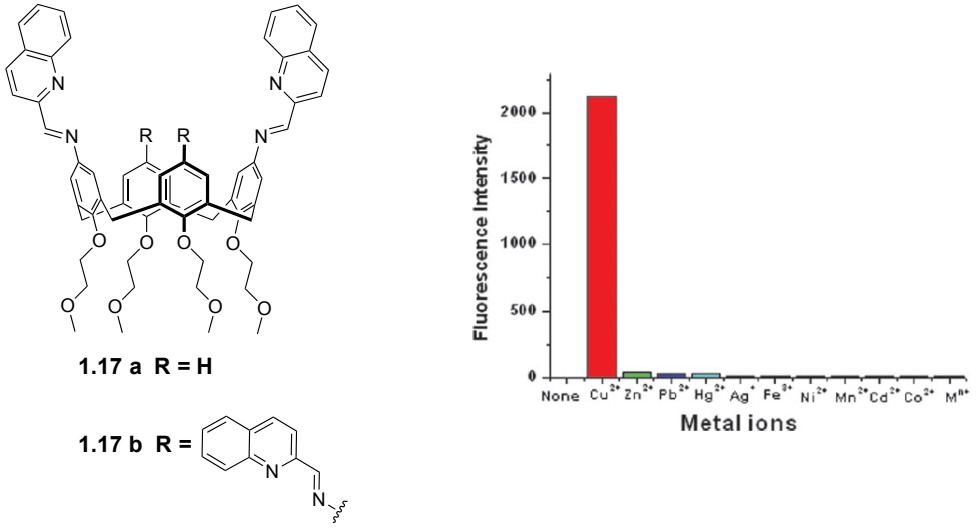

Figure 1.16: 1,3-Alternative two iminoquinoline substituted calix[4]arenes, **1.17a** and **1.17b**. Fluorescent intensity of compound **1.17b** (10^{-5} M) recorded in acetonitrile after the addition of 11.0 equiv. of various metal ions (M^{n+} denotes Li^+, Na^+, K^+, Mg^{2+}, Ca^{2+}, and Ba^{2+}). All cations were studied as the perchlorate salts. This result was originally published in *Chem. Commun.* **2008**, 1774-1776. Reproduced with permission. Copyright The Royal Society of Chemistry.

In 2003, Zheng and Huang reported another calixarene-derived Cu^{2+} chemosensor (**1.18)** that contains two lower rim imidazoles and a single naphthyl derivative. This compound not only could selectively discriminate Cu^{2+} and Zn^{2+}, but also acted as on/off fluorescent switch by modulating the pH of a methanol-water solution.[29] These researchers adopted imidazoles as preorganized ionophores to recognize selectively transition metals by combining a calix[4]arene with a fluorophore consisting of a naphthly ring with the goal achieving a modulated signal upon ion recognition. A marked decrease in fluorescence was observed as the concentration of Cu^{2+} was raised in methanol/water (9:1, v/v, pH 10). In contrast, a slow increase at the emission maximum

was observed in the presence of Zn^{2+}. On the basis, it was concluded that compound **1.18** can effectively recognize Cu^{2+} and Zn^{2+}. The system also displayed showing different fluorescent behaviors in the presence and absence of these cationic inputs, thus functioning as a molecular switch. By modulating the pH, the evidence of on-off fluorescent switching was demonstrated as a function of acid, base, and Cu^{2+}.

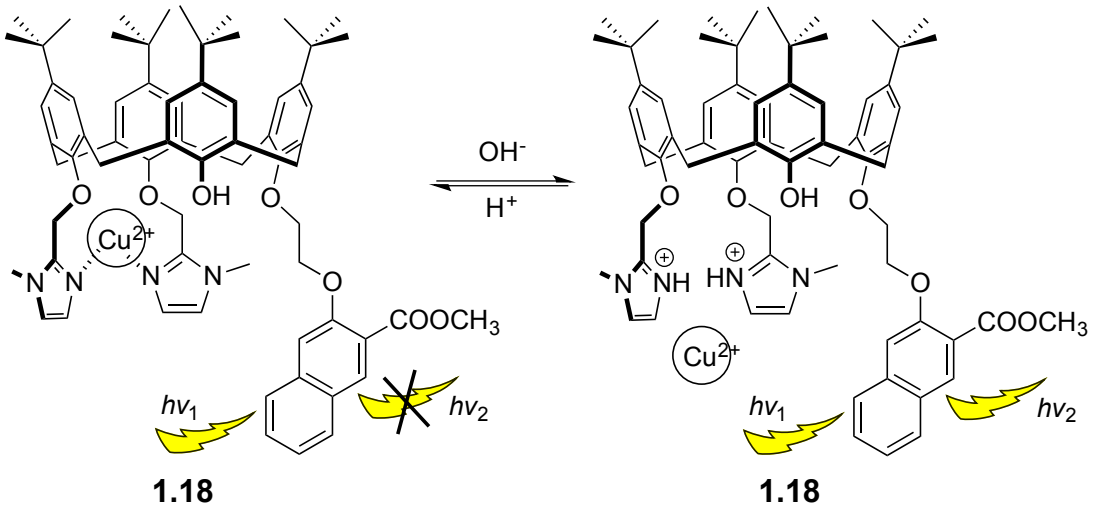

Figure 1.17: pH-dependent on/off molecular switching seen in the case of compound **1.18**.

The first calix[4]arene-based fluorogenic mercury selective extractant was discovered by Bartsch in 1999.[30] He and his coworkers used a dansyl fluorophore moiety in conjunction with a N-X-sulfonyl carboxamide group to create a system capable of recognizing the Hg^{2+} ion (Figure 1.18). The fluorescence spectrum of compound **1.19** in a chloroform solution was characterized excitation and emission bands at λ_{ex} = 340 and λ_{em}

= 520 nm, respectively. However, after upon the extraction of Hg^{2+} from an aqueous solution, the fluorescence of the dansyl group is quenched. This quenching reflects a PET process that is a general characteristic of transition metal ions and in this case involves the transfer electrons from the excited dansyl moiety to the proximate mercuric ion. As a result, fluorescence quenching is observed upon Hg^{2+} complexation that is not seen with other cations, including alkali metals, alkaline earth metals or transition metals.

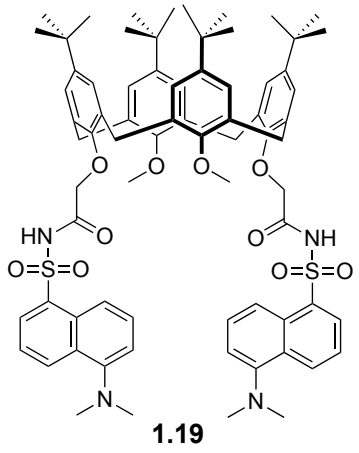

1.19

Figure 1.18: A calix[4]arene extractant **1.19** that relies on dansyl moieties for the sensing Hg^{2+}.

Over the past few years, Kim and coworkers developed a series of calix[4]arene-based fluorescent chemosensors for Pb^{2+} detection. Within these series, compound **1.20** was considered prototypical. It was designed to act as a Pb^{2+} fluorogenic sensor as the result of a PET process.[31] In this compound, amide groups serve to capture not only cations through the carbonyl oxygen atoms, but also anions as the result of the hydrogen bonding interactions involving the bound anions and the acidic hydrogen atoms on the nitrogen atoms (Figure 1.19).

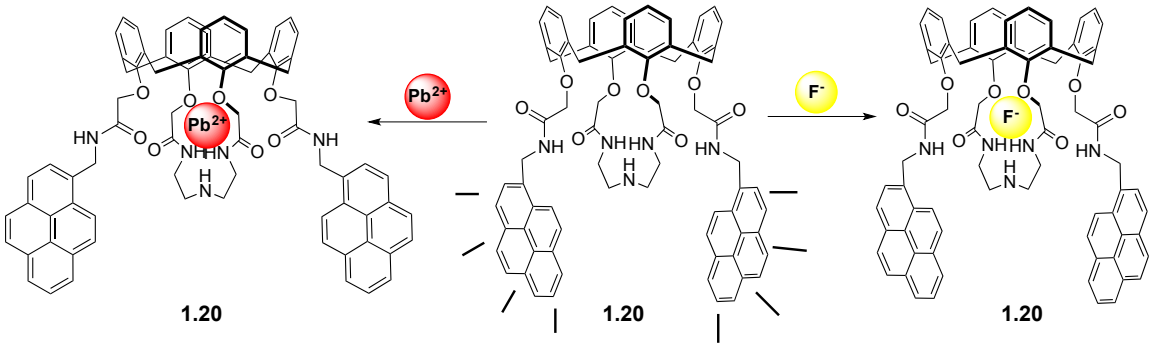

Figure 1.19: Structure of fluorescence chemosensors **1.20** and the response produced upon complexation of Pb^{2+} and F^-.

When Pb^{2+} and Co^{2+} were bound to compound **1.20**, both the monomer and excimer emissions were quenched due to the combination of a heavy metal effect, reverse-PET and conformational changes. The association constants (K_a) corresponding to the interaction for **1.20** and Pb^{2+} and Co^{2+} were 4.65×10^7 and 4.96×10^6 M^{-1} respectively, in acetonitrile. Compound **1.20** also demonstrated an ability to interact with anions, particularly the F^- anion. Addition of F^- ion (as the TBA salt) to an acetonitrile solution of **1.20** led to formation of a selective complex stabilized by H-bonding. This complexation led to a quenching of the monomer emission. However, a little change in the excimer emission was seen. Kim and colleague also synthesized the crown-6-ethered calix[4]arene compound **1.21a** bearing a N-(1-pyrenylmethyl)amide moiety. It and its analogous thiacalix[4]arene compound **1.21b** were then studied.[32] Both compounds, produced a significant fluorescence response upon the addition of Pb^{2+} selectively was seen over other cations. The Pb^{2+} cation was assumed to be bound via the two amido oxygen atoms with the aid of a crown ring. This, it was proposed, would lead to a reverse PET effect such that electrons transfer from the pyrene groups to the electron deficient amide oxygen atoms, an electron flow that results in fluorescence quenching (Figure 1.20).

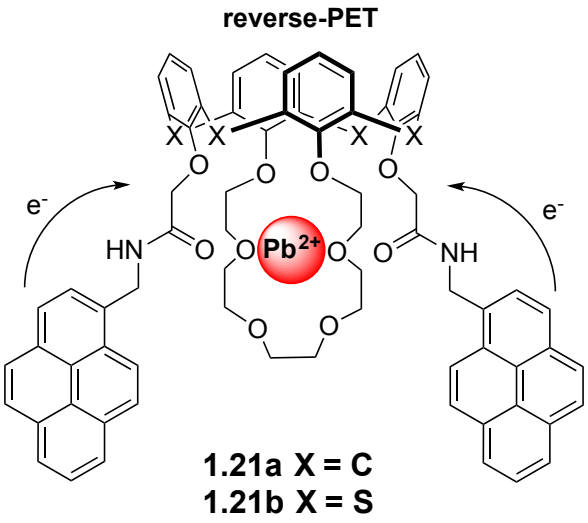

Figure 1.20: Structure of the fluorescence chemosensors **1.21a** and **b** and the proposed interactions with Pb^{2+}.

Mostly calix[4]arene-based derivatives have been designed to act as cationic receptors. However, anion recognition has been explored. For instance, Wong and Shuang demonstrated that a tetrakis-(4-carbamoylphenyl)-substituted calix[4]arene, **1.22** could be used to detect acetate ions (Figure 1.21).[33] Among various non-covalent interactions explored for anion recognition, hydrogen-bonding interactions are particularly effective for anion recognition. Some classic functional groups, including amides, ureas, thioureas and other positively charged groups have been widely used to recognize anions via hydrogen bonding interactions. On the other hand, the carbamate functionality has rarely used for this purpose. Recently, however, Wong and Shuang introduced a carbamate groups at the upper rim of a calix[4]arene to create a new class of anion receptors. They found that in their hands the carbamate functionality proved as an useful H-bond donor for the recognition of various anions, including F^-, CH_3COO^-, $PhCOO^-$, and $H_2PO_4^-$ (all studied as the Bu_4N^+ salts) in acetonitrile.

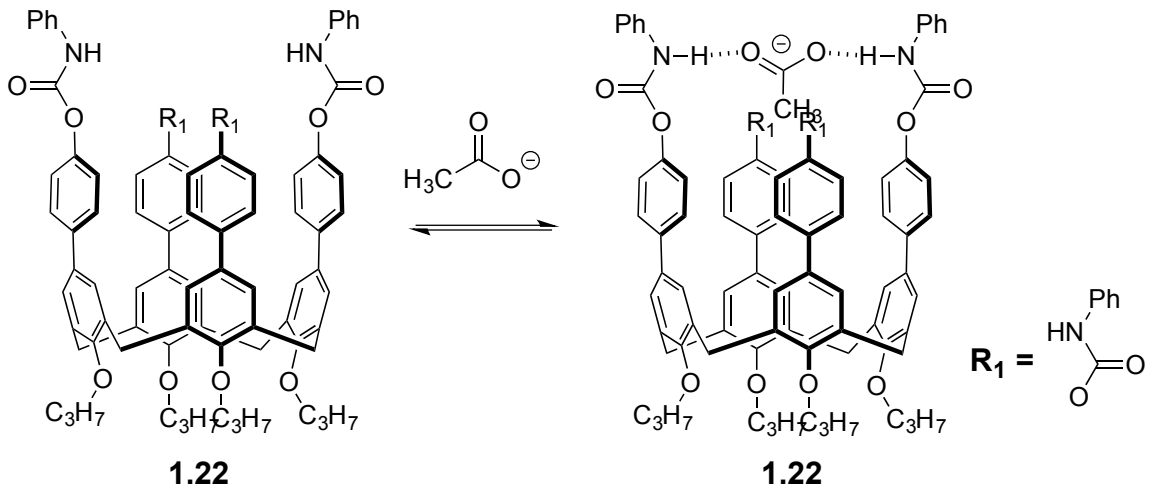

Figure 1.21: Tetrakis-(4-carbamoylphenyl)-substituted calix[4]arene, **1.22**, and its proposed interactions with the acetate anion.

1.3.2 Photo-Induced Charge Transfer Fluorescent Sensors

Sensors based on PCT are less popular and have not proved as useful as probe based on other mechanisms, such as PET or FRET. Electron excitation requires some degree of charge transfer. However, in fluorophores containing both electron withdrawing and electron donating substituents, this charge transfer may occur over a long distance. It can also be associated with major dipole moment changes. This makes it particularly sensitive to the microenvironment of the fluorophore. Therefore, it can be expected that cations or anions that are in a close interaction with either the donor or the acceptor moiety will give rise to discernable changes in the photophysical properties of the fluorophore. For instance, complexation of a cationic electron donating fluorophore will give rise to optical changes since the electron donating character of the donor will be reduced. The resulting reduction causes a blue shift in the absorption spectrum along with

a decrease in the molar absorptivity. On the other hand, metal ion binding to an acceptor group in expected to enhance its electron withdrawing character is seen. As the absorption spectrum is red-shifted and an increase in the molar absorptivity is seen. Valeur and coworkers have studied calixarene-based fluorescent sensors based on a PCT mechanism. These systems, compound **1.23** and **1.24,** possess one and four 6-acyl-2-methoxynaphthalene fluorophores at the lower rim respectively. They also contain a methoxy group as a donor and carbonyl groups that can function as acceptors in PCT processes.[34] These compounds show selectivity toward Na^+ and K^+ and are characterized by stability constant ratios of 500 for **1.23** and 407 for **1.24**, respectively in an EtOH/H_2O mixture (4:1, v/v) (Figure 1.22).

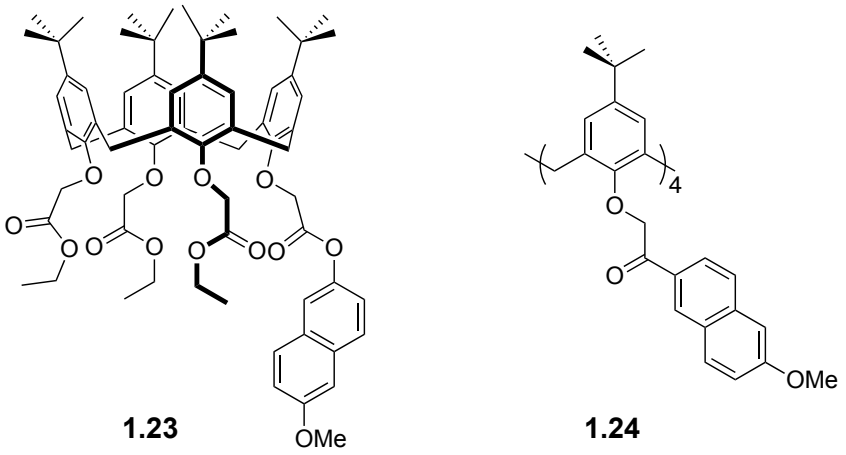

1.23 **1.24**

Figure 1.22: *p*-Tert-butyl calix[4]aren receptors **1.23** and **1.24** containing one and four methoxynaphthylene subunits respectively.

Although cation sensing via PCT mechanism has been widely exploited, there are only a handful examples of fluorogenic sensors based on calix[4]arene that function for anion recognition via a similar mechanism. Kim reported a PCT-based chemosensor bearing coumarin units, compound **1.25** and used it to detect F^- salts (Figure 1.23).[35] In this work, it was found that complexation of F^- by **1.25** caused a selective red-shift in the UV-Vis absorption and in the fluorescence emission, presumably as the result of the H-bonding between the NH-amide groups and the bound F^- anion. The proposed interaction between amide hydrogen atoms with the bound F^- promotes delocalization of the π-electrons from the anionic nitrogen atoms to the coumarin units provoking a change in the π–π interaction between the appended chromophores.

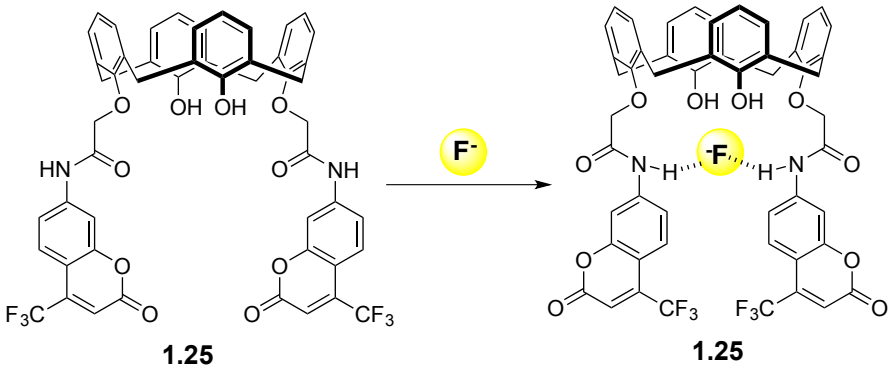

Figure 1.23: Two coumarin units attached calix[4]arene, **1.25** and its proposed interaction with the F- anion.

1.3.3 Fluorescence Resonance Electron Transfer Fluorescent Sensors

While the ability to introduce different fluorophores onto the upper and lower rims of calixarene would seem to make FRET (fluorescence resonance energy transfer) sensors an obvious target for researchers, there are very few reports in the literature. One of leaders in the area of FRET sensor research, Kim has reported several luminescence receptors based on this mechanism. As shown in Figure 1.24, Kim and his colleagues designed and synthesized a rhodamine-dansyl (energy acceptor-energy donor) fluorophore using a tren linker. This system (**1.26**) acts as a FRET sensor for the Cu^{2+} ion.[36] Upon irradiation at 420 nm, a strong emission feature was observed around 510 nm, which was ascribed to the fluorescence emitted from the dansyl donor unit. After exposure to Cu^{2+} ions were added, an emission band at approximately 580 nm is observed. This emission feature is the region of an energy acceptor (rhodamine unit). The complexation of a Cu^{2+} ion induced the opening of the spirolactam ring present in **1.26**. This leads to a shift in the absorption spectrum of rhodamine. This spectral shift leads to an enhanced overlap between the emission of the donor and the absorption of the acceptor greatly. This, in turn, leads to an increase in the extent of intramolecular FRET, allowing for the observed increase in emission from the energy acceptor unit present in compound **1.26.**

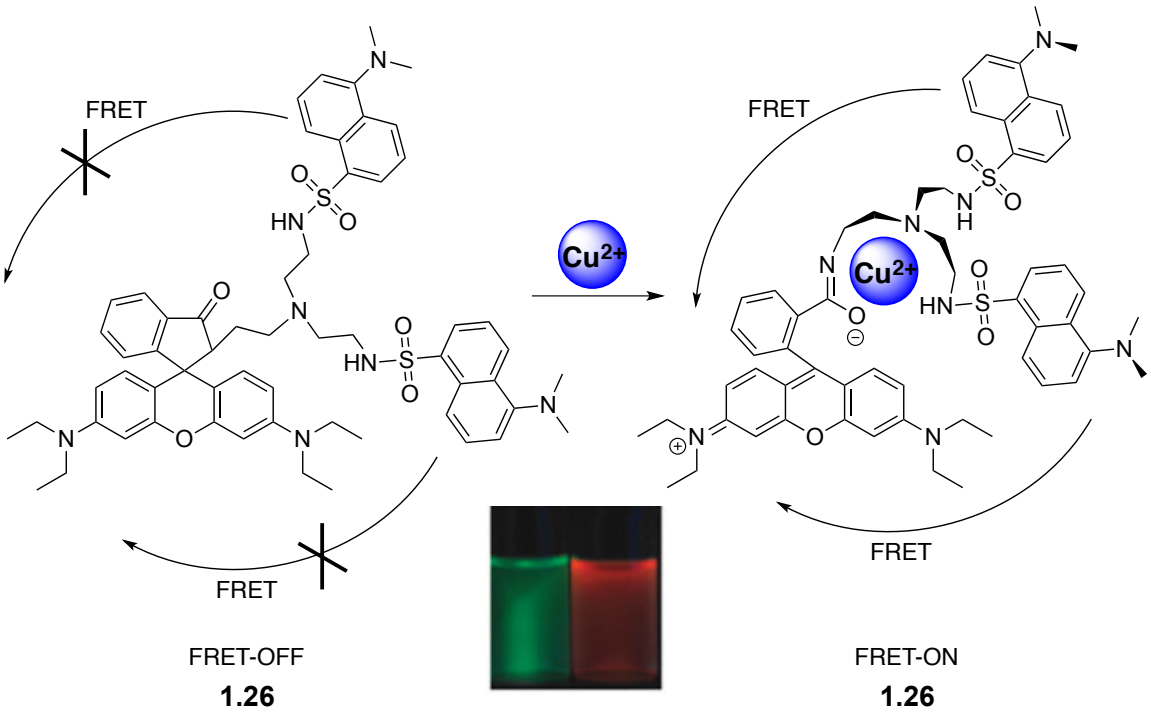

Figure 1.24: Schematic representation of the FRET OFF-On approach to Cu^{2+} sensing developed by Kim, et al. Also shown are the color changes seen upon irradiation at 420 nm. This figure was originally published in *Chem. Soc. Rev.* **2008**, 1465-1472 and reproduced with permission. Copyright The Royal Society of Chemistry.

Kim also reported several FRET receptors, namely **1.27** and **1.28**, that act as sensors for heavy metal ions such as In^{3+} and Pb^{2+}. They are based on the use of pyrene moieties as electron donors (Figure 1.25).[37, 38] It was considered that electron transfer from the pyrene units to the nitro groups leads to a partial reduction in the emission of **1.27**. Complexation of In^{3+} in acetonitrile led to a dramatic bathochromic shift in the fluorescence emission maximum from 380 nm to 507 nm. Such a finding is consistant with the In^{3+} cation being bound to the phenolate oxygens formed by deprotonation of the phenolic OH groups produced from quinone-hydrozone tautomerization. In the case of

compound **1.28**, a significant spectral overlap between the fluorescence emission band of the pyrene donor unit and the absorption band of the azophenyl accept unit was inferred. This results in a notable fluorescence quenching. Exposure to Pb^{2+} (as the perchlorate salt) in acetonitrile induced an enhancement in the pyrene emission. This increase can be rationalized in terms of reduced overlap between the donor and acceptor bands arising from the blue shift in the absorption band of the azo unit as the result of absorption by complexation. The net result is a diminished FRET effect. Compound **1.28,** a FRET-based fluorescent sensor, showed high selectivity towards the Pb^{2+} cation when tested as the perchlorate salt in acetonitrile.

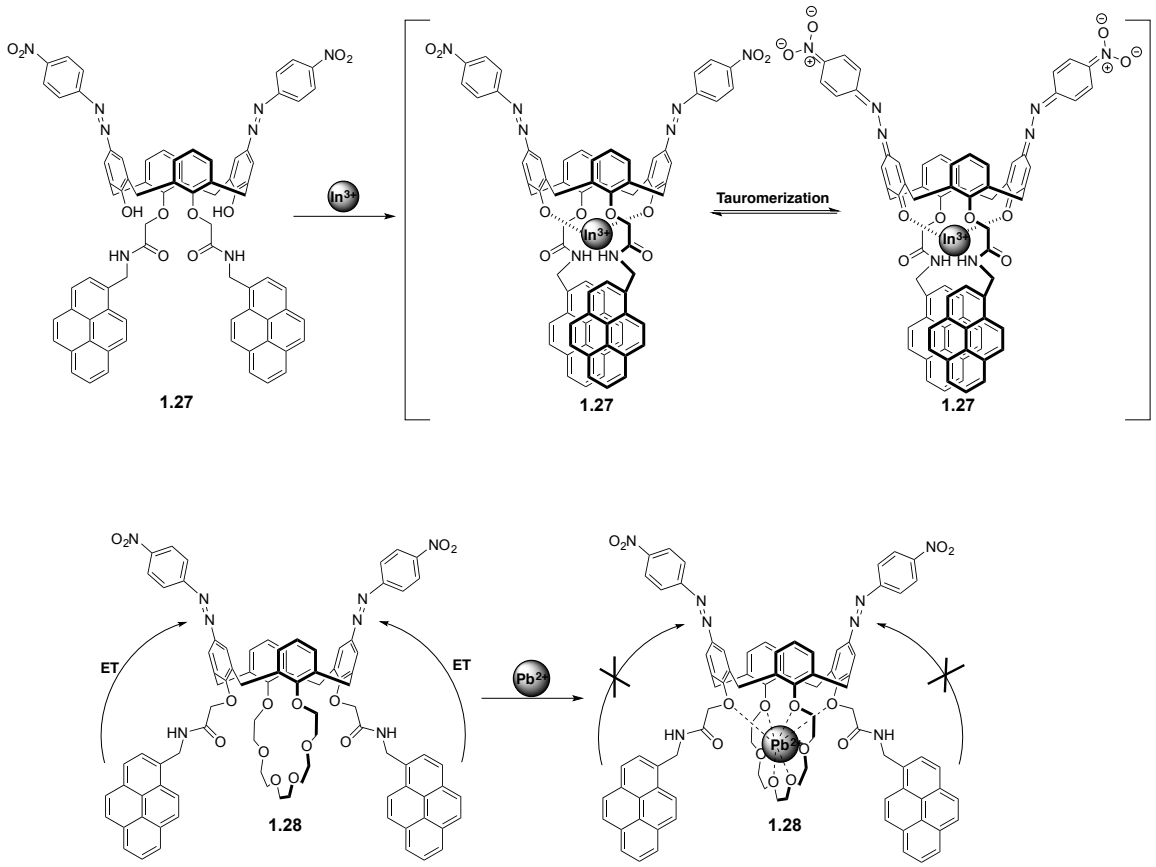

Figure 1.25: Compounds **1.27** and **1.28**.

In 2007, Vicens and Kim reported the calix[4]arene-rhodamine based chemosensor **1.29.** With this system fluorescence changes were observed in the case of only two metal cations, namely Hg^{2+} and Al^{3+}.[39] When Hg^{2+} (as the ClO_4^- salt) was added to compound **1.29** in acetonitrile, a dramatic enhancement in the fluorescence intensity was observed at 575 nm. This increase was rationalized in terms of a FRET-ON process involving the pyrene units and the rhodamine moiety that accompanies ring-opening with excitation at 343 nm, as illustrated schematically in Figure 1.26. Different behavior was seen for **1.29** when bound to Al^{3+}. Specifically, the addition of Al^{3+} gave rise to strong emission feature characteristics of a pyrene excimer. A weak rhodamine emission at 575 nm was also seen, leading to the conclusion that Al^{3+} did not induce ring-opening of the spirolactam on the basis two different metal-bound structures were inferred for **1.29**. Mercury ion, the metal ion interacts with the tren-spirolactam unit leading to ring-opening of the rhodamine to produce a FRET-ON signal. However, Al^{3+} complexes with the tren-diamide unit and it do induce ring-opening.

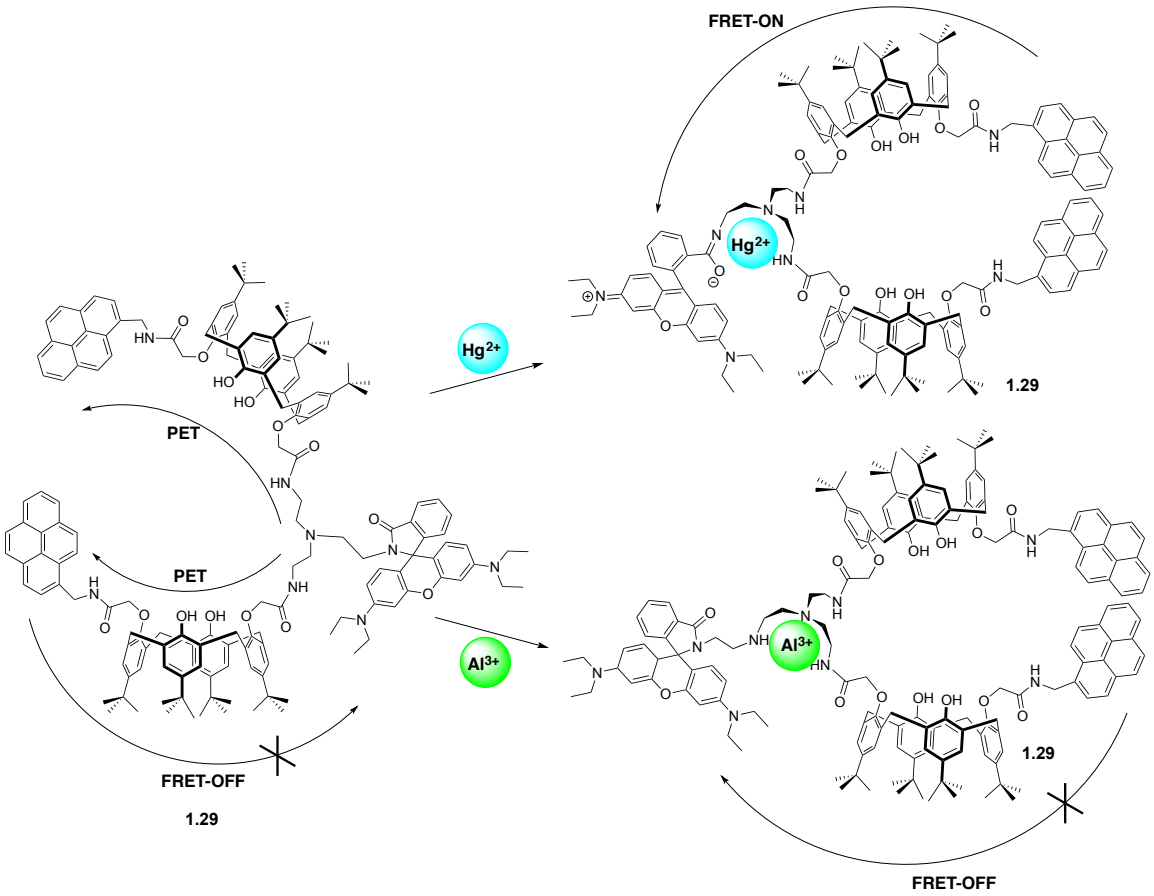

Figure 1.26: Differing complexation pathways for compound **1.29** proposed to be operational in the case of Hg^{2+} and Al^{3+}.

1.3.4 Excimer Sensors

Calixarene sensors based on excimer effects appear to be limited to compounds that have well-known fluorescent pyrenyl moieties. Moreover, almost every example reported to date has the fluorophores attached to the lower rim of a calix[4]arene core. A fluorescent unit, pyrene is considered as one of the most the useful because it may emit as a monomer around at 375 nm (I_m) or as an excimer at 480 nm (I_E), and these two emission processes are clearly distinguishable.[40]

Compound **1.30** (Figure 1.27) is one of the first calixarenes to be reported that showed excimer formation. This system prepared by Koyama proved to be a good chemosensor for the Na^+ ion (studied as the SCN salt) in chloroform.[41] In **1.30**, *p*-t-butylcalix[4]arene core is bound to the lower of a ester linkages. Ethyl ester substituents are focus on the other aromatic subunit. The two pyrene units are close enough to support excimer formation. The fluorescence spectrum of **1.30** is characterized by a dual emission, with that of the excimer seen at 480 nm and that of the monomer at 390 nm. In the absence of Na^+, the excimer emission dominates: The intensity ratio of excimer to monomer emission is about 4. When a Na^+ cation is bound to the **1.30**, the I_E:I_M ratio is altered, presumably reflecting a change in the relative configuration of the two pyrene moieties. That is induced by the reorientation of the four carbonyl groups of **1.30** to bind the Na^+ ion. Examination of Corey-Pauling-Koltun molecular model led the authors to suggest that the distance between the two pyrene moieties increases upon Na^+ ion complexation. When other alkali metals, such as Li^+, K^+, Cs^+ and Rb^+ were tested, relatively small changes in the ratio was seen, leading to the conclusion that **1.30** may be useful for the selective sensing of the Na^+ cation.

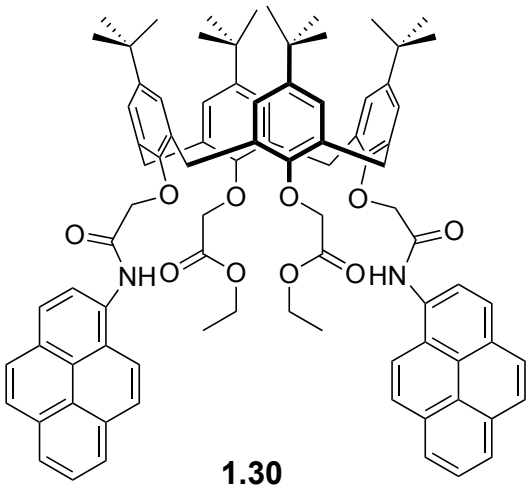

1.30

Figure 1.27: Compound **1.30**.

In 1996, Matsumoto and Shinkai reported a calix[4]arene derivative **1.31**, which possesses an ionophoric cavity at the lower rim and two pyrene units on the upper rim and showed that it can be used for the fluorescence sensing of Li^+ and Na^+ (as the perchlorate salt in CH_3CN: THF = 1000:1 (v/v)) (Figure 1.28).[42] Complexation of Li^+ and Na^+ into the ionophoric cavity induces a change in distance between the two pyrene units, which is reflected in a change in the I_E:I_M ratio. The addition of up to a 250-fold excess of K^+ did not affect significantly the fluorescence spectrum of the preformed complexes 1.31•Na^+ or 1.31•Li^+.

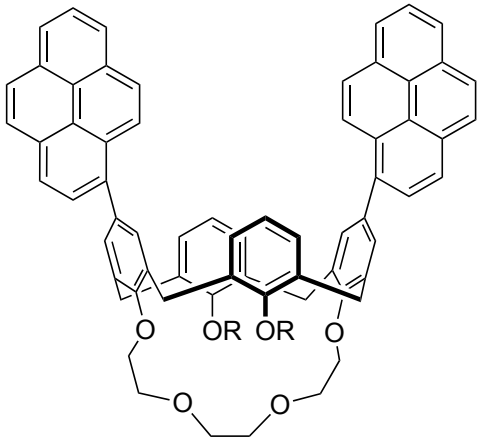

1.31

Figure 1.28: Compound **1.31**.

Reinhoudt et al. prepared compounds **1.32** and **1.33** with two substituents attached to a distal calix[4]arene via amide linkages as shown in Figure 1.29.[43] Monomer emission of compound **1.32** was observed at λ_{max} 385 nm and 395 nm along with a broad excimer

emission feature centered around at 480 nm. The addition of Na^+ in methanol to a monolayer of **1.33** immobilized on a silicon surface led to a decrease in the monomer emission and an increase in the eximer emission. Presumably, the distance between the two pyrenyl groups is reduced upon Na^+ cation omplexation. This finding was taken as evidence that an immobilized receptor could prove useful as a fluorescence-based metal ion sensor.

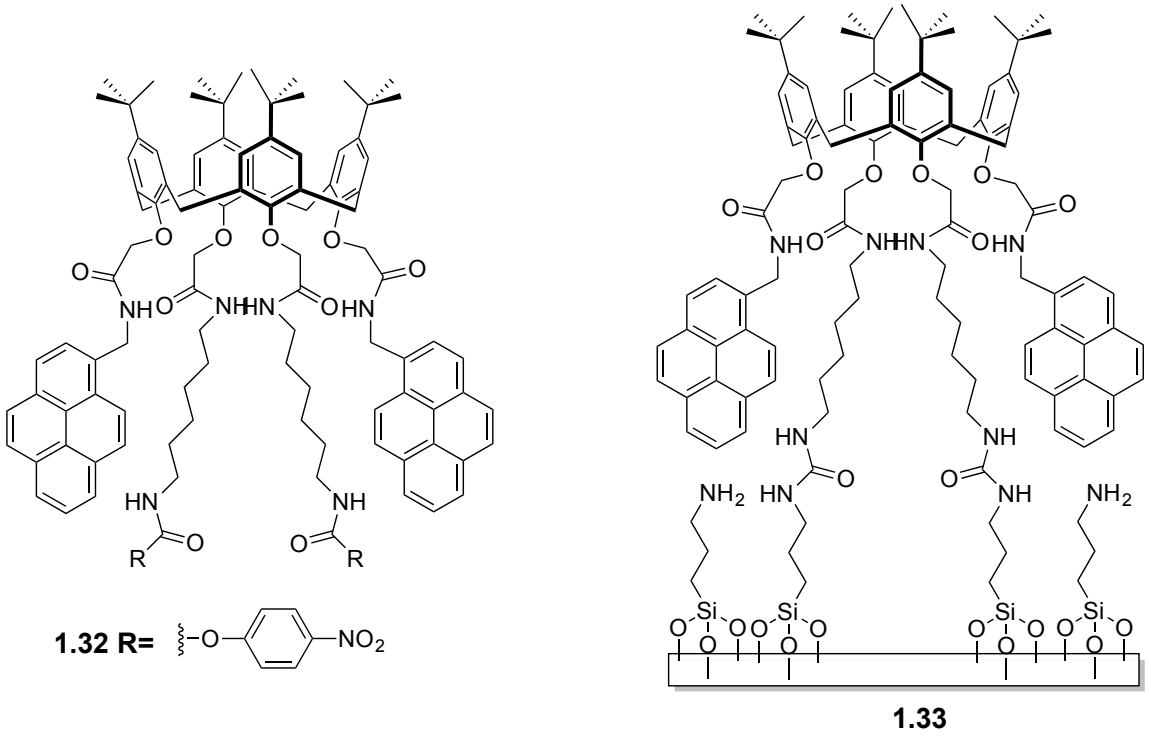

Figure 1.29: Compounds **1.32** and **1.33**.

In 2005, Kim and coworkers reported two fluorescent calix[4]arenes (**1.34** and **1.35**) that contain a pair of amide-linked pyrene units as shown in Figure 1.30. Even though these two molecules are ostensibly similar, they show very distinct emission fluorescent properties.[44] Whereas the bis-phenyl system **1.34** exhibits only monomer emission at 398 nm, its ester functionalized analogue **1.35** shows a strong excimer emission. It is assumed that the two pyrene units are in close proximity as the result of π–π stacking in the case of **1.35** but not in the case of **1.34**. This difference is rationalized interms of intramolecular H-bonding being possible in **1.34,** but not in **1.35**. A X-ray crystal structure of **1.34** supported this hypothesis (Figure 1.31). It revealed that the pyrenyl substituents diverge and are thus too remote for excimer formation.

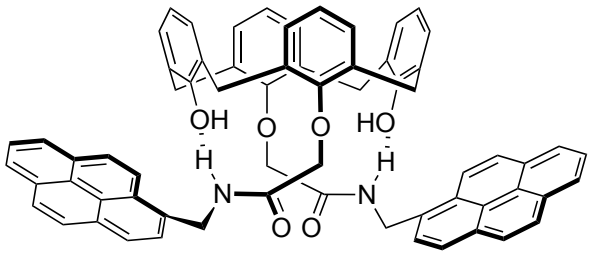

1.34

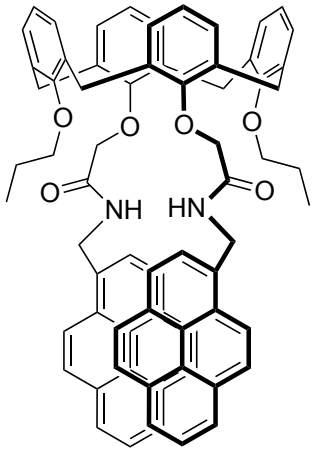

1.35

Figure 1.30: Compounds **1.34** and **1.35**

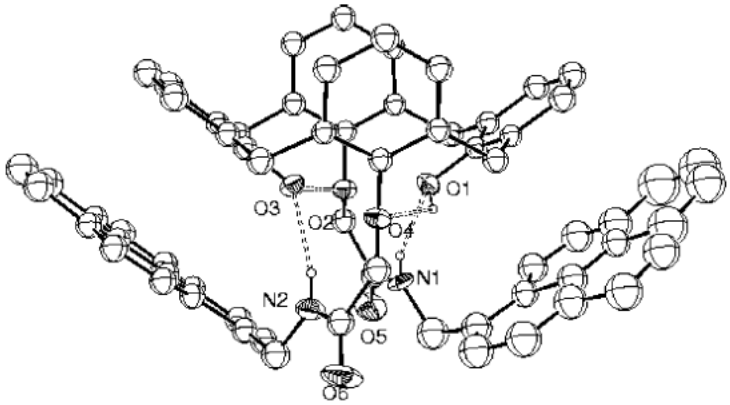

Figure 1.31: X-ray crystal structure of compound **1.34** with hydrogen bonds represented by dotted bonds. This figure was originally published in *Inorg. Chem.* **2005**, 7866-7875. Reproduced with permission. Copyright American Chemical Society.

The addition of In^{3+} (as its ClO_4^- salt) to **1.34** in CH_3CN led to an enhancement in the excimer emission and quenching of the monomer emission. This finding was explained in terms of In^{3+}-induced deprotonation of the phenolic OH groups, which leads to the elimination of the hydrogen bonding interaction between the phenolic OH groups and the amide groups. In contrast, upon the addition of In^{3+} to an acetonitrile solution of **1.35**, the excimer emission is quenched. This is rationalized in terms of a conformational change in the initially divergent amide carbonyl oxygen atoms that occurs when the ion is bound. These structural changes preclude the face-to-face π-stacking of the two pyrenes.

In 2006, Kim and Ham reported a tetrahomodioxacalix[4]arene pyrenylamide **1.36** which displayed Pb^{2+} selective sensing characteristics (Figure 1.29).[45] In the case of compound **1.36**, neither monomer nor excimer emission features were observed upon addition of Pb^{2+} (as perchlorate salts) in chroroform:acetonitrile (1:3, v/v). It appears that

1:1 coordination evidenced by Job plot experiment of Pb^{2+} (Figure 1.32) resulting in a conformational change, which set at least two of the pyrene groups well apart.

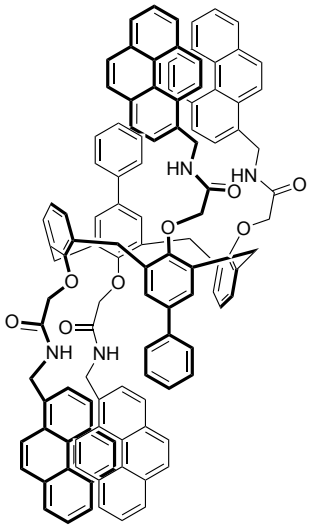

1.36

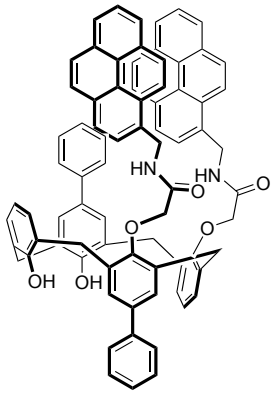

1.37

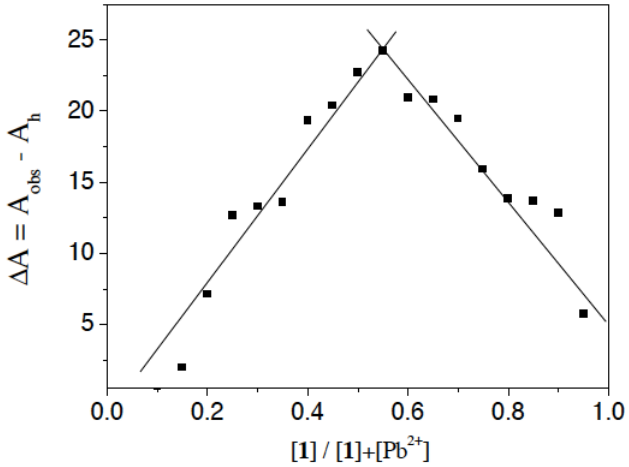

Figure 1.32: Compounds **1.36** and **1.37**. Job plot of **1.36** with Pb^{2+} in $CHCl_3/CH_3CN$ (1:3, v/v). $\Delta A = A_{obs}-A_h$, where A_{obs} and A_h denote the absorbance at 375 nm upon metal ion and **1.36**, respectively. This figure was originally published in *Org. Lett.* **2006**, 1601-1604. Reproduced with permission. Copyright American Chemical Society.

A more significant effect of Pb^{2+} addition is seen with **1.37**. Here, binding to the amide carbonyl oxygen donors to form a 1:1 complex inevitably eliminates any possibility of excimer formation. However, when Ca^{2+} ion was added to a chroroform:acetonitrile (1:3, v/v) of compound **1.37**, an increase in the excimer emission and a concomitant decrease in monomer emission was seen. These differing fluorescence response phenomena can be interpreted in terms of different coordination modes in the case of Ca^{2+} and Pb^{2+}. Figure 1.33 shows the result of computational geometry optimizations of **1.37** after in the form of its Ca^{2+} and Pb^{2+} complexes, respectively. In the case of Ca^{2+}, a chelate complex involving both the phenolic donors and the amide oxygen atoms is stabilized. This serves to bring the two pyrene units into closer proximity.

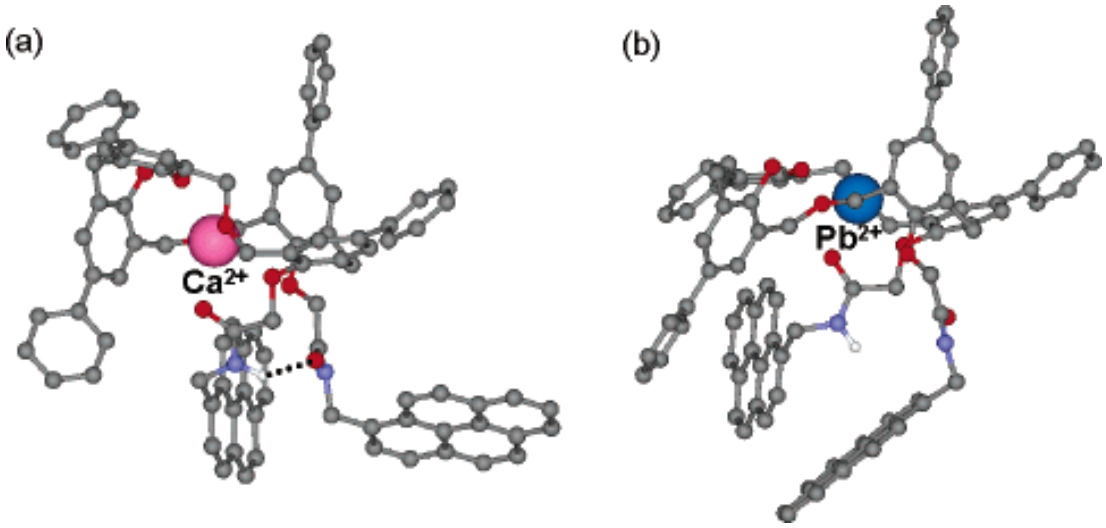

Figure 1.33: Calculated geometries for (a) **1.37•**Ca^{2+} and **(b) 1.37•**Pb^{2+}**.** Hydrogen atoms are omitted for clarity, except the hydrogen involved in NH•••OC bonding interaction. In the **1.37•**Ca^{2+} complex, the hydrogen bonding interaction between the amides in shown in the dotted line. Oxygen atoms are shown in red; nitrogen atoms are in blue. This figure was originally published in *Org. Lett*. **2006**, 1601-1604. Reproduced with permission. Copyright American Chemical Society.

As mentioned above, most works involving fluorescent calix[4]arene sensors has focused on metal ions detection. Recently, however, the interest fluoregenic anion sensors have emerged. Calixarene-based anion sensors include those where H-bonding donor groups serve as the anion recognition sites. For example, a 1,3-alternate calix[4]arene bearing two pyrenylurea units (**1.38)** was studied as an anion sensor. In the absence of anions, this system displayed a monomer emission at 398 nm and much broader (intramolecular) excimer emission at 452 nm upon photoexcitation.[46] Four urea groups, providing eight hydrogen bonds for anion bonding, are in close proximity to pyrene units. The relative orientation of these urea groups is thought to change upon

anion complexation, as seen in Figure 1.34. Of the anions tested, Cl^- anion (as its TBA salt) produced the greatest change in the emission spectrum of compound **1.38** in solvent of acetonitrile: chloroform (95:5). A strong quenching of the excimer emission was observed concurrent with an with an enhancement in the monomer emission.

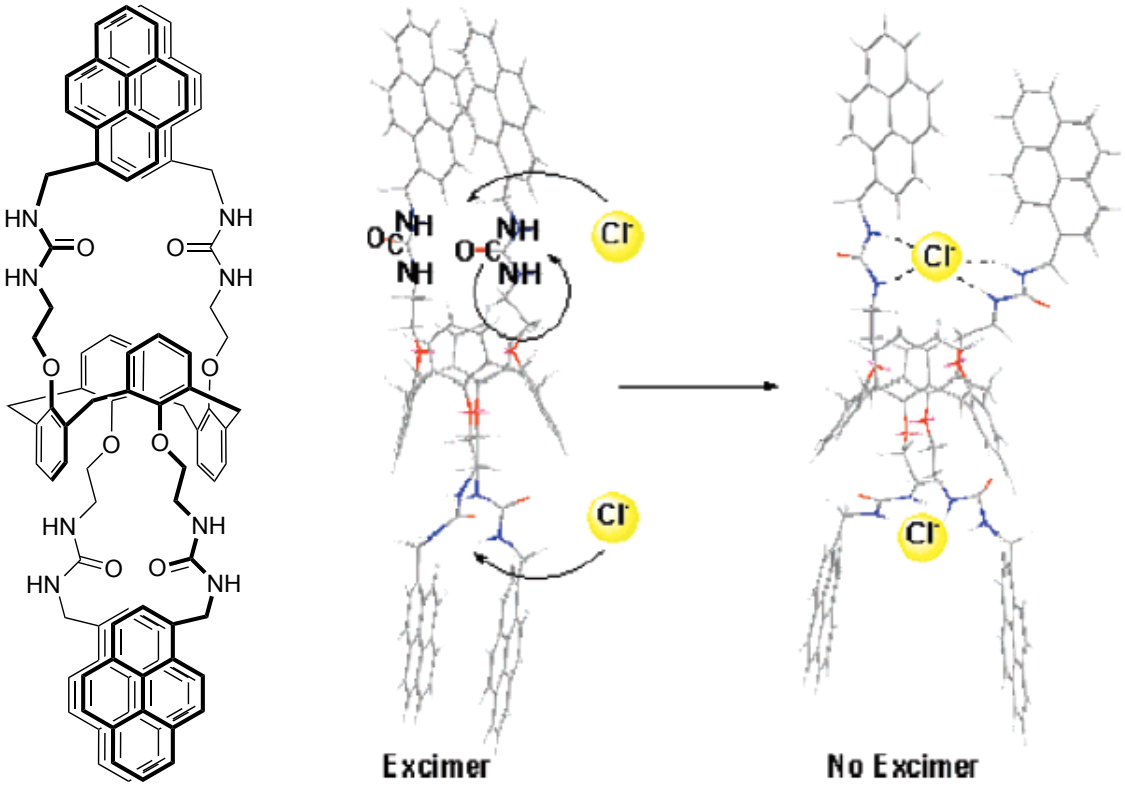

Figure 1.34: Compound **1.38** and binding of Cl^- ions by **1.38**. Quenching of excimer emission (452 nm) caused by perturbation of the pyrene π–π interaction by the conformational 'unstacking' of pyrene moieties. This was published originally in *J. Am. Chem. Soc.* **2006**, 8607-8614. Reproduced with permission. Copyright American Chemical Society.

In 2006, Kim et al. reported that calix[4]arenes bearing (4-nitrophenyl)azo and pyrene groups displayed selectivity and sensitivity for F^- when excited at 343 nm.[47] Upon the addtion of F^- ion (as its TBA salt) in acetonitrile to compound **1.39**, the eximer emission (480 nm) seen in its absence is quenched while new emission bands at 385 nm and 460 nm appear. These changes can be ascribed to formation of a static pyrene dimer in the ground state. That results from the hydrogen bonding interaction between the F^- ion and the amide protons (Figure 1.35).

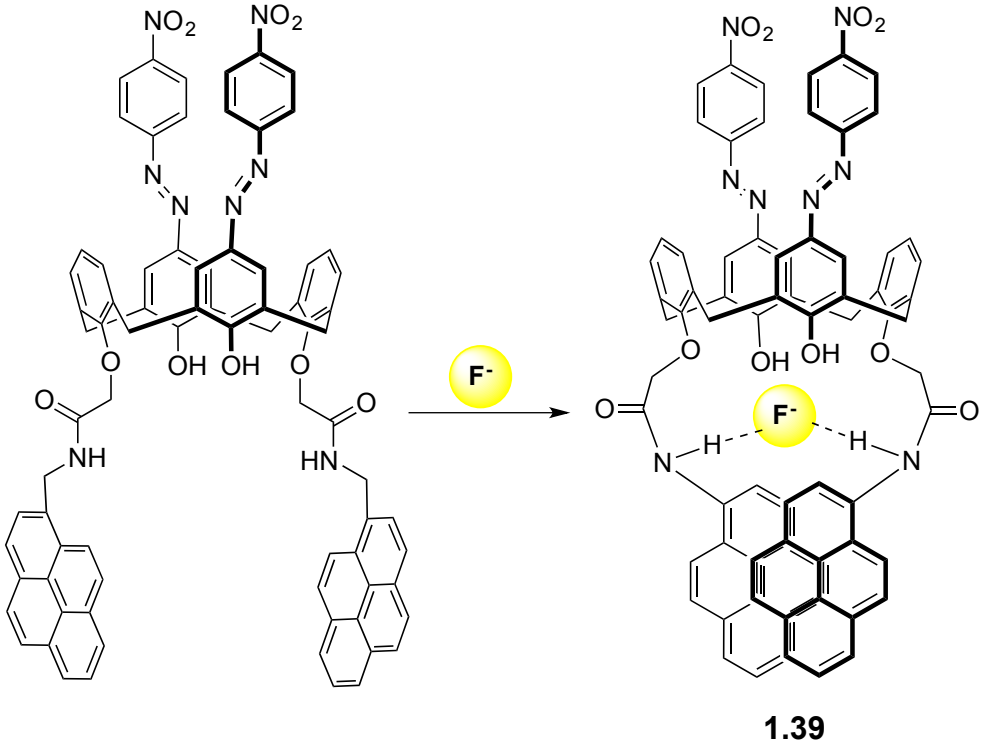

Figure 1.35: Structure of the pyrene- and (4-nitrophenyl)azo appended calix[4]arene **1.39**.

Various efforts have been made to develop sensors for nonmetallic cations. Among the first reports was that of Takeshida and Shinkai.[48] In 1994, they described the calix[6]arene and calix[3]arene derivatives **1.40** and **1.41** that can recognize guanidinium ions selectively through fluorescence changes (Figure 1.36). In the absence of a guest, compound **1.40** shows monomer and excimer emission features at 396 nm and 487 nm in chloroform/THF (4:1. v/v) solvent, respectively. As the concentration of added guanidinium ion (TBA salt) increases, the excimer emission intensity decreases while that of monomer emission increases. It was suggested that the intramolecular interaction between two pyrenes is prevented by complexation of a guanidinium ion within the ester-rich calixarene cavity. Notably, the fluorescence changes seen with the guanidinium ion are not produced upon exposure to other organic cations, including the *t*-butyl ammonium, protonated L-alanine methyl ester, or *n*-hexylammonium ions. In the case of compound **1.41**, an ability to bind the guanidinium ion was also inferred on the bases of the induced changes in the fluorescence characteristics. However, in this case competitive binding by primary ammonium ions was observed.

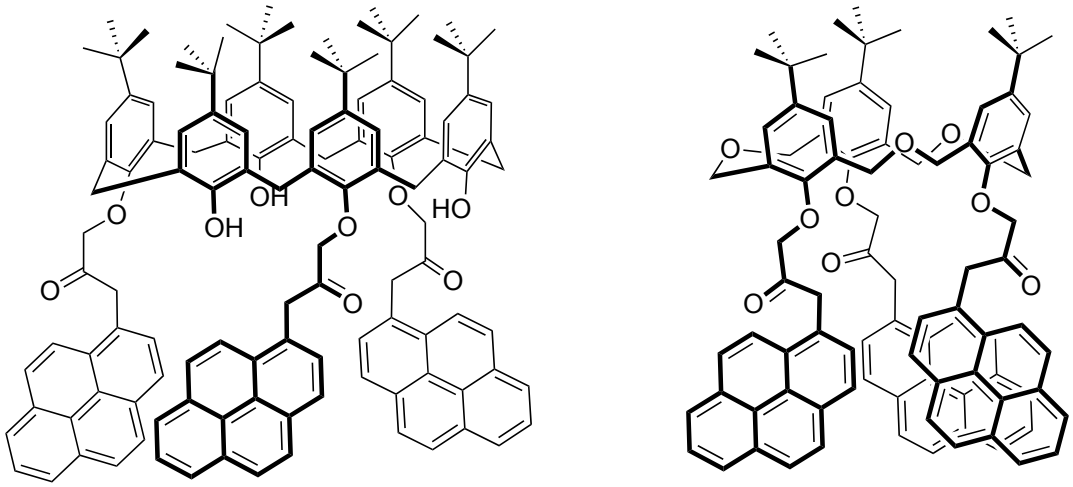

1.40 **1.41**

Figure 1.36: Guanidium ion selective calix[4]arene derivatives **1.40** and **1.41**.

1.4 CROWN ETHER STRAPPED CALIX[4]ARENE-BASED FLUORESCENT CESIUM ION SENSORS

There is significant need for the development of cesium ion selective sensors. Major environment threat is the cesium in nuclear waste materials from reactor failure, such as that occurring at the Daiichi nuclear plant in March of 2011. A key goal is detect the cesium cation where other salts are present with large excess. In order to achieve good cesium cation selectivity, the design of the core recognition unit is of importance. In this respect, 1,3-alternate crown-6-ether strapped calix[4]arenes are attractive because the parent member of this receptor series exhibits remarkable selectivity towards the cesium ion over other alkali metals.[49]

The first crown strapped calix[4]arene, based on a penta-ethylene glycol linker, was developed by Ungaro and coworkers in 1983.[50] Specifically, this team prepared a set of crown-6-ether strapped calix[4]arenes, **1.42a-d** (Figure 1.37) and found that their cation binding affinities were determined by the number of oxygen atoms in the polyethylene glycol subunits, as well as by the conformation of the calix[4]arene skeleton.[51]

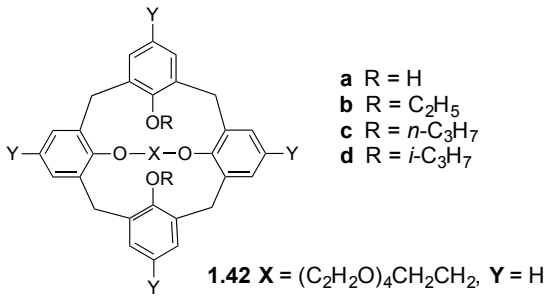

Figure 1.37: Schematic representation of 1,3-alternate crown-6-ether strapped calix[4]arene derivatives, **1.42a-d**.

As shown in Table 1.2, receptors **1.42a-d** proved to be effective the cesium cation receptors with especially high Cs^+/Na^+ selectivity when studied in chloroform. Among the series **1.42**, the cone conformation of **1.42d** is more exposed to the chloroform solvent compared to the 1,3-alternate **1.42d** isomer. Moreover, in this conformation, the butyl isopropyl site serves to limit access of the cesium ion to the binding which accounts for the low binding affinity.

Ligand	Conformation	Cs^+	Na^+
1.42a	mobile	6.0	4.3
1.42c	1,3-alt.	8.6	5.1
1.42d	1.3-alt.	8.8	5.2
1.42d	cone	<4	<4

Table 1.2: Association constants (log K_a) of compounds **1.42a,c** and **d** for cesium and sodium picrate salts in chloroform.

A crystal structure of the cesium picrate complex of the 1,3-alternate system, **1.42d,** revealed that the cesium cation is coordinated to all six oxygen atoms provided by the hexa-ethylene glycol and to the two phenyl moieties (Figure 1.38). These finding were taken as support of the notion that in this system, the crown-6-ether calix[4]arene is highly preorganized. Moreover, this conformation allows for favorable cation-π interactions between the bound Cs^+ cation and the two aromatic walls.

To date, numerous approaches have been pursued successfully to creat cesium ion recognition receptors based on the basic crown ether strapped calix[4]arene approach. However, few of these act as effective sensors under the conditions that might make them

attractive for use in the field. In this chapter, different examples of fluoregenic crown ether strapped calix[4]arene-based Cs^+ ion sensors are reviewed. In chapter 2, our own efforts to address this need will be described.

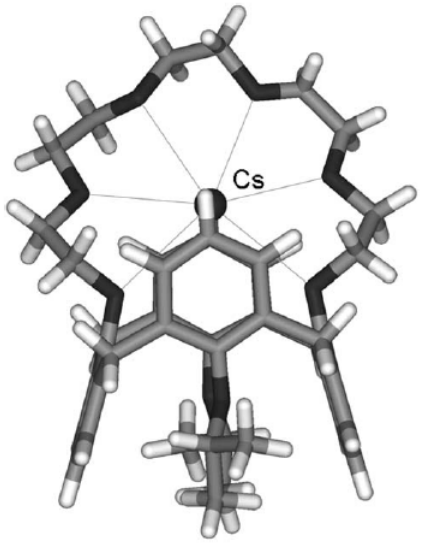

Figure 1.38: Crystal structure of the complex **1.42d•**CsPic in the 1,3-alternate conformation (the picrate counter ion has been omitted for clarity). This figure was originally published in *J. Am. Chem. Soc.* **1995**, *117*, 2767-2777. Reproduced with permission. Copyright American Chemical Society.

In Chapter 1.3.1 section, several fluoregenic crown-6-ether strapped calix[4]arene sensors (**1.13**-**1.16**) for the cesium ion were mentioned as examples of systems whose sensing function relied on photo-induced electron transfer (PET) processes. In the present section, various functional groups that may be attached as fluorophores to the crown ether-linked calix[4]arene derivatives will be described. One of important examples of this class of sensor was reported by Dabestani and coworkers. These researchers synthesized **1.43** and showed that it can detect either the K^+ ion or Cs^+ ion (ClO_4^-,

counterion) by control of pH (Figure 1.39).[52] Under basic conditios in methanol, fluorescence enhancement was observed upon complexation of the K^+ ion because of a PET process involving the azacrown ether (donor) to the anthracene fluorophore (acceptor). In contrast, in acidic medium, the complexation of the Cs^+ ion results in a 3.8-fold enhancement of the fluorescence because of a PET process from the dialkoxybenzene subunits to the fluorophore. Protonation of the amine changes the energetics of the fluorophore. This allows the dialkoxy benzene to quench the fluorescence. This emission is unchanged upon addition of the K^+ ions because of the low affinity of the crown ether ring of **1.43** for the K^+ ion.

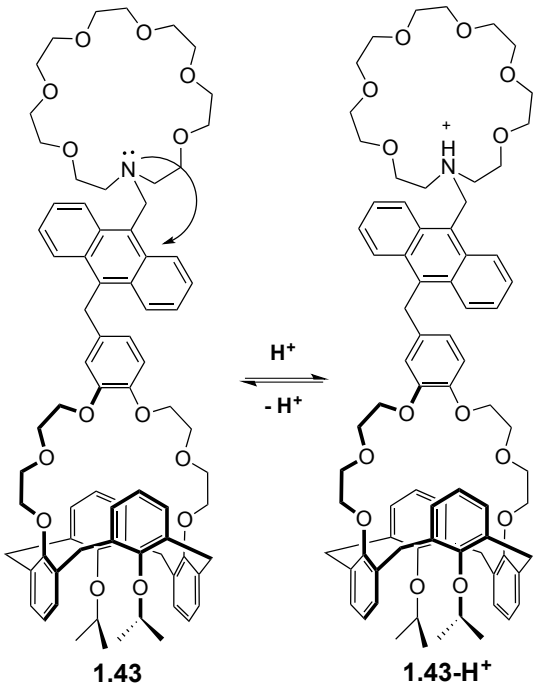

Figure 1.39: Molecular structures of **1.43** and **1.43**-H^+ and schematic representation of how they can function via pH modulation.

Compounds **1.44a** and **b** are composed of bis-crown-6-ether linked calix[4]arenes in which a dioxycoumarin subunit is incorporated into each crown ring.[53] In receptor **1.44a**, a PCT process occurs between the two oxygen atoms linked to the phenyl part of coumarin and the lactone carbonyl group. Association constants were obtained from fluorescence spectral titrations involving by addition of cesium acetate in ethanol. This gave log K_{11} and log K_{21} of 6.68 and 3.81, respectively. With a view towards of practical applications, water soluble receptor, **1.44b**, that is an analogue of **1.44a,** was synthesized. This was done by appending four sulfonyl groups onto the calix[4]arene core (Figure 1.40). Receptor **1.44b** is highly fluorescent and its emission spectrum was found to be are independent of pH (in the pH 6-9 range). Upon addition of the Cs^+ ion (acetate salt) to a solution of **1.44b** in MES-NaOH buffer pH 7, a 10 nm bathochromic shift in the UV-vis spectral maximum and an enhancement in the fluorescence intensity was observed. The Cs^+-induced enhancement in the fluorescence intensity was rationalized in term of the coumarin itself being poorly fluorescent. However, the introduction of electron-donating methoxy groups at the 6- and 7-positions led to substantial fluorescence intensity. This increase in intensity is ascribed to intramolecular charge transfer from these methoxy groups to the lactone carbonyl group. In **1.44a**, the fluorescence intensity was reduced upon the complexation of the cesium ion. This was ascribed to a reduction in the electron-donating groups of the oxygen atoms linked to the coumarin phenyl moieties. In contrary, in the cesium cation complex of **1.44b**, the electron-donating character is reinforced by the negative charges of sulfonate groups appearing in the vicinity of the oxygen atoms. This, it was proposed, should lead of fluorescence intensity seen by experiment.

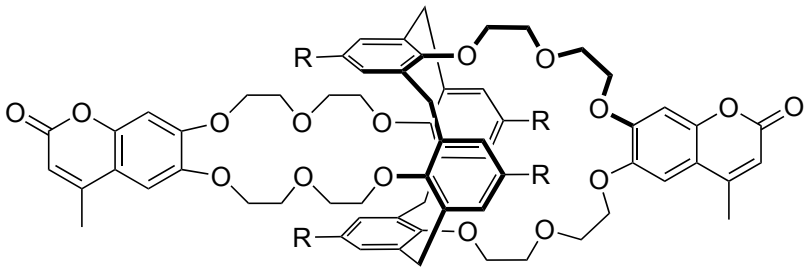

1.44a R = H
1.44b R = SO_3^-

Figure 1.40: Molecular structures of **1.44a** and **1.44b**

Compound **1.45** contains a calix[4]arene bearing one 2,3-naphthocrown-6-ether and two coumarin amide subunits at the lower rim in a partial-cone conformation as shown in Figure 1.41.[54] This compound showed a high selectivity for the cesium ion over other metal cations when studied in. It is known that cesium ion (using the perchlorate salt) encapsulation is favorable with a crown-6-ether strapped calix[4]arene ring because of size complementary. An enhancement of the coumarin-based emission is observed upon the addition of the cesium ion. This finding was ascribed to the inhibition of a PET process as involving the oxygen atoms bound to naphthalene group in acetonitrile solvent. In contrast, addition of the cesium ion to the receptor **1.45** provided an enhanced level of FRET because of the more effective spectral overlap (FRET) between the donor emission (naphthalene) and the acceptor absorption (coumarin).

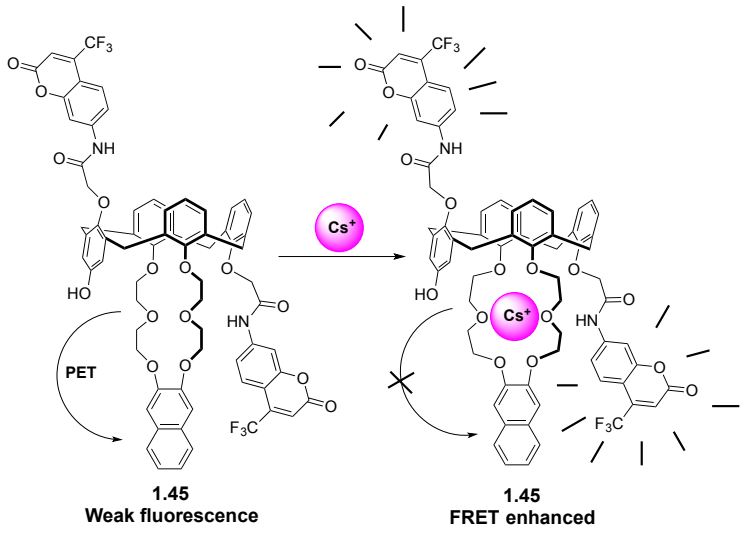

Figure 1.41: Cesium ion complexation mechanism believed to be operative in the case of the calix[4]arene derivative, **1.45**. beaing 2,3-naphtocrown-6-ether and two coumarin amide fluorophores.

1.5 CONCLUSION

Calixarenes, with their robust and preorganized structures, have been explored extensively as chemical sensors. Much of the untility derives from the ease with which various functional groups can be added on synthetically to a well-studied core. Analytes can be bound within the macrocyclic cavity itself or by substituents appended at either the upper or lower rim. In this chapter, multiple sensing methods were described. They were catagorized based upon the underlying mechanism of action and the means of detection. Among these methods, the most convenient method involves simple monitoring of analyte-induced color change. However, a limitation of such systems is that the intensity of the response needs to be intense enough to be observable, even at a low analyte concentration. Calixarene-based sensors that incorporate fluoregenic signaling groups on the upper or lower rim are as a general rule, more sensitive. In fact, of the sensors described in this chapter, the greatest sensitivity is observed for the fluorescent sensor systems, in particular those that function through excimer or PET mechanisms.

Although chromogenic and fluoregenic calixarene sensors are effective in many instances, there are still a few drawbacks. First, as with all chemical sensors, the main problem is the selectivity of the sensor for the analyte. In many cases, the binding sites of various calixarene-based sensors were elaborately designed to target a specific analyte. Nevertheless, interference from ostensibly a similar species is often observed. Other problems can come from the targeted anions themselves. This is particularly true for F^-, which can either bind to receptors or deprotonate them, as the specific chemistry dictates. Additionally, there are only a handful of water-soluble calixarene receptors that permit sensing to be carried out effectively in aqueous media. Therefore, the development of

new highly selective sensing systems that address some or all of these shortcomings remains as an important challenge.

In Chapter 1, an effort has been made to classify the various known calix[4]arene-based colorimetric and fluoregenic ion receptors. While a summary introduction of this nature cannot encompass all advancements, a strong attempt has been made to describe the advantages of chromogenic and fluoregenic receptors for anions and cations. As the present summary serves to underscore, cesium sensing systems have attracted relatively little attention as compared to other small ion targets. The lack of success in cesium sensing achieved to date could reflect, probably this is due to synthetic difficulties, as well as experimental limits to function as a result of the binding phenomena involved. Against this background of perceived need, the candidate sought to prepare new cesium receptors. That could allow for sensing via colorimetric or electrical means. As part of this effort, a colorimetric anion receptor, namely an amidoindole-based calix[4]arene, was developed. This work is described in the ensuing chapters.

1.6 REFERENCE

1) von Baeyer, A. Ber. Dtsch. Chem. Ges., 1872, 5, 25-26.

2) Iqbal, M.; Mangiafico, T.; Gusche, C. D. *Tetrahedron* **1987**, *43*, 4917-4930.

3) Chawla, H. M.; Singh, S. P.; Upreti, S. *Tetrahedron,* **2006**, *62*, 7854-7865. (b) Kim, J. Y.; Kim, G.; Kim, C. R.; Lee, J. H.; Kim, J. S. *J. Org. Chem.* **2003**, *68*, 1933-1937. (c) Ludwig, R. *Fresenius J. Anal. Chem.* **2000**, *367*, 103-128. (d) Chawla, H. M.; Srinivas, K.; Meena. *Tetrahedron* **1995**, *51*, 2709-2718.

4) McCarrick, M.; Wu, B.; Harris, S. J.; Diamond, D.; Barret, G.; Mckervey, M. A. *J. Chem. Soc. Chem. Commun.* **1992**, 1287-1289.

5) Gutsche, C. D. *Calixarenes*, The Royal Society of Chemistry, Cambridge, UK, **1989**, Vol 1.

6) Kubo, Y.; Hanaguchi, S, -I.; Kotani, K.; Yoshida, K. J. *Tetrahedron Lett.* **1991**, *32*, 7419-7420.

7) Kubo, Y.; Hamaguchi, S. -I.; Niimi, A.; Yoshida, K.; Tokita, S. *J. Chem. Soc. Chem. Commun.* **1993**, 305-307.

8) Chang, K. -C.; Su, I, -H.; Lee, G. -H.; Chung, W. -S. *Tetrahedron Lett.* **2007**, 7274-7278.

9) Kao, T. –L.; Wang, C. –C.; Pan, Y. –T.; Shiao, Y. –J.; Yen, J. –Y.; Shu, C. –M.; Lee, G. –H.; Peng, S. –M.; Chung, W. –S. *J. Org. Chem.* **2005**, *70*, 2912-2920.

10) Ho, I. –T.; Lee, G. –H.; Chung, W. –S. *J. Org. Chem.* **2007**, *27*, 2434-2442.

11) Liang, Z.; Liu, Z.; Gao, Y. *Tetrahedron Lett.* **2007**, *48*, 3587-3590.

12) Kubo, K.; Maeda, S.; Nakamura, M.; Tokita, S. J. *Chem. Soc. Chem. Commun.* **1994**, 1725-1726.

13) Quinlan, E.; Matthews, S. E.; Gunnlaugsson, T. *Tetrahedron Lett.* **2006**, *47*, 9333-9338.

14) Quinlan, E.; Matthews, S. E.; Gunnlaugsson, T. *J. Org. Chem.* **2007**, *72*, 7497-7503.

15) Kubo, E.; Maeda, S.; Tokita, S.; Kubo, Y. *Nature* **1996**, *382*, 522-524.

16) McCarrick, M., Harris, S. J.; Diamond, D. *J. Mat. Chem.* **1994**, *4*, 217-221.

17) (a) Hines, J. H.; Wanigasekara, E.; Rudkevich, D. M.; Rogers, R. D. *J. Mat. Chem.* **2008**, *18*, 4050-4055. (b) Ohira, S. –I.; Wanigasekara, E.; Rudkevich, D. M.; Dasgupta, P. K. *Talanta* **2008**, *77*, 1814-1820.

18) (a) de Silva, A. P.; Gunaratne, H. Q. N.; Gunlaugsson, T.; Huxley, J. M.; Mchoy, C. P.; Rademacher, J. T.; Rice, T. E. *Chem. Rev.* **1997**, *97*, 1515- 1566. (b) Kim, J. S.; Quang, D. T. *Chem. Rev.* **2007**, *107*, 3780-3799.

19) Beer, P. D.; Gale, P. A. *Angew. Chem. Int. Ed.* **2001**, *40*, 486-516.

20) (a) Kim. S. K.; Lee, S. H.; Lee. J. Y.; Bartsche, R. A.; Kim, J. S. *J. Am. Chem. Soc.* **2004**, *126*, 16499-16506. (b) Lee, S. H.; Kim, Kim, S. H.; Kim, S. K.; Jung, J. H.; Kim, J. S. *J. Org. Chem.* **2005**, *70*, 9288-9295.

21) (a) Agnihotri, P.; Suresh, E.; Paul, P.; Ghosh, P. K.; *Eur. J. Inorg. Chem.* **2006**, 3369-3381. (b) Patra, S.; Maity, D.; Sen, A.; Suresh, E.; Ganguly, B.; Paul, P.; *New J. Chem.* **2010**, *34*, 2796-2805. (c) Patra, S.; Paul, P. *Dalton Trans.* **2009**, 8683-8695.

22) (a) Calestani, G.; Ugozzoli, F.; Arduini, A.; Ghidini, E. Ungaro, R.; *J. Chem. Soc. Chem. Commun.* **1987**, 344-345. (b) Sabbatini, N.; Guardigli, M.; Mecati, A.; Balzani, V.; Ungaro, R.; Ghidini, E.; Casnati, A.; Pochini, A.; *J. Chem. Soc. Chem. Commun.* **1990**, 878-879.

23) Casnati, A; Ungaro, R.; Asfari, Z.; Vincens, J. Crown Ethers Derived from Calix[4]arenes. In Asfari, Z; Böhmer, V.; Harrowfield, J.l Vincens, J. Calixarenes **2001**, Kluwer Academic Publishers, Dordrecht, 365-384.

24) Ji, H. –F.; Brown, G. M.; Dabestani, R. *Chem. Commun.* **1999**, 609-610.

25) Kim, J. S.; Noh, K. H.; Lee, S. H.; Kim, S. K.; Kim. S. K.; Yoon, J. *J. Org. Chem.* **2003**, *68*, 597-600.

26) Kim, J. S.; Shon, O. J.; Rim, J. A.; Kim, S. K.; Yoon, J. *J. Org. Chem.* **2002**, *67*, 2348-2351.

27) Ji, H. F.; Dabestani, R.; Brown, G. M.; Sachleben, R. A. *Chem. Commun.* **2000**. 833-834.

28) Li, G. –K.; Xu, Z. –X.; Chen, C. –F.; Huang, Z. –T. *Chem. Commun.* **2008**, 1774-1776.

29) Cao, Y.-D.; Zheng, Q. –Y.; Chen, C. –F.; Huang, Z. –T. *Tetrahedron Lett.* **2003**, 4751-4755.

30) Talanova, G. G.; Elkarim. N. S. A.; Talanov, V. S.; Bartsch, R. A. *Anal. Chem.* **1999**, *71*, 3106-3109.

31) Lee, J. Y.; Kim, S. K.; Jung, J. H.; Kim. J. S. *J. Org. Chem.* **2005**, *70*, 1463-1466.

32) (a) Kim, S. K.; Lee, J. K.; Lim, J. M.; Kim, J. W.; Kim, J. S. *Bull. Korean Chem. Soc.* **2004**, *25*, 1247-1250. (b) Lee, S. H.; Kim, J. Y.; Kim, S. K.; Lee, J. H.; Kim, J. S. *Tetrahedron* **2004**, *60*, 5171-5176.

33) Sun, X. H.; Li, W.; Xia, P. F.; Luo, H. –B.; Wei, Y.; Wong, M. S.; Cheng, Y. –K.; Shuang, S. *J. Org. Chem.* **2007**, *72*, 2419-2426.

34) (a) Leray, I.; O'Reilly, F.; Jiwan, J. –L. H.; Soumillion, J. –Ph.; Valeur, B. *Chem. Commun*. **1999**, 795-796. (b) Leray I.; Lefevre, J. –P.; Delouis, J. –F.; Delaire, J.; Valeur, B. *Chem. Eur. J*. **2001**, *7*, 4590-4598.

35) Lee, S. H.; Kim, H. J.; Lee, Y. O.; Vicens, J.; Kim, J. S. *Tetrahedron Lett*. **2006**, *47*, 4373-4376.

36) Lee, M. H.; Kim, H. J.; Yoon, S.; Park, N.; Kim, J. S. *Org. Lett*. **2008**, *10*, 213-216.

37) Kim, S. K.; Kim, S. H.; Kim, H. J.; Lee, S. H.; Lee, S. W.; Ko, J.; Bartsche, R. A.; Kim, J. S. *Inorg. Chem*. **2005**, *44*, 7866-7875.

38) Lee, S. H.; Kim, S. K.; Bok, J. H.; Lee, S. H.; Yoon, J.; Lee, K.; Kim, J. S. *Tetrahedron Lett*. **2005**, *46*, 8163-8167.

39) Othman, A. B.; Lee, J. W.; Wu, J. –S.; Kim, J. S.; Abidi, R.; Thuery, P.; Strub, J. M.; Dorsselaer, A. V.; Vicens, J. *J. Org. Chem*. **2007**, *72*, 7634-7640.

40) Winnik, F. M. *Chem. Rev*. **1993**, *93*, 587-614.

41) Jin, T.; Ichikawa, K.; Koyama, T. *J. Chem. Soc. Chem. Commun*. **1992**, 499-501.

42) Matsumoto, H.; Shinkai, S. *Tetrahedron Lett*. **1996**, *37*, 77-80.

43) Van der Veen, N. J.; Flink, S.; Deij, M. A.; Egberink, R. J. M.; van Veggel, F. C. J. M.; Reinhoudt, D. N. *J. Am. Chem. Soc*. **2000**, *122*, 6112-6113.

44) Kim, S. K.; Kim, S. H.; Kim, H. J.; Lee, S. H.; Lee, S. W.; Ko, J.; Bartsch, R. A.; Kim, J. S. *Inorg. Chem*. **2005**, *44*, 7866-7875.

45) Choi, J. K.; Lee, A.; Kim, S.; Ham, S.; No, K.; Kim, J. S. *Org. Lett*. **2006**, *8*, 1601-1604.

46) Schazmann, B.; Alhashimy, N.; Diamond, D. *J. Am. Chem. Soc*. **2006**, *128*, 8607-8614.

47) Kim, H. J.; Kim, S. K.; Lee, J. Y.; Kim, J. S. *J. Org. Chem*. **2006**, *71*, 6611-6614.

48) Takeshita, M.; Shinkai, S. *Chem. Lett*. **1994**, 1349-1352.

49) (a) Vicens, J. *J. Inclusion Phenom. Macrocyl. Chem*. **2006**, *55*, 193-196. (b) Thuery, P.; Nierlich, M.; Asfari, Z.; Vincens, J. Dozol, J. F. *Polyhedron* **2000**, *19*, 1749-1756.

50) Alfieri C.; Dradi, E.; Pochini, A.; Ungaro, R.; Andreetti, G. D. *J. Chem. Soc. Chem. Commun*. **1983**, 1075-1077.

51) Casnati, A.; Pochini, A.; Ungaro, R.; Ugozzoli, F.; Arnaud, F.; Fanni, S.; Schwing, M. J.; Egbering, R. J. M.; de Jong, F.; Reinhoudi, D. N. *J. Am. Chem. Soc*. **1995**, *117*, 2767-2777.

52) Ji, H. –F.; Dabestani, R.; Brown, G. M. *J. Am. Chem. Soc*. **2000**, *122*, 9306-9307.

53) a) Leray, I.; Asfari, Z.; Vincens, J.; Valeur, B. *J. Fluoresc*. **2004**, *14*, 451-458. (b) Leray, I.; Asfari, Z.; Vincens, J.; Valeur, B. *J. Chem. Soc. Perkin Trans. 2*, **2002**, 1429-1434. (c) Souchon, V.; Leray, I.; Valeur, B. *Chem. Commun*. **2006**, 4224-4226.

54) Lee, M. H.; Quang, D. T.; Jung, H. S.; Yoon, J.; Lee, C. –H.; Kim, J. S. *J. Org. Chem*. **2007**, *72*, 4242-4245.

Chapter 2: 3-(Dicyanomethylidene)indan-1-one-Appended Calix[4]arene-Calix[4]pyrrole System:

Colorimetric Ion-Pair Sensor for Cesium Salts

2.1 INTRODUCTION

The detection and remediation of radioactive materials are topical areas of research due to whose importance is underscored by current events, such as the Daiichi nuclear disaster. Of the isotopes released during the associated reactor breach, ^{137}Cs (half-life, 30.2 years), produced during the nuclear fission of uranium-235, is particularly insidious. This isotope comprises a significant fraction of the radioactive waste produced from early military-director efforts, which also replaces potassium in muscles and red blood cells and spreads out throughout the body.[1,2] As a result there is a critical need for chemosensors that can be used to detect the cesium ion with selectivity relative to other metal cations, particular Na^+ as found in sea water.

In recent years, Sessler and coworkers reported several artificial cesium selective ion-pair receptors containing both a calix[4]arene and calix[4]pyrrole subunits.[3] In general, ion-pair receptors display significantly enhanced binding affinities for specific ions as compared with simple ion receptors.[4] This improvement, which often translates to increased selectivity, can generally be rationalized in terms of favorable electrostatic interactions between co-bound ions. Such an appreciation underlies to the approach pursed within the Sessler group, which has anion-binding cores and cation recognizing subunits within the same framework. While considerable success has been encountered for the recognition cesium ions, unfortunately the receptors studied to date do not possess optically absorbance or emission features that can be detectable via optical means, such as a change in the absorption spectra or the fluorescence intensity. Therefore, the existing systems could be used as chemosensors. This problem is not limited to systems generated

in the Sessler group. Chromophores and fluorophores have often been attached to core receptor motifs to permit fluorogenic cesium ion receptors have been reported over a decade ago.[5] However, to the best of our knowledge, chromogenic or colorimetric chemical sensors capable of recognize cesium ion-pair are still lacking, have not been reported thus far. Hence, given the potential utility of a Cs^+ ion pair sensors, we have attempted to append a chromogenic subunit to a previously studied, cesium-selective calix[4]arene-calix[4]pyrrole hybrid system. It relies on a merocyanine type donor-π-acceptor (D-π-A) subunit. This class of chromophores is frequently used to create pull-push systems with useful spectral properties.[6-7] In this chapter, a first chromogenic Cs^+ selective ion-pair receptor **2.1** is presented. The key chromogenic unit is 3-(dicyanomethylidene)indan-1-one, which was appended to a β-formylated calix[4]pyrrole in analogy to what was done previously by Anzenbacker and coworkers to produce calix[4]pyrrole based anion sensors[10]. As will be detailed below. The optical spectra of the indane-incorporated calix[4]arene-calix[4]pyrrole system was perturbed upon the addition of cesium ions. 3-(Dicyanomethylidene)indan-1-one is an electron deficient moiety that may be a pull-push chromophore. In this event, complexation of a cesium ion between the two ethylene glycol subunits of **2.1** induces a conformational change in **2.1** and results in modest, but detectable, change in color.

2.2 RESULTS AND DISCUSSIONS

2.2.1 Synthesis and NMR and UV-Vis Spectroscopic Studies

The synthesis of receptor **2.1** is shown in Scheme 2.1. It starts with the calix[4]arene-calix[4]pyrrole **2.3**, was synthesized using known procedures.[3] Vilsmeier-Hacck formylation, then give, **2.2**.[8] Although two β-monoformylated regioisomeric compounds might be expected from this reaction[9], in fact one product proved dominant. Unexpectedly, it was the regioisomer reaction of **2.2** with where formlyation at the more hindered β-position. Reaction of **2.2** with 3-(dicyanomethylidene)indan-1-one in a mixture of solvents (THF: EtOH) at room temperature for 24 hours in the absence of an added base, then gave receptor target **2.1** in quantitative yield. Receptor **2.1** was fully characterized by standard spectroscopic means, as well as by single crystal X-ray diffraction analysis (Figure 2.1).

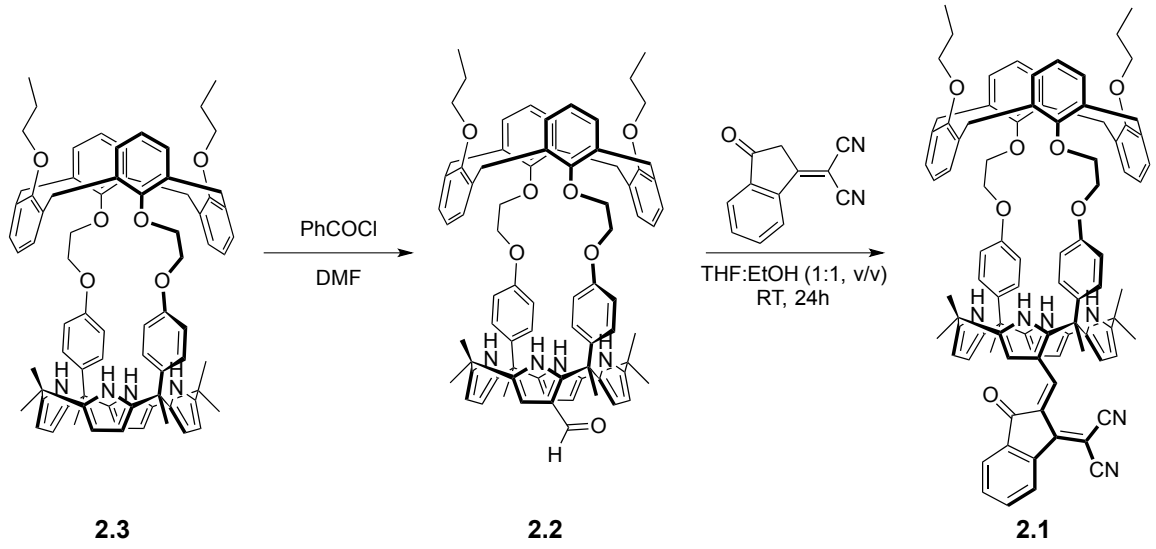

Scheme 2.1: Synthetic pathway used to prepare compound **2.1**.

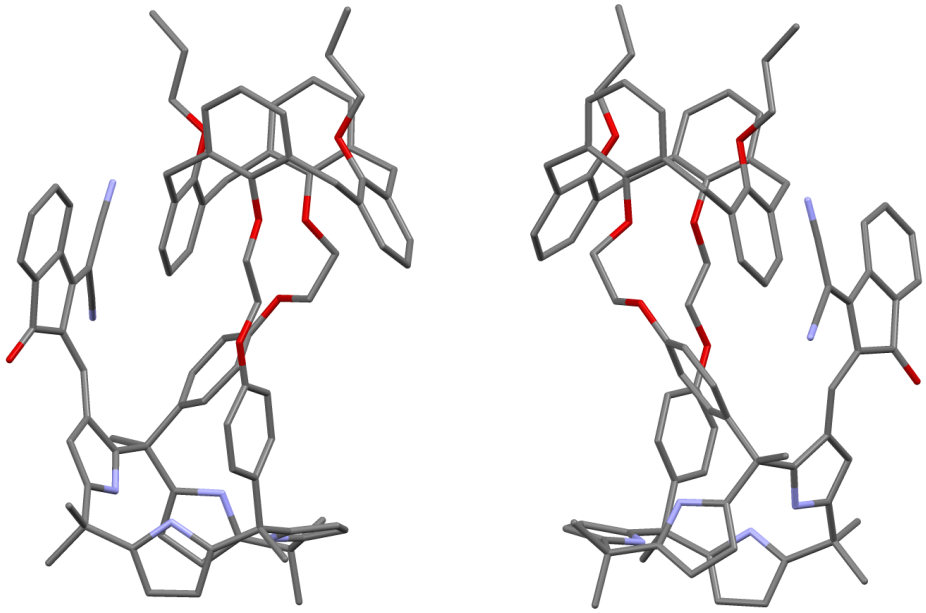

Figure 2.1: Two different views of the single crystal X-ray diffraction structures of **2.1**. Solvent molecules and hydrogen atoms have been omitted for clarity.

Based on prior studies by the Sessler group[3], it was anticipated that receptor **2.1** would possess structural feature that would favor the binding of cesium ion pairs. In particular, it was expected that the Cs^+ cations would be bound to the ethylene glycol moieties between the calix[4]pyrrole and calix[4]arene subunits. Likewise, it was expected that the counter anions, if appropriately size would be bound by the calix[4]pyrrole unit. This anticipated complexation of cesium ion salts was expected to a partial change in the conjugation of within dicyanoindaneone chromophore unit leading to an overall color change. The ability of **2.1** to act as a cesium selective ion-pair receptor was investigated using various cesium and TBA salts via UV-Vis spectroscopic and ^1H NMR spectroscopic analyses. In fact, discernable spectral changes were seen for **2.1** upon exposure to CsF, CsCl, and $CsNO_3$ in mixed organic media (Figure 2.2). These color changes proved anion dependent.

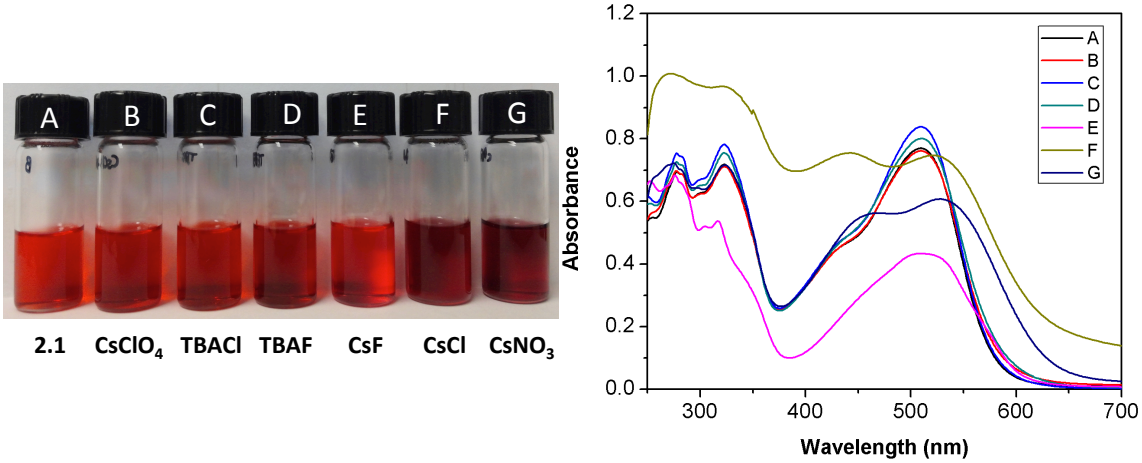

Figure 2.2: (Left) solutions of receptor **2.1** (150 μM) in MeOH/$CHCl_3$ (1/9, v/v) photographed in the absence and presence of excess ions (100 equiv), (Right) UV-Vis absorption spectra of receptor **2.1** (50 μM) in MeOH/$CHCl_3$ (1/9, v/v) in the absence (A) and presence of 100 equiv of (B) $CsClO_4$ (C) TBACl, (D TBAF, (E) CsF, (F) CsCl and (G) $CsNO_3$.

In analogy to what is true for receptor **2.3** (studied previously), receptor **2.1,** lacks a strong cation recognition site (e. a., crown ether subunit). As a result, it fails to interact with single ions such as Cs^+, F^- or Cl^- when exposed to these ions in the form of salts lacking a charge-dense counterion (e.g., ClO_4^- for Cs^+ and TBA^+ for F^- and Cl^-, respectively). Thus, only modest enhancements in spectral intensity were observed in the UV- Vis absorption spectrum when these single ion were added to organic solutions of **2.1** in the form of these weakly coordinating salts.

Support for the above findings came from ^{1}H NMR spectroscopic studies. In contrast to what is seen with $CsClO_4$, TBAF, and TBACl, the addition of CsF, CsCl and $CsNO_3$ to a solution of receptor **2.1** in 10 % CD_3OD in $CDCl_3$ caused significant changes in the ^{1}H NMR spectrum of **2.1** (Figure 2.3). After exposure to the latter cesium salts, the proton signal of the allylic proton shifts to lower field, with the degree of this shift is

different depending on the cesium salts. In addition, the pyrrolic amine proton signals shift downfield in the case of the coordinating cesium salts. On this basis, it is inferred that CsF, CsCl and $CsNO_3$ are bound to receptor **2.1** to form ion pair complexes. No evidence of substantial shifts in seen unless both a strongly coordinating cation (i. e., Cs^+ rather than TBA^+) and anion (e. g., F^-, Cl^-, or NO_3^-) are present.

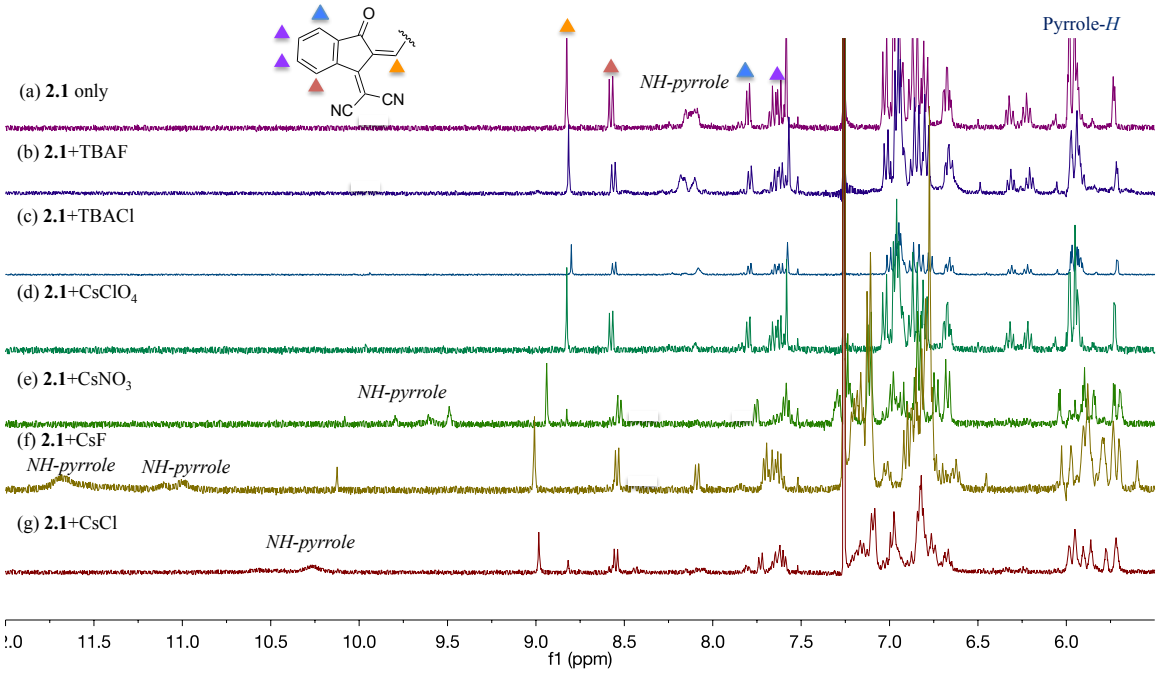

Figure 2.3: Partial ^{1}H NMR spectra of (a) **2.1** only, (b) **2.1** + 5 equiv of TBAF, (c) **2.1** + 5 equiv of TBACl, (d) **2.1** + 5 equiv of $CsClO_4$, (e) **2.1** + 5 equiv of $CsNO_3$, (f) **2.1** + 5 equiv of CsF and (g) **2.1** + 5 equiv of CsCl in $CD_3OD/CDCl_3$ (1:9, v/v).

The interaction between **2.1** and CsF were further studied by ^{1}H NMR and UV/Vis spectroscopy. The concurrent addition of both TBAF and $CsClO_4$, neither of which is individually bound to **2.1**, gives rise to UV-Vis and ^{1}H NMR spectral changes in

10% methanol chloroform solution that are very similar to those seen upon addition of CsF (Figure 2.4). While no discernable color changes are observed (cf. Figure 2.4), significant spectral perturbations are seen in the UV-Vis spectrum. Additionally, ^{1}H NMR spectroscopic study (Figure 2.4) also revealed notable changes. In particular, the combination of TBAF and $CsClO_4$ proved changes in the pyrrole NH resonances of **2.1** that were eventually identical to those produced when CsF was added directly to the initial solution of **2.1**. Such findings suggest that receptor **2.1** is capable of trapping both the Cs^+ cation and the F^- counter anion concurrently in this solvent system.

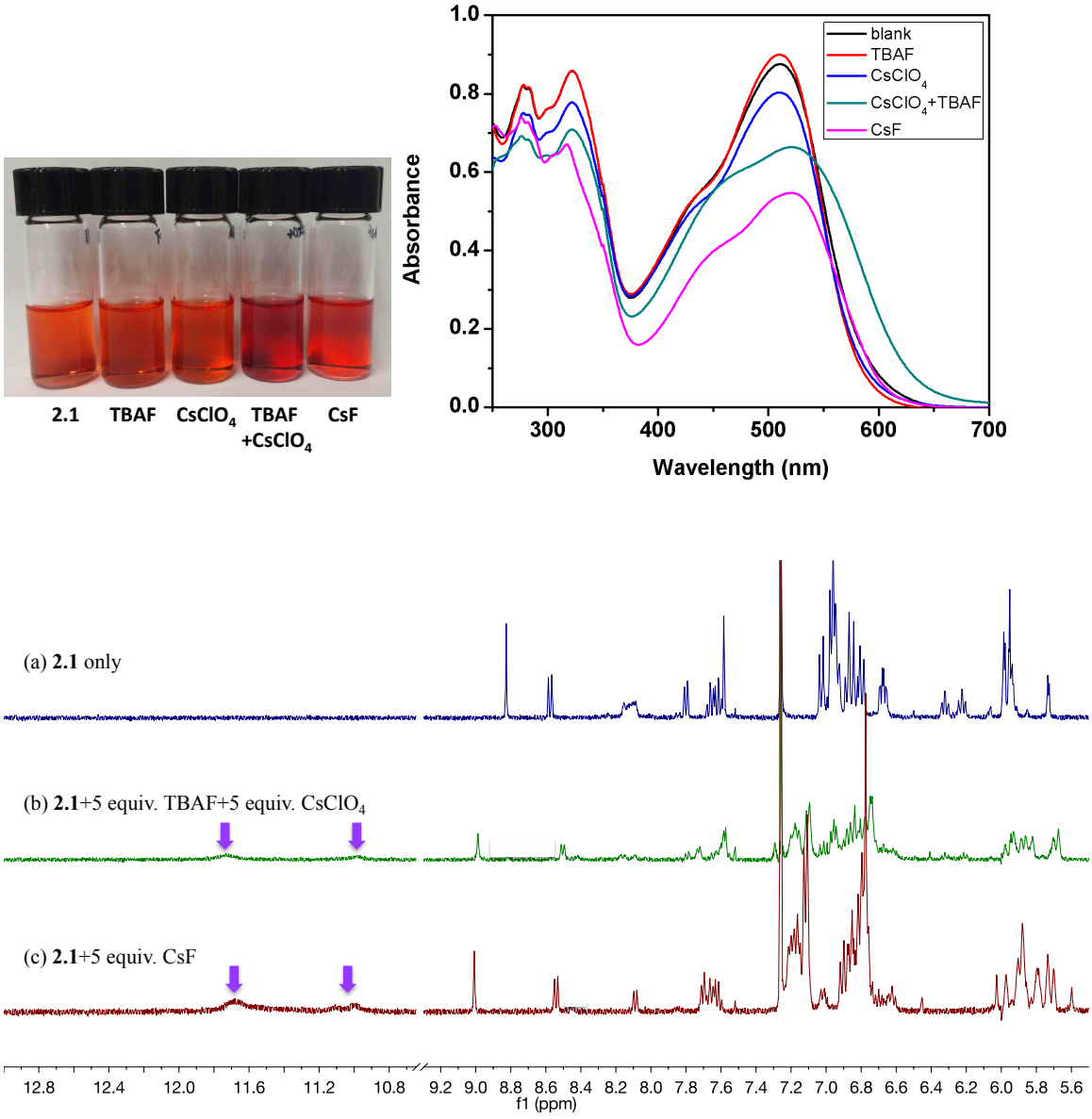

Figure 2.4: **Upper**: (Left) solution of receptor **2.1** (50 μM) in MeOH/$CHCl_3$ (1/9, v/v) in the presence of excess ions, (Right) UV-Vis absorption spectra of receptor **2.1** (50 μM) in MeOH/$CHCl_3$ (1/9, v/v) (A) and in the presence of 100 equiv of (B) TBAF + $CsClO_4$ (5 equiv, respectively), and (C) 5 equiv. of CsF, **Below**: Partial ^{1}H NMR spectra of (a) **2.1** only, (b) **2.1** + 5 equiv of TBAF and 5 equiv of $CsClO_4$, and (c) **2.1** + 5 equiv of CsF, in $CD_3OD/CDCl_3$ (1:9, v/v). The purple arrows indicate the NH-pyrrole resonances.

Further evidence that receptor **2.1** forms strong complexes with cesium salts came from UV-Vis absorption titrations carried out with CsF. Assuming a 1:1 binding stoichiometry, $K_a = 1.1 \times 10^4$ M^{-1} could be derived for this moderately polar solvent system (10% CH_3OH in $CHCl_3$) (Figure 2.5). Unfortunately, the fit to a 1:1 binding profile was characterized by large residuals. So this value should be approximate. The binding constants corresponding to the interaction of **2.1** with CsCl and $CsNO_3$ could not be determined by UV-Vis or ^1H NMR spectroscopic titration methods because of the poor solubility of these salts in this and other readily accessible solvent systems.

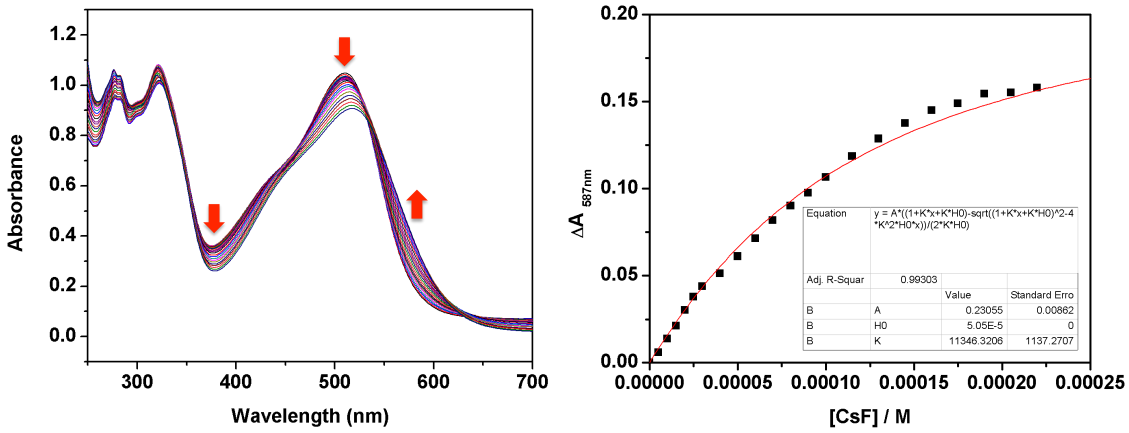

Figure 2.5: Titration of receptor **2.1** (50 μM) with CsF in 10% of CH_3OH in $CHCl_3$.

Receptor **2.1** was exposed to other alkali metal chloride anion salts in this solvent system to test the cesium ion selectivity. The resulting UV-Vis spectra reveal the changes in the absorption features of **2.1** in the case of CsCl as compared to the other alkali metal salts (cf. Figure 2.6). This findings leads us to suggest that receptor **2.1** binds the chloride anion through the calix[4]pyrrole conjugated moiety (which is the indaneone unit) and

that the cesium cation is bound to the ethylene glycol moieties. The maximum absorption (λ_{max}) of ion-free receptor **2.1** appears around 520 nm. In the presence of excess LiCl, NaCl, or KCl, no discernible change in the λ_{max} of **2.1** is seen. However, the intensity of the absorbance decreased. This finding is taken as evidence of a relatively weak interaction between receptor **2.1** and these three ion pair salts. In contrast, exposure to CsCl ion pair causes the absorption band at 520 nm to be split into two bands with λ_{max} 440 nm and 540 nm, respectively. This spectral change is ascribed to the chloride anion to the calix[4]pyrrole unit with the cesium cation being cocurrently bound to the ethylene glycol subunits. The high selectively of **2.1** for CsCl inferred from the UV-Vis spectral studies supported by ^{1}H NMR spectroscopic analysis. For instance, upon exposure to CsCl the allylic proton shifted from 8.7 ppm to 9.0 ppm. However, when LiCl or NaCl was added to the solution of receptor **2.1**, no discernible shifts were observed. Under conditions where CsCl fully bound to **2.1**, KCl given rise to relatively minor changes in the ^{1}H NMR spectrum, leading to the conclusion that it is but weakly bound (Figure 2.7).

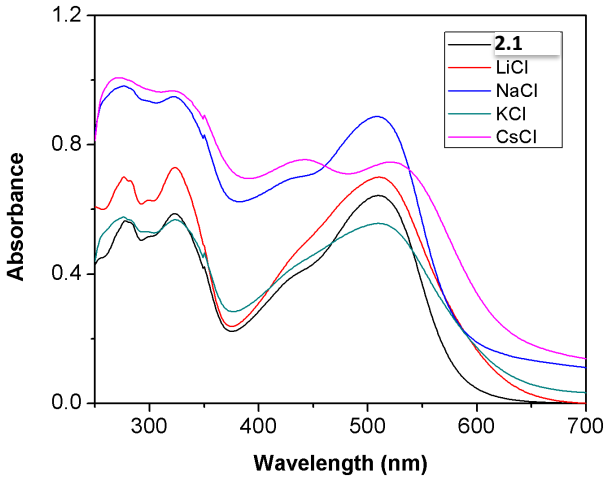

Figure 2.6: UV-Vis absorption spectra of receptor **2.1** (50 μM) in MeOH/$CHCl_3$ (1/9, v/v) recorded in the absence and presence of 100 equiv of excess of various salts, namely LiCl, NaCl, KCl, and CsCl.

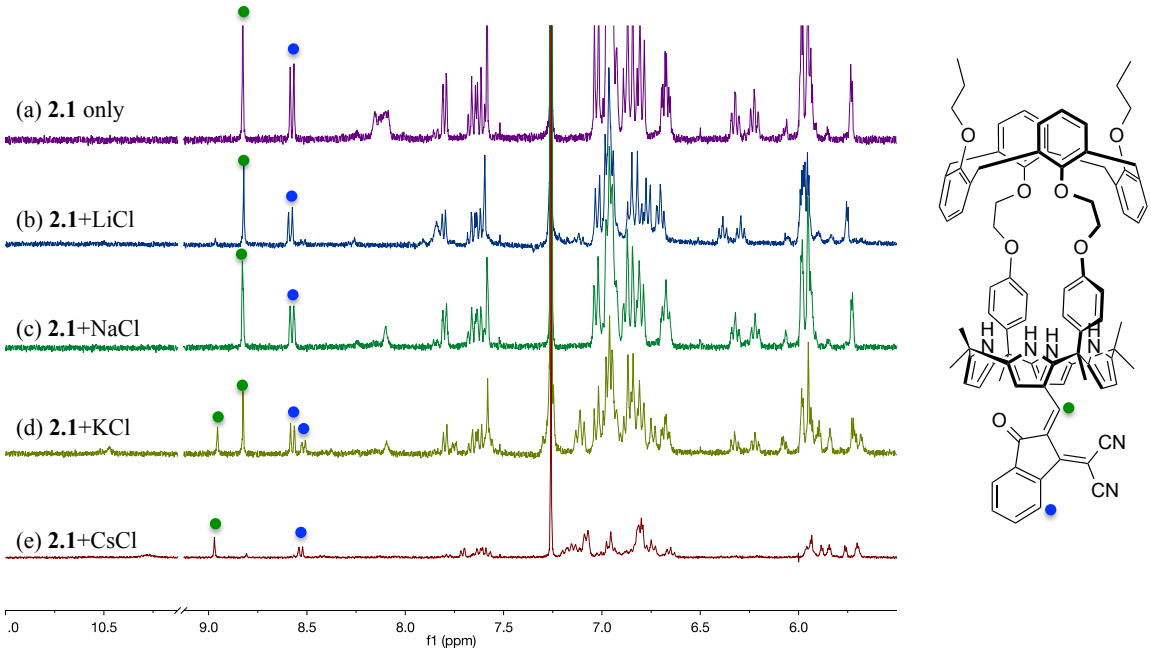

Figure 2.7: Partial ^{1}H NMR spectra of (a) **2.1** only, (b) **2.1** + 5 equiv of LiCl, (c) **2.1** + 5 equiv of NaCl, (d) **2.1** + 5 equiv of KCl, and (e) **2.1** + 5 equiv of CsCl recorded in $CD_3OD/CDCl_3$ (1:9, v/v).

The ability of receptor **2.1** to promote the liquid-liquid extraction of cesium salts was examined on the basis of visible color changes as well as chemical shift changes in the ^{1}H NMR spectrum. The experiments were carried out by contacting nitrobenzene solution ($C_6D_5NO_2$) of **2.1** with an aqueous (D_2O) solution of various cesium salts, such as CsF, CsCl, CsBr, $CsNO_3$, and $CsClO_4$. When contacted with $CsNO_3$, receptor **2.1** gives rise to noteworthy spectral changes in both the UV-Vis and ^{1}H NMR spectra of the organic phase (Figures 2.8 and Figure 2.9, respectively).

This finding was taken as evidence that receptor **2.1** is able to extract $CsNO_3$ from water into the nitrobenzene phase with high efficiency and selectivity. UV-Vis and ^{1}H NMR spectral data also provide support for the notion that receptor **2.1** can extract other cesium salts, such as CsF, CsCl, and CsBr, albeit with relatively low efficiency compared to $CsNO_3$. No spectral changes were observed when the nitrobenzene solution of **2.1** was

exposed to cesium ion salts containing non-coordinating counter anions such as ClO_4^-. Nor, were changes seen when the Cs^+ cation was replaced by TBA^+. Taken in aggregation, these findings support the conclusion that receptor **2.1** is capable of functioning as an extractant for rather specific cesium salts. On some level, therefore, this system can be considered to be a rudimentary AND Logic device (Figure 2.10).

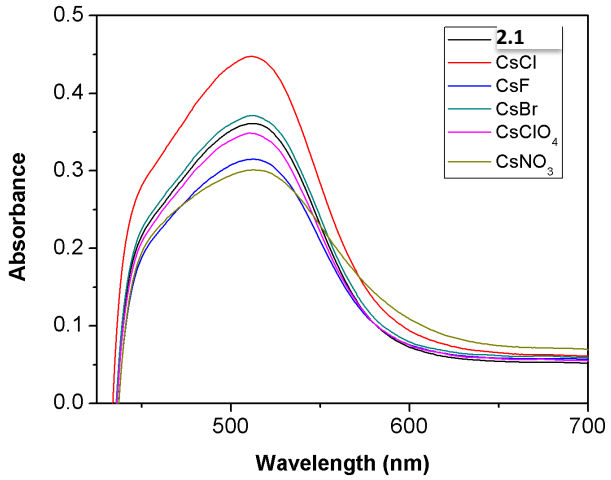

Figure 2.8: Liquid-Liquid extraction, UV-Vis absorption spectra of compound **2.1** (50 μM) in nitrobenzene recorded before and after contacting with 100 equiv of $CsClO_4$, CsF, CsCl, CsBr and $CsNO_3$ dissolved in H_2O. The spectra were recorded after roughly 30 min. of sonication.

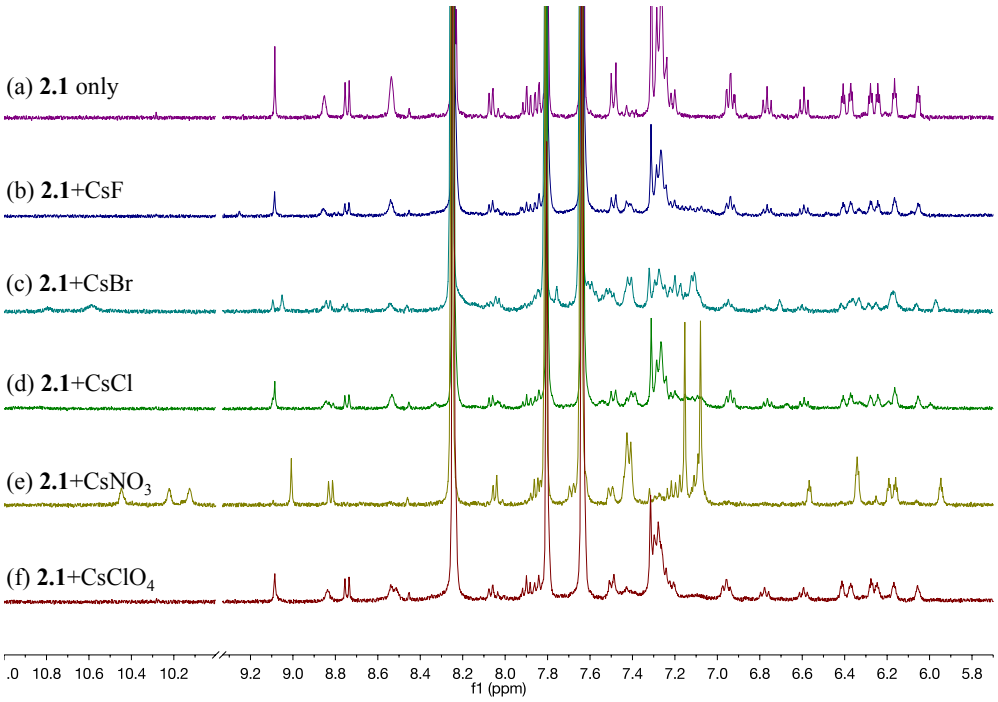

Figure 2.9: Partial ^{1}H NMR spectra of (a) **2.1** only, (b) **2.1**+10 equiv. of CsF, (c) **2.1**+10 equiv. of CsBr, (d) **2.1**+10 equiv. of CsCl, (e) **2.1**+10 equiv. of $CsNO_3$ and (f) **2.1**+10 equiv. of $CsClO_4$ in nitrobenzene-d_5. The spectra were recorded after roughly 30 min. of sonication.

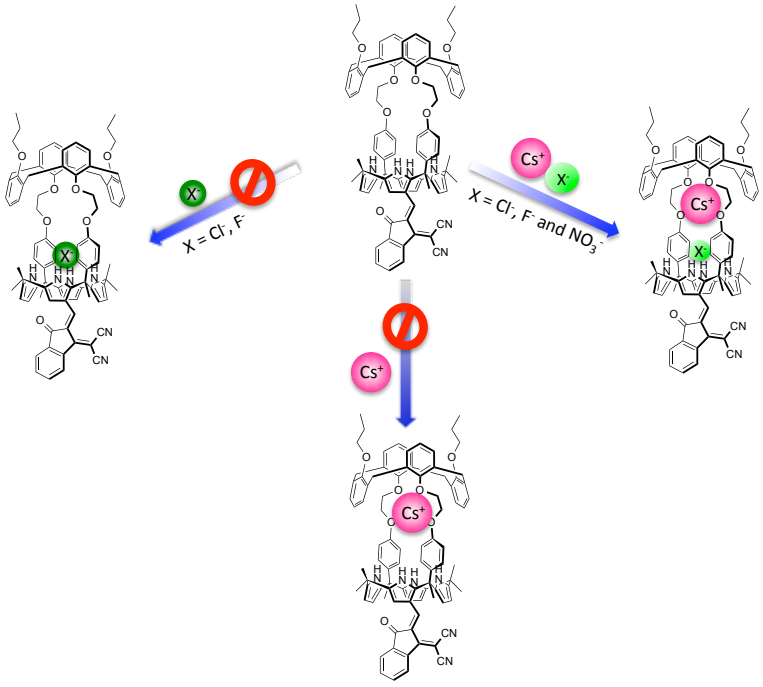

Figure 2.10: Proposed AND logic gate binding behavior of **2.1** towards Cs salts ion pair in $CD_3OD/CDCl_3$.

2.3 CONCLUSIONS

In summary, a chromogenic ion-pair sensor **2.1**, specific for certain cesium salts, was successfully synthesized. It was prepared via the condensation of a calix[4]arene-calix[4]pyrrole pseudodimer with 3-(dicyanomethylidene)indan-1-one. Its ability to form complexes of cesium ion salts was investigated using visual and spectroscopic methods. In a solvent mixture of methanol and chloroform (1/9,v/v), noticeable color changes were seen upon treatment with various cesium salts, including CsF, CsCl or $CsNO_3$. Spectroscopic changes were also seen, leading to the conclusion that receptor **2.1** is able to bind CsF, CsCl, and $CsNO_3$ with high selectivity and efficiency. This binding mimics

an AND Logic gate in that receptor **2.1** fails to recognize appreciately either $CsClO_4$ or TBA^+ anion salts (Cl^- and F^-). Furthermore, the colorimetric ion pair sensor (**2.1**) proved capable of extracting CsF, CsCl, and particularly, $CsNO_3$ from an aqueous phase into an organic phase consisting of nitrobenzene. This extraction could be followed by the naked-eye.

2.4 FUTURE DIRECTIONS

3-(Dicyanomethylidene)indan-1-one was used as the chromogenic moiety in this work. However, the color changes produced by receptor **2.1** upon exposure to Cs^+ salts are not as large as desired building on the work of metal complexation occasionally. Anzenbacher, it is proposed to extend the range of chromogenic 1,3-indanes used to functionalize the calix[4]pyrrol subunit of **2.2.** for anion sensing.[10] Several of Anzenbacher's anion sensors are shown in Figure 2.11. Receptors **2.4a-d** gave rise to yellow, orange, and pink colors upon exposure to different anions. Based on this prior work, it is suggested that the dicyanomethylidene, which increases the acidity of the NH-pyrrole proton, would be particularly worthwhile to consider in the context of designing yet-improved Cs^+ ion pair sensors. This and other targets are shown in Figure 2.12.

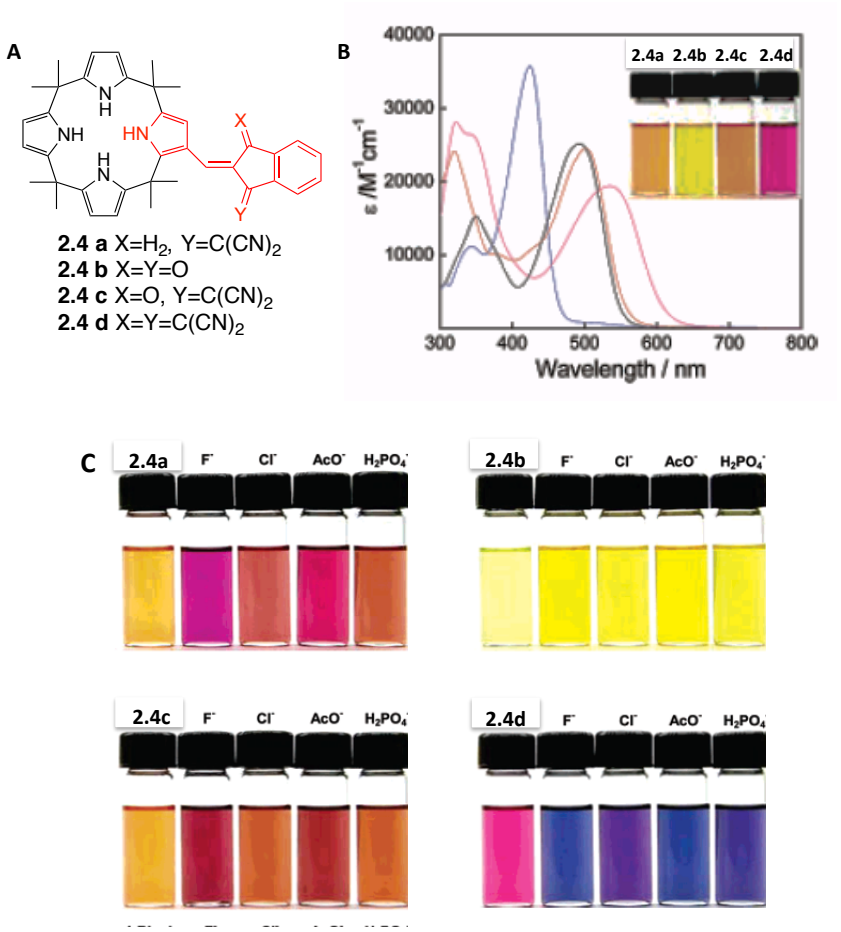

Figure 2.11: A) Structures of **2.4a-d**. B) Absorption spectra of **2.4a** (black line), **2.4b** (blue line), **2.4c** (orange line) and **2.4d** (pink line) in CH_2Cl_2 (50 μM). C) The solution of sensors **2.4 a-d** (50 mM in CH_2Cl_2) in the presence of anions (10 equiv. excess). This figure was originally published in *Org. Lett.* **2006**, *8*, 359-362. Reproduction was permitted. Copyright American Chemical Society.

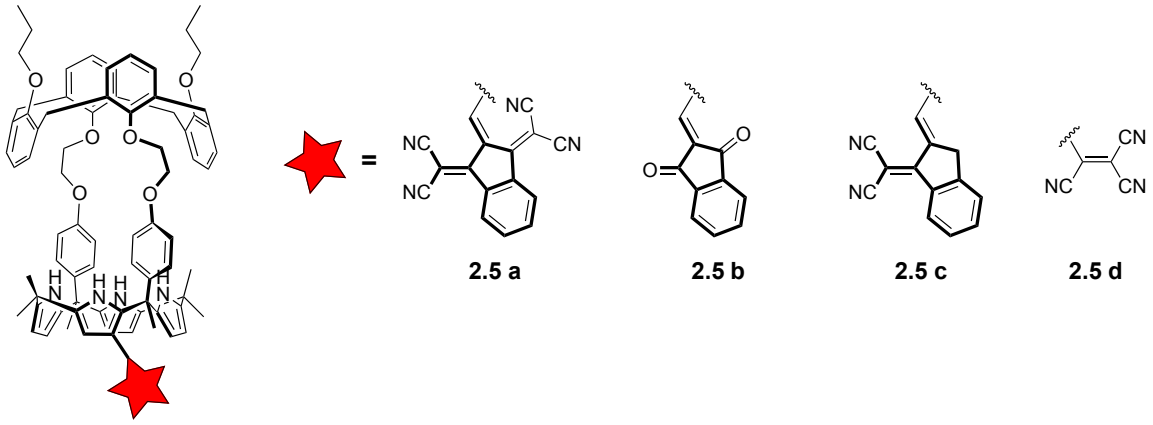

Figure 2.12: Candidates proposed as ion pair sensors that may prove more effective than **2.1** as colorimetric Cs^+ ion pair sensors.

2.5 REFERENCE

1) Delacroix, D.; Guerre, J. P.; Leblanc, P.; Hickman, C. Radionuclide and Radiation Protection Data Handbook; Nuclear Technology Publishing, **2002**.

2) Relman, A. S. *Yale J. Biol. Med.* **1956**, *29*, 248-262.

3) (a) Kim, S. K.; Sessler, J. L.; Gross, D. E.; Lee, C. –H.; Kim, J. S.; Lynch, V. M.; Delmau, L. H.; Hay, B. P. *J. Am. Chem. Soc.* **2010**, *132*, 5827-5836. (b) Kim, S. K.; Lynch, V. M.; Young, N. J.; Hay, B. P.; Lee, C. H.; Kim, J. S.; Moyer, B. A.; Sessler, J. L. *J. Am. Chem. Soc.* **2012**, *134*, 20837-20843. (c) Kim, S. K.; Hay, B. P.; Kim, J. S.; Moyer, B. A.; Sessler, J. L. *Chem. Commun.* **2013**, *49*, 2112-2114.

4) (a) Custelcean, R.; Delmau, L. H.; Moyer, B. A.; Sessler, J. L.; Cho, W. –S.; Gross, D.; Bates, G. W.; Brooks, S. J.; Light, M. E.; Gale, P. A. *Angew, Chem, Int. Ed.* **2005**, *44*, 2537-2542. (b) Bush, L. C.; Heath, R. B.; Feng, X. U.; Wang, P. A.; Maksimovie, L.; Song, A. L.; Chung, W. –S.; Berinstain, A. B.; Scaiano, J. C.; Berson, J. A. *J. Am. Chem. Soc.* **1997**, *119*, 1406-1415. (c) Sato, W.; Miyaji, H.; Sessler, J. L.; *Tetrahedron Lett.* **2000**, *41*, 6731-6736.

5) (a) Leray, I.; Valeur, B. *Eur. J. Inorg. Chem.* **2009**, 3525-3535. (b) Kim, J. S.; Quang, D. T. *Chem. Rev.* **2007**, *107*, 3780-3799.

6) Reichardt, C. Solvents and solvent effects in organic chemistry. 3rd ed. Weinheim: Wiley-VCH; 2003.

7) (a) Bella, S. D. *Chem. Soc. Rev.* **2001**, *30*, 355-366. (b) Whittall, I. R.; McDonagh, A. M.; Humphrey, M. P.; Samoc, M. *Adv. Organomet. Chem.* **1998**, *42*, 291-362. (c) Planells, M.; Robertson, N. *Eur. J. Org. Chem.* **2012**, 4947-4953.

8) Brinas, R. P.; Bruckner, C. *Tetrahedron* **2002**, *58*, 4375-4381.

9) Kim, S. –H.; Hong, S. –J.; Yoo, J.; Kim, S. K.; Sessler, J. L.; Lee, C. –H. *Org. Lett.* **2009**, *11*, 3626-3629.

10) (a) Nishiyabu, R.; Anzenbacher, Jr., P. *Org. Lett.* **2006**, *8*, 359-362. (b) Nishiyabu, R.; Anzenbacher, Jr., P. *Am. Chem. Soc.* **2005**, *127*, 8270-8271.

Chapter 3: Tetra-Amidoindole Substituted Calix[4]arene for Anion and Ion Pair Recognition

3.1 INTRODUCTION

In recent years, it has come to be appreciated that anions play pivotal roles in the biological and environmental fields. This importance has spawned to investigate artificial anion receptors.[1] Key goals have been recognition, extraction, and sensing. Traditionally, anion sensing has been relatively difficult to achieve in comparison to cation sensing.[2] This is rationalized as being due to their wide range of geometries and pH sensitivity, as exemplified by phosphate. Therefore, spatial arrangements and orientation of anion binding units are critical to anion recognition and sensing. Consequently, many of the early synthetic anion receptors relied on charged framework[3] or metal complexes, which are able to directly coordinate anions.[4] Later, neutral receptors, such as calix[4]pyrroles, were developed for the purpose of anion recognition. As the importance of spatial pre-organization of the ion binding units became increasingly appreciated, attention has been paid to elaborated calix[4]arene-based ion receptors wherein various ancillary ion recognition sites targeting calix[4]pyrrole rims, or both. Beyond calix[4]pyrroles, either anions or cations are incorporated into the overall framework through either the upper or lower has been widely explored.[5] Indeed, neutral anion receptors, based on, amides, sulphonamides, pyrroles, ureas, and thioureas are all known. Urea substituents have proved particularly popular due to their ability to bind anions very strongly via hydrogen bonding interactions.[6] Reinhoudt and coworkers reported the first urea-derived calix[4]arenes in 1994.[7] In these receptors (**3.1a-e** and **3.2**; Figure 3.1), two and four urea substituents were introduced to the calix[4]arene frameworks to provide four and eight hydrogen bond donors for anion recognition. Since it is well known that Cl^- and Br^-

anions are good hydrogen bond acceptors and the hydrogen bond donor sites of the urea moiety act as hard Lewis acids were bound by these receptors. It was expected and indeed found that Lewis basic anions, Cl^- and Br^- ions were bound these receptors. The data in Table **3.1** reveals that in chloroform solvent, the anion binding affinities are follow the order $Cl^- > Br^- > CN^-$, with limited binding affinities being observed for $I^- > SCN^-$. Interestingly, although F^- ion is a very strong hydrogen bond acceptor, no complexation with receptors **3.1a-e** and **3.2** was observed. In addition, little appreciable affinity was seen in the case of $H_2PO_4^-$. All anions studied as their TBA salts. Presumably the tetrahedral $H_2PO_4^-$ anion is too large to fit into the receptor cavity and is unable to interact well with the urea sites. Therefore, receptor **3.2** was designed to evaluate how the number of hydrogen bond donor sites affected the affinity. In fact, receptor **3.2** showed increased selectivity for the Cl^- anion as compared to receptors **3.1a-e**, even though it contains fewer donor sites. These researchers proposed that **3.2** adopts a less pre-organized conformation and is less prone to self-association, an effect that would lead to a reduction in anion affinity. To the extent such rationalizations are correct, they would account for why chloride anion binding is energetically favorable in the case of **3.2** than **3.1**.

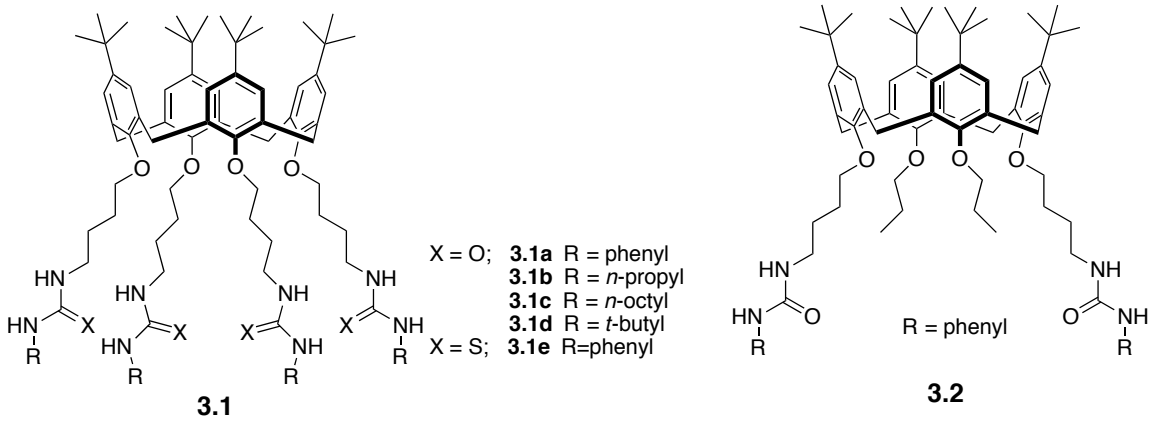

Figure 3.1: Urea-based calix[4]arene anion receptors **3.1a-e** and **3.2**.

	Cl^-	Br^-	I^-	CN^-	SCN^-
3.1a	2660	1735	<25	855	<25
3.1b	<25	<25	<25	<25	<25
3.1c	285	450	-	550	-
3.1d	2015	1225	-	80	-
3.1e	335	575	<25	855	<25
3.2	7105	2555	605	1115	<25

Table 3.1: Associate constants, K_a (M^{-1}) of urea-derived *p*-tert-butylcalix[4]arenes in $CHCl_3$. All counter ions are TBA^+ salts.

Inspired by the ability of urea-substituted calix[4]arene derivatives to act as anion receptors, two calix[4]arene bearing tetra-amidoindole substituents, **3.3** and **3.4**, were designed and synthesized. Indole-amide subunits are expected to be superior hydrogen bond donors than ureas. Therefore, these new receptors were expected to bind anionic guests more strongly than the Reinhaudt receptors. This chapter summarizes our work on receptors **3.3** and **3.4**.

3.2 RESULTS AND DISCUSSIONS

Two tetra-amidoindole incorporated calix[4]arenes were synthesized. Both involve the use of amides to link indole subunits to a calix[4]arene core. As compared with **3.4**, compound **3.3** possess four additional electron-withdrawing nitro groups on each amidoindole moiety. We investigated the ability of these receptors to bind anions and ion pairs by monitoring analyte-induced ^{1}H NMR and optical spectral changes. The synthesis of compound **3.3** and **3.4** is outlined in Scheme 3.1. Compound **3.5** was synthesized by known synthetic pathway.[8] Briefly, 5-nitroindole-2-carboxylic acid **3.6** was obtained by subjecting to ethyl 5-nitroindole-2-carboxylate acidic hydrolysis.[9] Compound **3.6** was then reacted with the amine-functionalized calix[4]arene **3.5** in DMF in the presence of *N*-(3-dimethylaminopropyl)-*N'*-ethylcarbodiimide hydrochrolide (EDCI) and 1-hydroxybenzotriazole. This gave the amide-nitroindole substituted calix[4]arene **3.3** in moderate yield. Compound **3.4** was also obtained by following a similar pathway as used to obtain compound **3.3** but using indole-2-carboxylic acid instead of 5-nitroindole-2-carboxylic acid. Compound **3.3** was contains an electron-withdrawing -NO_2 group at each amidoindole groups, whereas compound **3.4** has the same tetra-amidoindole moieties but without the –NO_2 groups.

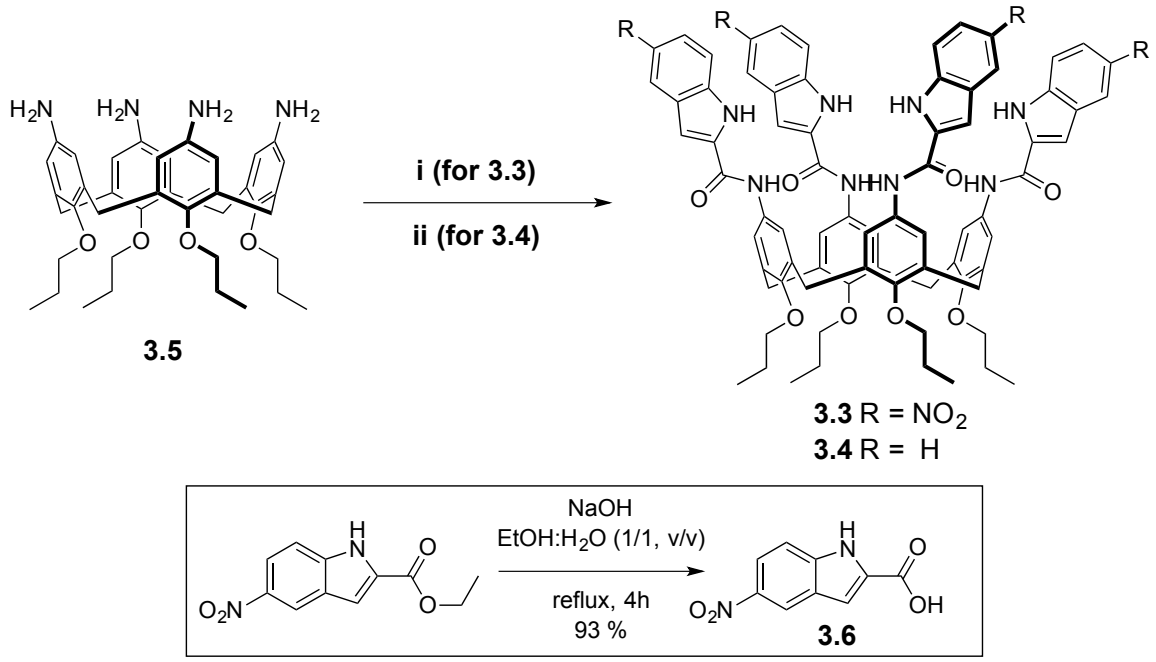

Scheme 3.1: Syntheses of compounds **3.3** and **3.4**. i) 5-Nitroindole-2-carboxylic acid, EDCI, HOBt, DMAP, DMF at room temperature for 6 h; ii) indole-2-carboxylic acid, HOBt, DMAP, DCM/THF (2:1, v/v) at room temperature for 4h.

The use of amidoindole motifs for anion recognition is very attractive because these subunits provide additional hydrogen bonding donors as compared to simple indole or urea-factionalized calix[4]arene derivatives. In addition, indoles conjugated with amide groups absorb and emit light under coordination of UV/Vis irradiation. It was thus expected that compounds **3.3** and **3.4** would act as colorimetric sensors for anions.

Compounds **3.3** and **3.4** were found to be soluble in a moderately polar solvent mixture (5~10 % DMSO in $CHCl_3$). Poor solubility was seen in relatively less polar solvents, a finding attributed to the formation of strong inter- or intramolecular hydrogen bonds among the amidoindole groups. However, the addition of certain anions to

suspensions of these compounds led to an immediate increase in solubility in almost all cases. We propose that this increase reflects an anion-induced break up of the aforementioned hydrogen-bonding interactions.[10] Treatment of turbid mixture of compound **3.3** with approximately 5.0 molar equivalents of various anions as their TBA salts allowed visual differentiation. Figure 3.2 shows photos of receptor **3.3** in 5% DMSO in chloroform before and after addition of various anions (as their TBA salts). As can be seen from an inspection of a Figure 3.2, all anions but bromide and iodide resulted in complete solubilization of the receptor as reflected by production of a clear solution from the original turbid suspension. A discernable color change was seen in the case of F-, which likely reflects a degree of NH deprotonation.

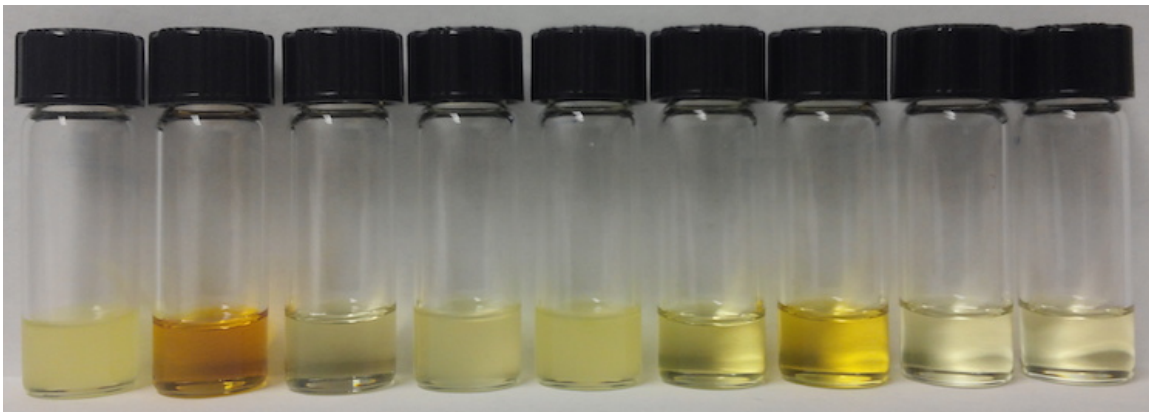

Figure 3.2: Solutions of receptor **3.3** (1 mM) in DMSO/$CHCl_3$ (1/9, v/v) photographed in the absence and in the presence of 5 equiv of various TBA anion salts. From left to right: **3.3** only, F^-, Cl^-, Br^-, I^-, $H_2PO_4^-$, $HP_2O_7^{3-}$, HSO_4^- and SO_4^{2-}.

In the first set of analyses (Figure 3.3), the ability of receptor **3.3** to bind various anions (I^-, Br^-, Cl^-, F^-, NO_3^-, $HP_2O_7^{3-}$, $H_2PO_4^-$, SO_4^{2-}, HSO_4^- and HCO_3^-) as their TBA^+ salts in $CDCl_3$/DMSO-d_6 (95/5, v/v) was investigated *via* ^1H NMR spectroscopy. In the case of Cl^- and $H_2PO_4^-$, the NH proton signals of both the indole and the amide groups were significantly shifted to lowerfield, presumably, as the result of strong hydrogen bond interactions between the NH protons and the bound anions. In contrast, compound **3.4** which lacks the nitro groups, was found to bind these anions with relatively low affinity in $CDCl_3$/DMSO-d_6 (95/5, v/v) compared to compound **3.3**, as inferred from similar ^1H NMR spectroscopic analyses. These findings can be attributed to the electron withdrawing nitro substituents of **3.3** resulting in the NH moieties being relatively more acidic and hence better hydrogen bond donors (Figure 3.4).

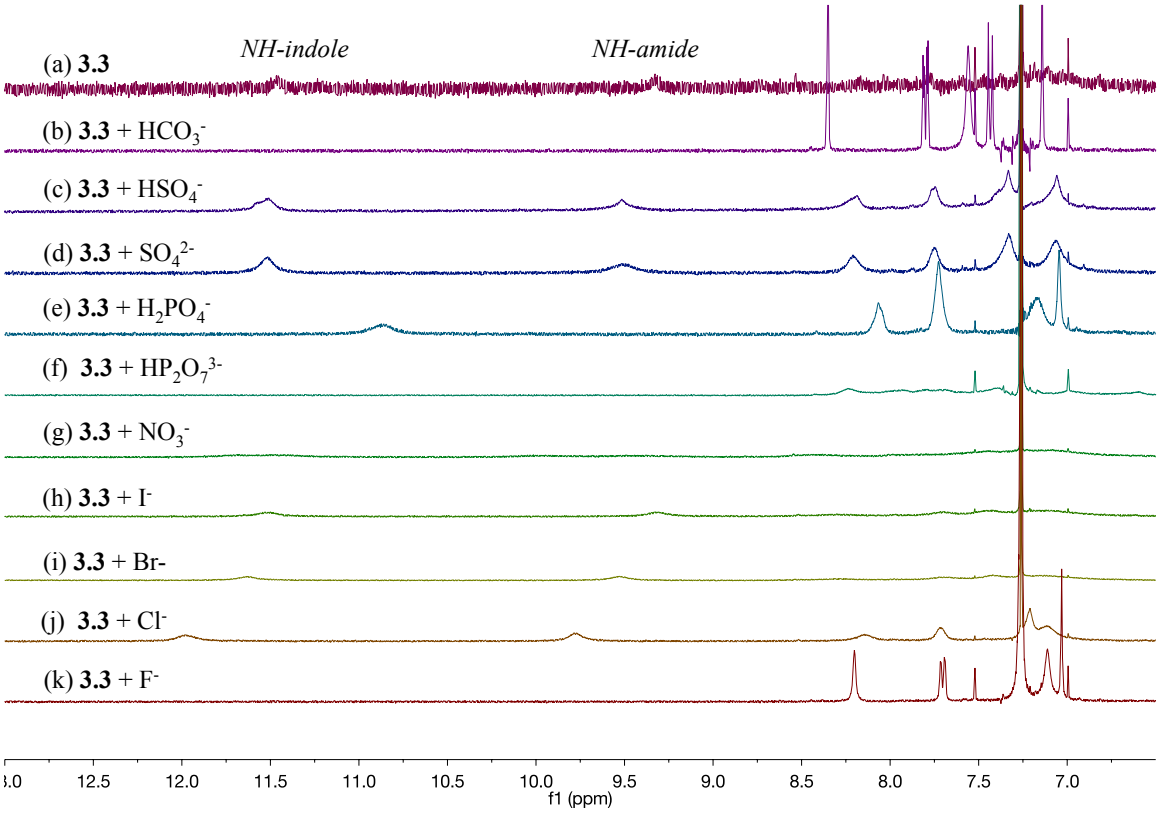

Figure 3.3: Partial ^{1}H NMR spectra of **3.3** (3 mM) recorded in DMSO-d_6/$CDCl_3$ (1:9, v/v) in the absence and in presence of excess ions (as their TBA^+ salts) (a) **3.3** only, (b) **3.3** + HCO_3^-, (c) **3.3** + HSO_4^-, (d) **3.3** + SO_4^{2-}, (e) **3.3** + $H_2PO_4^-$, (f) **3.3** + $HP_2O_7^{3-}$, (g) **3.3** + NO_3^- (h) **3.3** + I^- (i) **3.3** + Br^- (j) **3.3** + Cl^-, and (k) **3.3** + F^-.

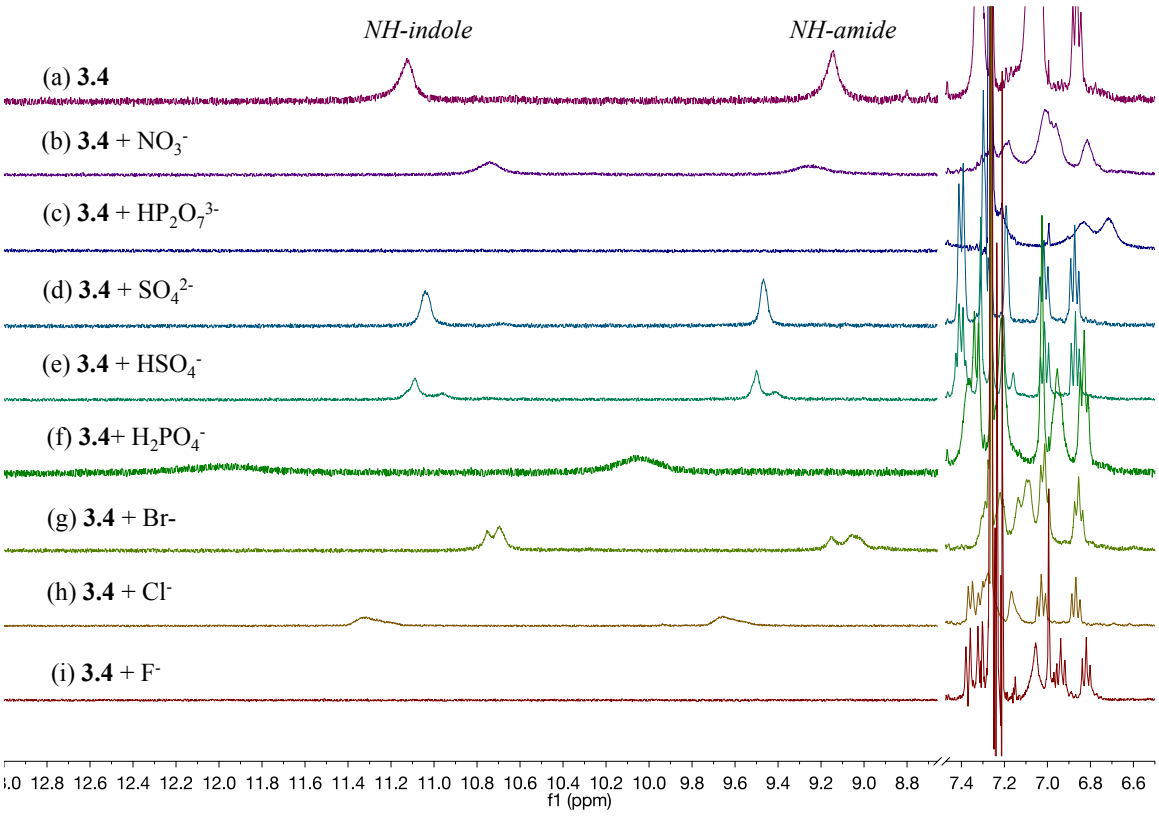

Figure 3.4: Partial ^{1}H NMR spectra of **3.4** (3 mM) recorded in DMSO-d_6/$CDCl_3$ (1:9, v/v) in the absence and in presence of excess ions (as their TBA salts) (a) **3.4** only, (b) **3.4** + HCO_3^-, (c) **3.4** + HSO_4^-, (d) **3.4** + SO_4^{2-}, (e) **3.4** + $H_2PO_4^-$, (f) **3.4** + $HP_2O_7^{3-}$, (g) **3.4** + NO_3^- (h) **3.4** + I^- (i) **3.4** + Br^- (j) **3.4** + Cl^-, and (k) **3.4** + F^-.

In an effort to quantify their affinities for anions, compounds **3.3** and **3.4** were subjected to UV-Vis spectroscopic titration experiments using 5% DMSO in $CHCl_3$ as the solvent for reasons of solubility (Figures 3.5 and 3.8). As compared to **3.4**, compound **3.3** showed relatively large absorption band changes upon being titrated with anion. This presumably reflects electronic changes involving the 4-nitrophenyl moiety which is a part of the overall amidourea anion receptor framework. When anions are hydrogen bonded to the NH of the indole, the nitro group gives rise to an internal charge transfer resulting in

absorption band shifts in the absorption spectrum for the 3.3, the maximum absorption peak is centered around 280 nm in 5% DMSO in $CHCl_3$. Upon the addition of anions, such as $H_2PO_4^-$ (as their TBA salt) to this solution, the absorption intensity of **3.3** at 280 nm was found to increase giving rise to an isosbestic point near 380 nm. The presence of an isosbetic point leads to suggest that receptor **3.3** binds the dihydrogenphosphate anion with a 1:1 binding stoichiometry. This suggestion is further supported by ^1H NMR spectral studies. Upon titration of **3.3** with dihydrogenphosphate ion (Figure 3.9), the NH proton signals of both the indole group and the amide group were seen to undergo downfield shift and to undergo broadening. These changes were concentration dependent. The interactions with the hydrogen pyrophosphate anion were studied in a similar manger. **3.3**, when titrated with $HP_2O_7^{3-}$, three isosbestic points were observed at 305 nm, 345 nm and 395 nm, respectively. This is taken as evidence for a 1:1 binding between **3.3** and this anion. In order to support for the proposed stoichiometry, Job plot experiments were carried out with the dihydrogenphosphate anion and the hydrogen pyrophosphate anion, respectively, using UV-Vis spectroscopy (Figure 3.10). It revealed a maximum in the complex absorbance at a mole fraction of 0.5 in the case of dihydrogenphosphate ion, as would be expected for a 1:1 binding stoichiometry. On the other hand, the Job plot produced with the hydrogen pyrophosphate ion proved difficult to interpret in terms of an integer stoichiometry. The association constants (K_a) were obtained under the assumption of 1:1 binding stoichiometry (Figure 3.6 and 3.7). However, some of anions bind likely more than 1:1 binding. Therefore, another UV-Vis titrations will be performed under the different host concentration and different equation will be also adopted to secure its binding mode.

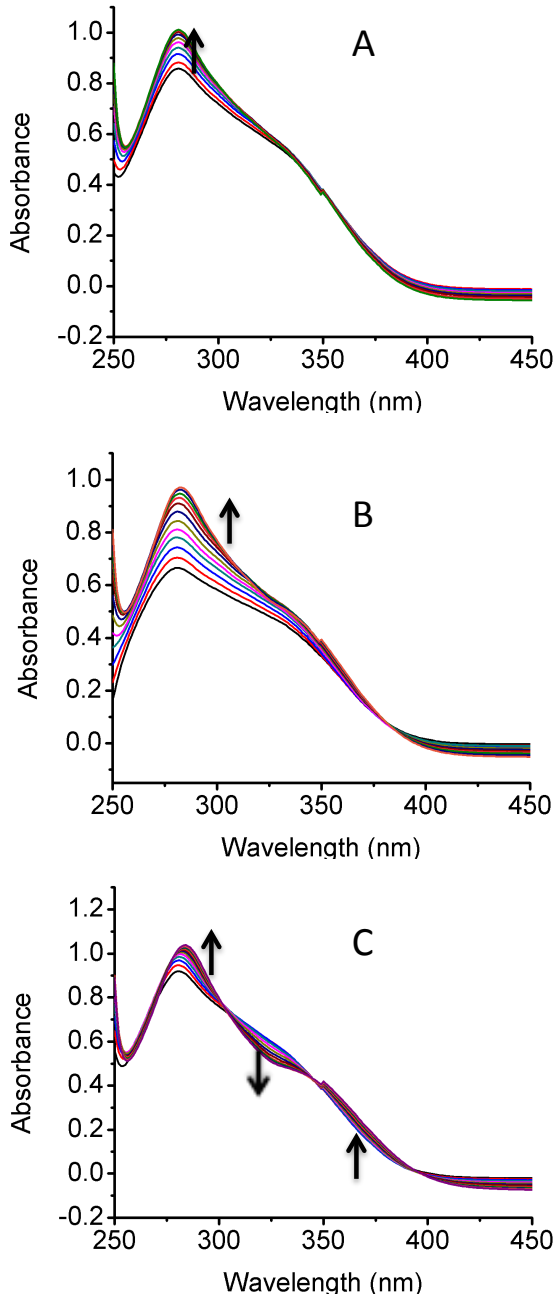

Figure 3.5: Partial UV-Vis spectra of compound **3.3** (10 μM) recorded in DMSO/$CHCl_3$ (5/95, v/v) upon the addition of various TBA^+ salts (A) Cl^-, (B) $H_2PO_4^-$, (C) $HP_2O_7^-$.

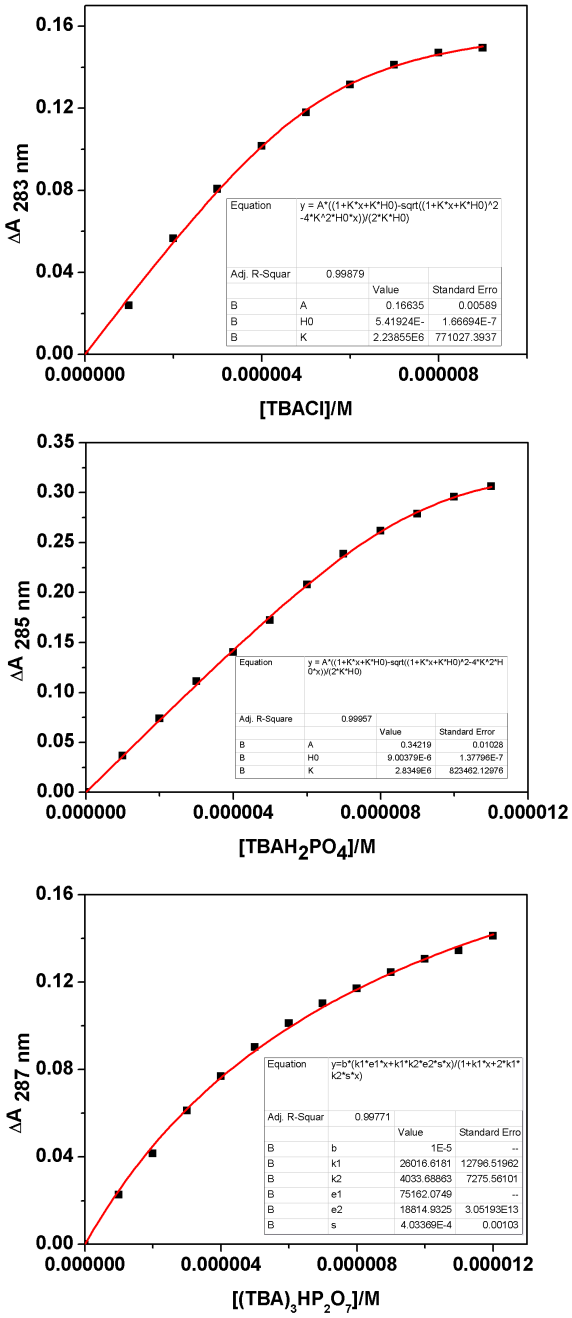

Figure 3.6: Association constants K_a (M^{-}) obtained from UV-Vis spectroscopic titration of compound **3.3** (10 μM) of (A) TBACl, (B) $TBAH_2PO_4$, (C) $(TBA)_3HP_2O_7$ in DMSO/$CHCl_3$ (5/95, v/v).

Binding constant (M^{-1})	
anions	**Compound 1**
Cl^-	4.5×10^5
$H_2PO_4^-$	2.8×10^6
$HP_2O_7^{3-}$	2.6×10^4, 4.0×10^3

Figure 3.7: Association constants (M^{-1}) obtained from UV-Vis spectroscopic titration of **3.3** (10 μM) with various TBA anion salts in DMSO/$CHCl_3$ (5/95, v/v).

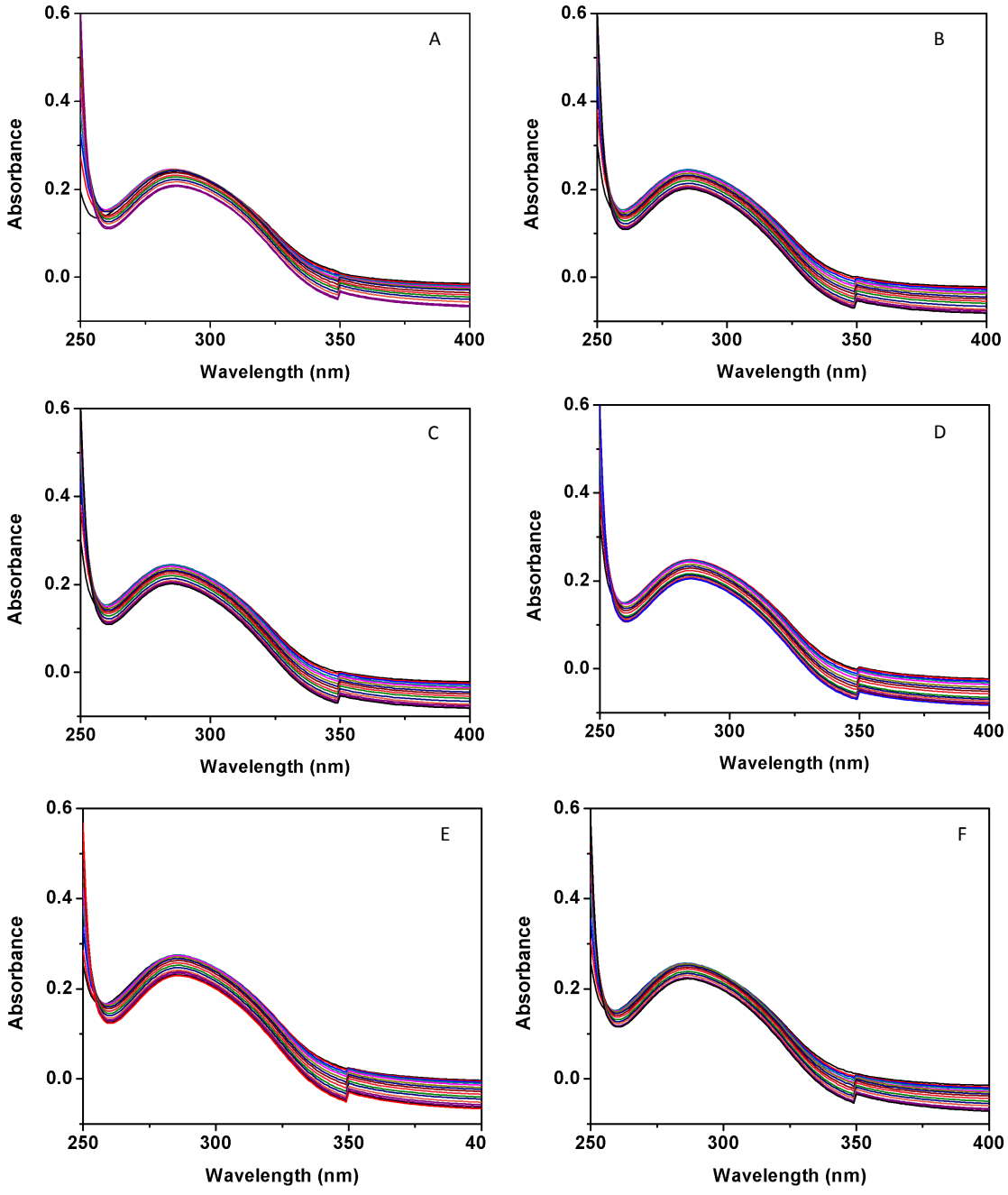

Figure 3.8: Partial UV-Vis spectra of compound **3.4** (10 μM) recorded in DMSO/$CHCl_3$ (5/95) upon addition of various TBA^+ salts (a) F^-, (b) Br^-, (c) Cl^-, (d) $H_2PO_4^-$, (e) $HP_2O_7^-$, and (f) HSO_4^-,

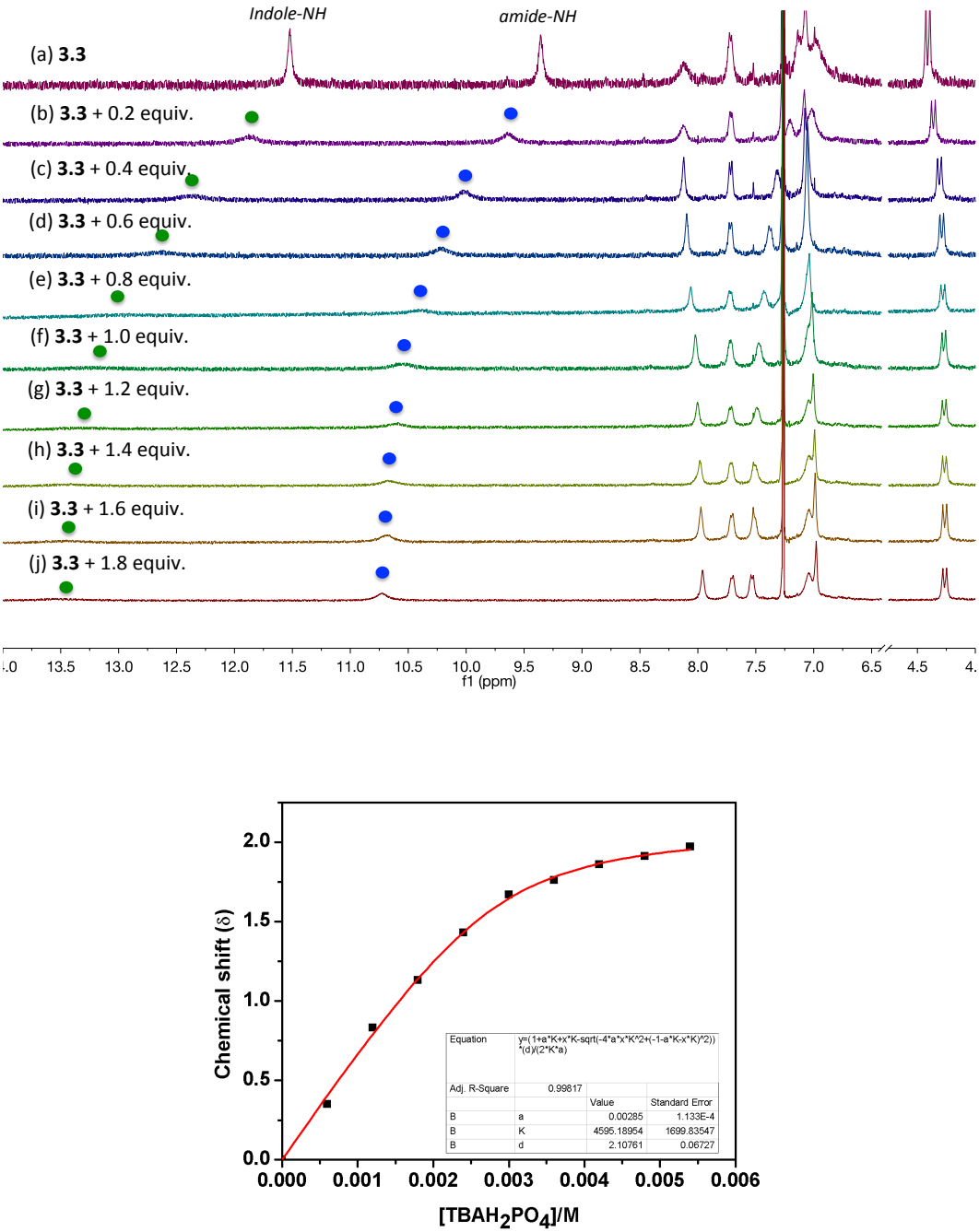

Figure 3.9: Partial ^{1}H NMR spectra recorded during the titration of compound **3.3** (3 mM) with $H_2PO_4^-$ (as TBA^+ salt) in 10% DMSO-d_6 in $CHCl_3$. Its association constant (K_a) is 4.6×10^3 M^{-1}.

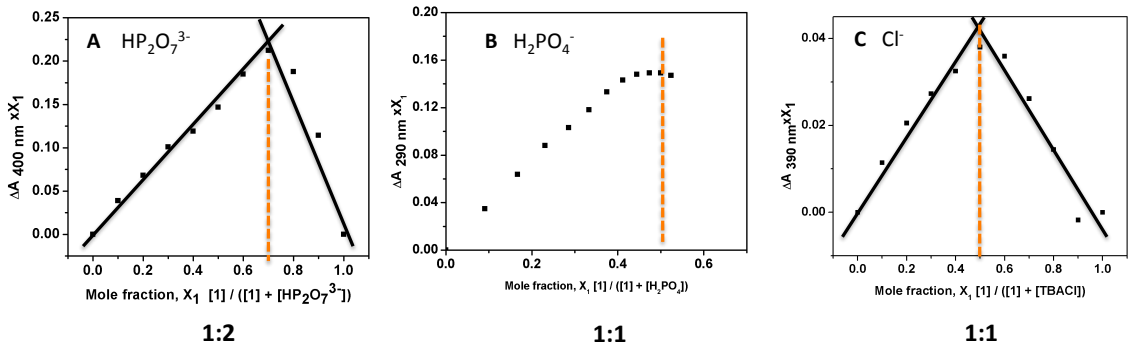

Figure 3.10: Job plots corresponding to the interaction of compound **3.3** (0.15 mM) with the TBA^+ salts of (A) $HP_2O_7^{3-}$, (B) $H_2PO_4^-$ and (c) Cl^- as recorded using UV-Vis spectroscopy in DMSO/ $CHCl_3$ (5/95, v/v).

Because compounds **3.3** and **3.4** have not only anion binding sites of amidoindoles but also a cooperative cation binding site consisting of four phenoxy groups, their ability to bind ion pairs such as LiCl and NaCl including relatively small cation was investigated. This was done using ^1H NMR spectroscopic methods. In the case of the nitro-substituted receptor **3.3**, little appreciable ^1H NMR spectral change was observed upon exposure to LiCl and NaCl (Figures 3.11 and 3.13). The observation leads us to suggest that neither LiCl nor NaCl is bound to receptor **3.3** strongly. This finding stands in sharp contrast in what was seen with compound **3.4**. For example, as seen in Figure 3.13, the two NH signals corresponding to the indole subunits and those of the amide NH protons underwent significant downfield shifts when exposed to LiCl but not to NaCl. This was ascribed to hydrogen bond formation between NHs and the chloride anion of LiCl. On the other hand, the downfield shift of the aromatic proton peak of the calix[4]arene presumably results from the binding of the lithium cation to the oxygen atoms of the phenoxyl groups. Taken together, these results lead us to propose that compound **3.4** is able to form an ion pair complex with LiCl. High resolution mass

spectroscopic analysis also supports complexation of the Li^+ ion with compound **3.4** (Figure 3.15).

The different LiCl binding behavior seen for **3.3** and **3.4** is ascribed to the relative acidity of the amidoindole moiety, which in the case of **3.4** results in intermolecular hydrogen bonding interaction between free receptors. As evidenced by a mass spectrometric analysis (Figure 3.19), compound **3.3** with its relatively more acidic amidoindole NHs protons, exists as an aggregated form in its free form. To prove this hypothesis, various concentration studies will be performed to observe concentration dependence.

In an effort to obtain support for the suggestion that Li^+ and Cl^- are co-bound to receptor **3.4**, more detailed binding studies using ^1H NMR spectroscopy were performed in DMSO-d_6/$CDCl_3$ (1,9/ v/v). When compound **3.4** was exposed to the lithium cation (as their perchlorate salt) the NH proton signals corresponding to the indole groups and the amide groups were slightly shifted, albeit in opposite directions as shown in Figure 3.14. In contrast, the aromatic proton signal of the calix[4]arene framework undergo a slight downfield shift, presumably as the result of the lithium cation being bound to the calix[4]arene, *via* its oxygen atoms. In contrast, treatment of **3.4** with the chloride anion (as its TBA salt) gives rise to a small downfield shift in the NH proton signals of the amidoindole groups ($\Delta\delta \approx 0.3$ ppm). Noticeably, in the presence of both the lithium cation and the chloride anion in the same solution (from LiCl or from a combination of salts that provide a mixture of these ions in situ), receptor **3.4** showed even larger downfield shift of the NH proton signals as well as the aromatic proton signals of the calix[4]arene. These changes are larger than what are seen in the presence of either Cl^- or Li^+ when the ions are added as salts containing noncompetitive counteranions (Figure

3.14). These findings are consistent with the proposition that **3.4** binds Li^+ and Cl^- concurrently to form an ion pair complex.

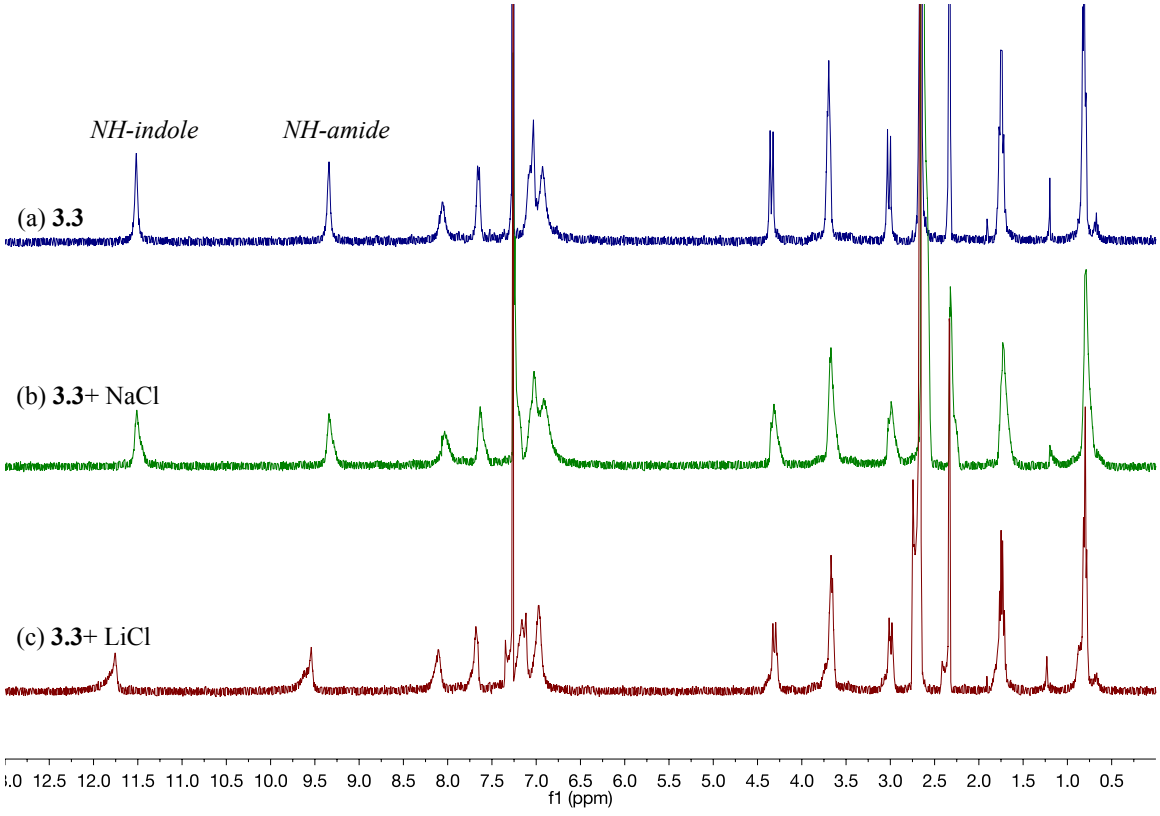

Figure 3.11: Partial ^{1}H NMR spectra of (a) **3.3** only, (b) **3.3** after exposure to an excess of NaCl, (c) **3.3** after exposure to an excess of LiCl in DMSO-d_6/$CDCl_3$ (1/9, v/v). The spectra were recorded after subjecting to sonication for roughly 30 min.

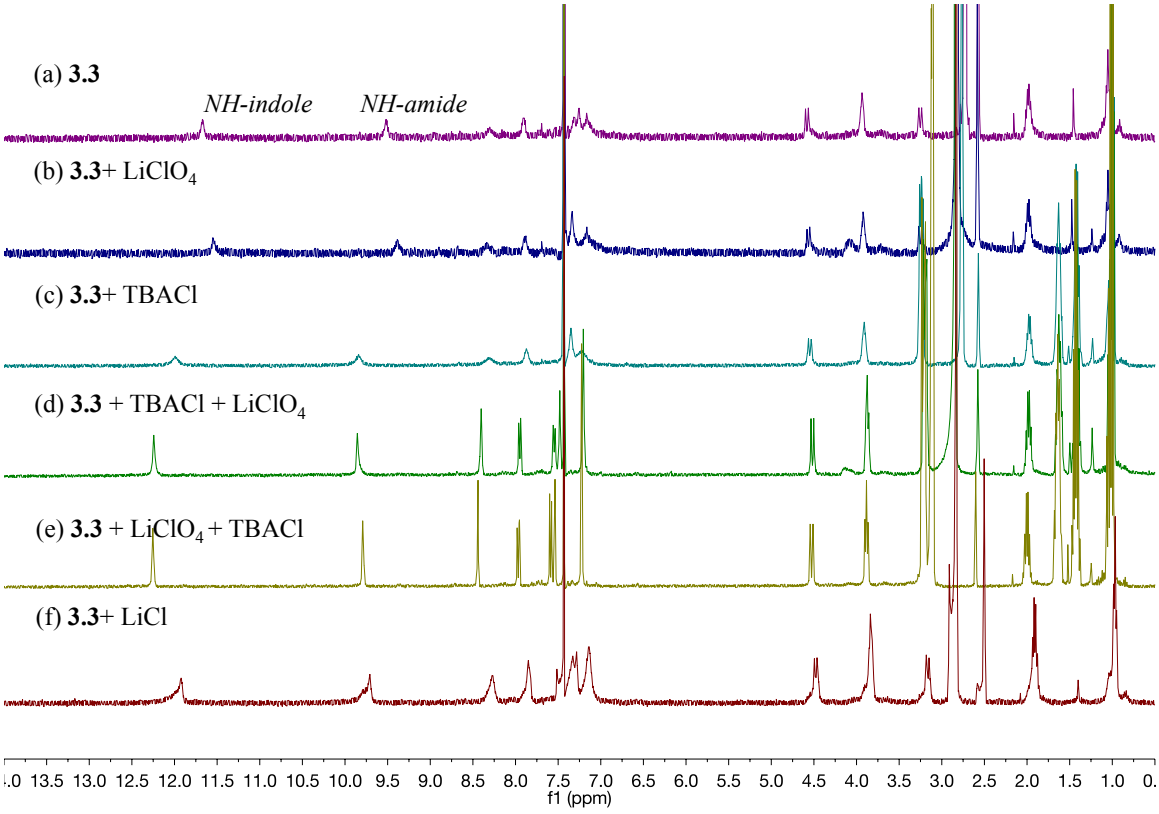

Figure 3.12: Partial ^{1}H NMR spectra of (a) **3.3** only, (b) **3.3** after exposure to an excess of $LiClO_4$, (c) **3.3** after exposure to an excess of TBACl, (d) **3.3** with excess of TBACl + $LiClO_4$, (e) **3.3** with excess of $LiClO_4$ + TBACl, (f) **3.3** with excess of LiCl in DMSO-d_6/$CDCl_3$ (1/9, v/v). The spectra were recorded after subjecting to sonication for roughly 30 min.

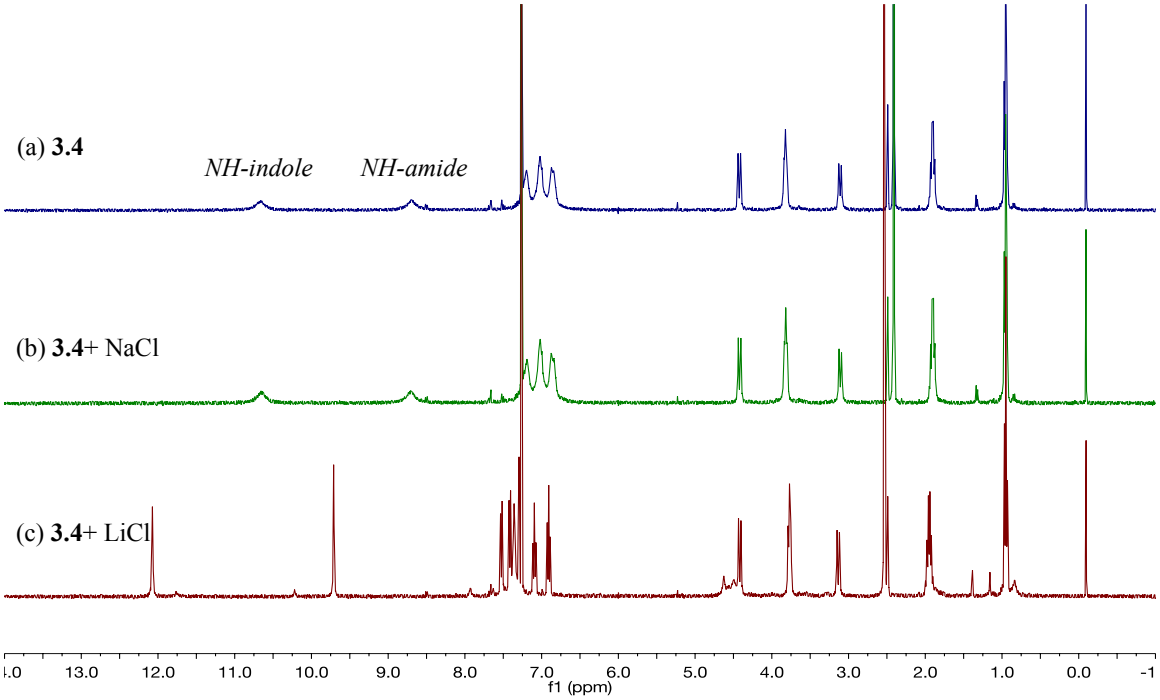

Figure 3.13: Partial ^{1}H NMR spectra of (a) **3.4** only, (b) **3.4** after exposure to an excess of NaCl, (c) **3.4** after exposure to an excess of LiCl in DMSO-d_6/$CDCl_3$ (1/9, v/v). The spectra were recorded after subjecting to sonication for roughly 30 min.

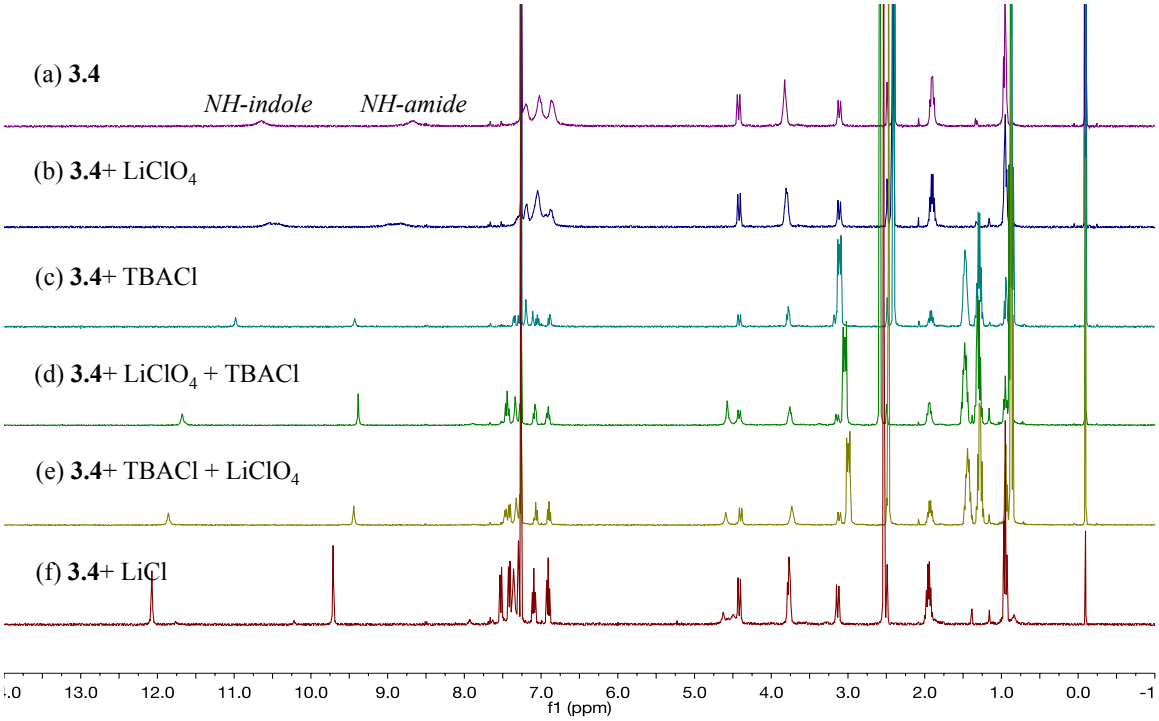

Figure 3.14: Partial ^{1}H NMR spectra of (a) **3.4** only, (b) **3.4** after exposure to an $LiClO_4$, (c) **3.4** after exposure to an TBACl, (d) **3.4** with excess of $LiClO_4$ + TBACl, (e) **3.4** with excess of TBACl + $LiClO_4$, (f) **3.4** with excess of LiCl in DMSO-d_6/$CDCl_3$ (1/9, v/v). The spectra were recorded after roughly 30 min. of sonication.

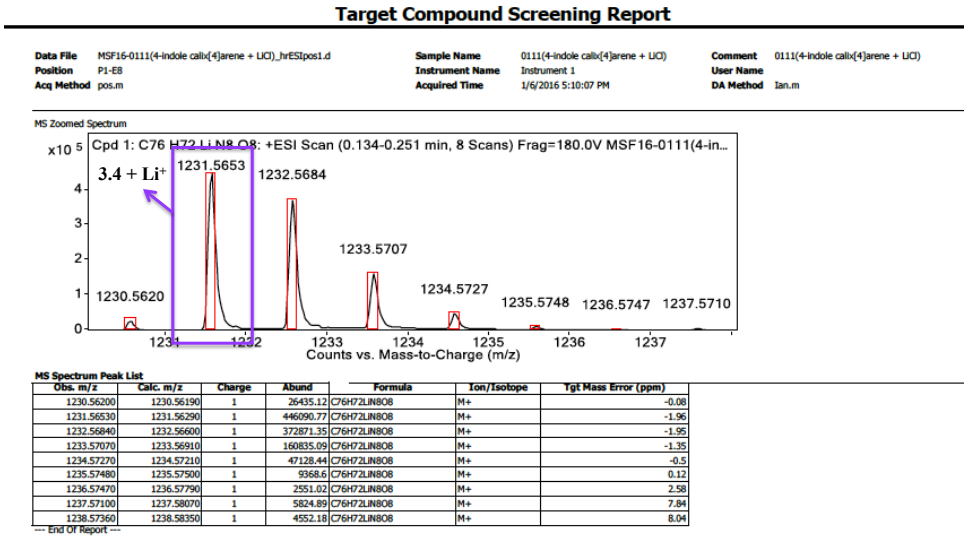

Obs. m/z	Calc. m/z	Charge	Abund	Formula	Ion/Isotope	Tgt Mass Error (ppm)
1230.56200	1230.56190	1	26435.12	C76H72LiN8O8	M+	-0.08
1231.56530	1231.56290	1	446090.77	C76H72LiN8O8	M+	-1.96
1232.56840	1232.56600	1	372871.35	C76H72LiN8O8	M+	-1.95
1233.57070	1233.56910	1	160835.09	C76H72LiN8O8	M+	-1.35
1234.57270	1234.57210	1	47128.44	C76H72LiN8O8	M+	-0.5
1235.57480	1235.57500	1	9368.6	C76H72LiN8O8	M+	0.12
1236.57470	1236.57790	1	2551.02	C76H72LiN8O8	M+	2.58
1237.57100	1237.58070	1	5824.89	C76H72LiN8O8	M+	7.84
1238.57360	1238.58350	1	4552.18	C76H72LiN8O8	M+	8.04

Figure 3.15: HRMS of Li^+ ion complexced compound **3.4**

The changes observed in ^{1}H NMR spectrum upon subjecting the lithium cation complex of **3.4** to titration with the chloride anion (as its TBA^+ salt) are shown in Figure 3.16. Upon addition of increasing quantities of Cl^-, the NH proton signals of both the amides and the indoles gradually move to lower field until saturation is observed after the addition of roughly 3.2 equiv. In the case of the indole NH proton signals the net change is substantial ($\Delta\delta \approx 1.2$ ppm). This observation lends further support to the above conclusion, namely that the lithium cation and the chloride anion are concurrently bound to receptor **3.4**. From these titrations, a binding constant for the complexation of Cl^- to the preformed complex **3.4**•Li^+ could be calculated as 6.26×10^2 M^{-1} (Figure 3.17). This value for chloride anion (as its TBA^+ salt) complexation is larger that seen in the case of the free receptor **3.4** (cf. Figure 3.18). The association constant for chloride anion (as

TBA^+ salts) cannot be determined because its chemical shifts were little in ^1H NMR spectroscopic studies.

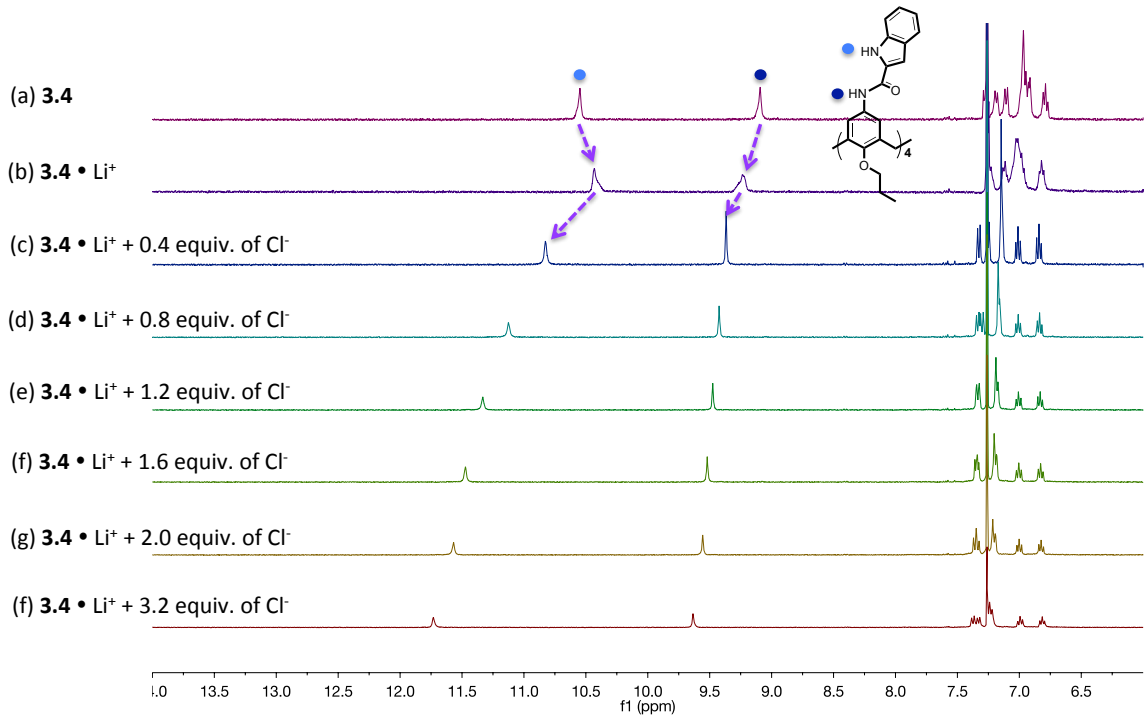

Figure 3.16: Partial ^1H NMR spectra recorded during the titration of compound **3.4** (3 mM) with Cl^- (TBA^+ salt) in presence of excess $LiClO_4$ in 10% DMSO-d_6 in $CDCl_3$. Its association constant (K_a) is 6.3×10^2 M^{-1}.

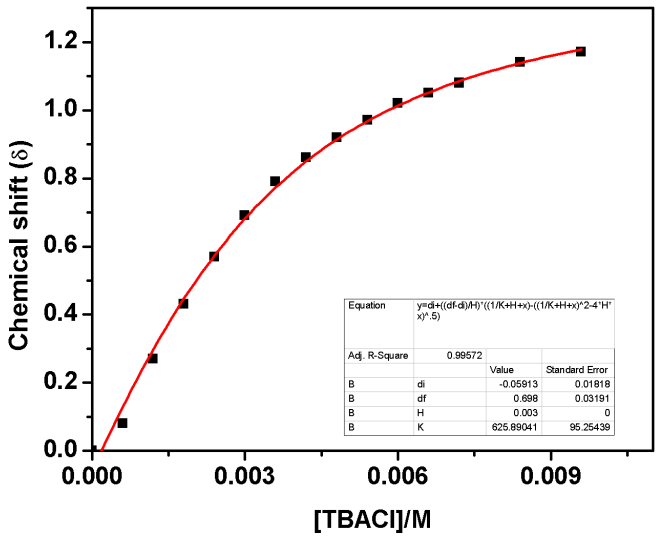

Figure 3.17: Binding isotherm (red line) and data points (black) used to calculate the binding constant (K_a; 6.3 × 10^2 M^{-1}) corresponding to the interaction of Cl^- (TBA salt) to the preformed complex **3.4**•Li^+ as obtained from a ^1H NMR spectroscopic titration carried out in DMSO-d_6/$CDCl_3$ (1/9, v/v).

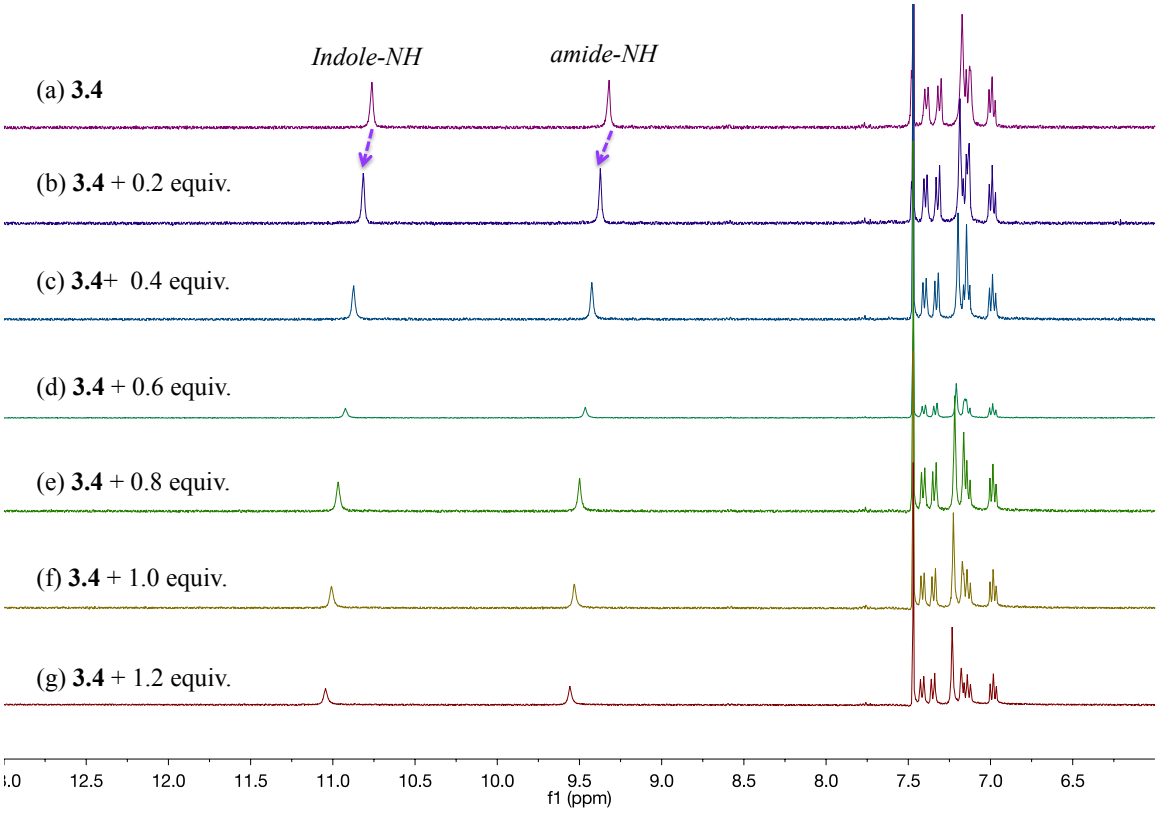

Figure 3.18: Partial ^{1}H NMR spectra recorded during the titration of compound **3.4** with Cl^{-} (TBA^{+} salt) in 10% DMSO-d_6 in $CHCl_3$.

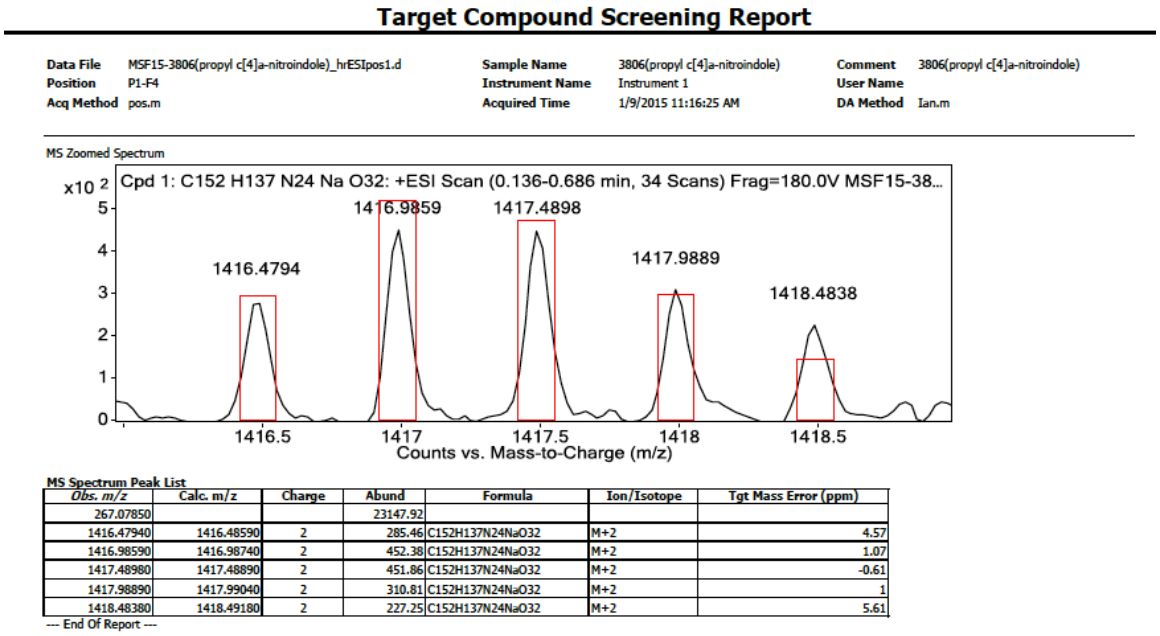

Figure 3.19: HRMS of compound **3.3**.

3.3 CONCLUSION

Calix[4]arene **3.3** and **3.4** containing four amidoindole groups at the upper rim have been synthesized as potential receptors for anions and ion pairs. Their ability to bind ions was analyzed by UV-Vis and ^{1}H NMR spectroscopy. Compound **3.3**, bearing electron withdrawing nitro groups, was found to bind anions, such as the dihydrogen phosphate and hydrogen pyrophosphate (as their TBA^{+} salts in organic media) as evidenced from spectral changes. However, as of this writing the nature of the underlying interactions has yet to be established either qualitatively or quantitatively. This is viewed as a major deficiency that needs to be addressed.

In contrast to **3.3**, its congener **3.4** shows little affinity for the phosphate salts that apparently interact well with **3.3**. However, the nitro group-free system appears to bind LiCl selectively under conditions of solid-liquid extraction, resulting in formation of an ion pair complex. In this case, the ^{1}H NMR spectroscopic data are consistent with a model wherein the chloride anion is bound to the amidoindole groups via multiple hydrogen bonds with the lithium cation cooperatively bound by the oxygen atoms of the calix[4]arene framework.

3.3 FUTURE DIRECTIONS

Interactions between both **3.3** and **3.4** with ions have yet to be established either qualitatively or quantitatively. Further efforts to support its binding stoichiometry and binding affinity addressed in this chapter will be required.

The tetra-amidoindole subsutituted calix[4]arenes receptors **3.3** and **3.4** are soluble in a moderately polar solvent system (5~10% DMSO in $CHCl_3$). The relatively poor solubility seen in less polar media was ascribed to the presence of strong inter- or intramolecular hydrogen bonds between the amidoindole subunits. The creation of analogues based on the use of ethyl ester moieties, which are expected to engage less in such hydrogen bonding interactions than their amide-containing analogues, might give more soluble systems that are suitable for use in less polar media, such as chloroform. Such an approach is embodied in calix[4]arene **3.7**.

Preliminary work has been carried out to prepare compound **3.7** as shown in Scheme 3.2. The preparation of **3.7** starts with the tetra-aminocalix[4]arene **3.8**, which

was synthesized using known procedures.[11] Reaction of **3.8** with **3.9** in THF at reflux for 4 hour gave receptor **3.7** in 31% yield. Compound **3.7** gave rise to a ^{1}H NMR spectrum consistent with the expected structure as shown in Figure 3.20. Moving forward, additional analyses, such as those coming from ^{13}C NMR spectroscopy, HRMS, and HPLC analyses, will be needed to confirm the identity and purity of compound **3.7**. Once its structure has been securely established, its ability to function as either an ion or an ion pair will be investigated.

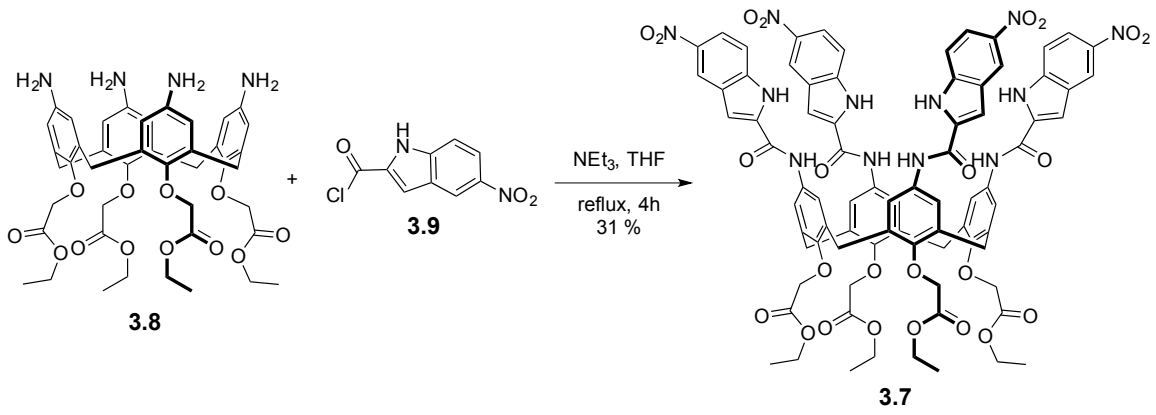

3.8 **3.9** **3.7**

Scheme 3.2: Target **3.7** and its synthesis.

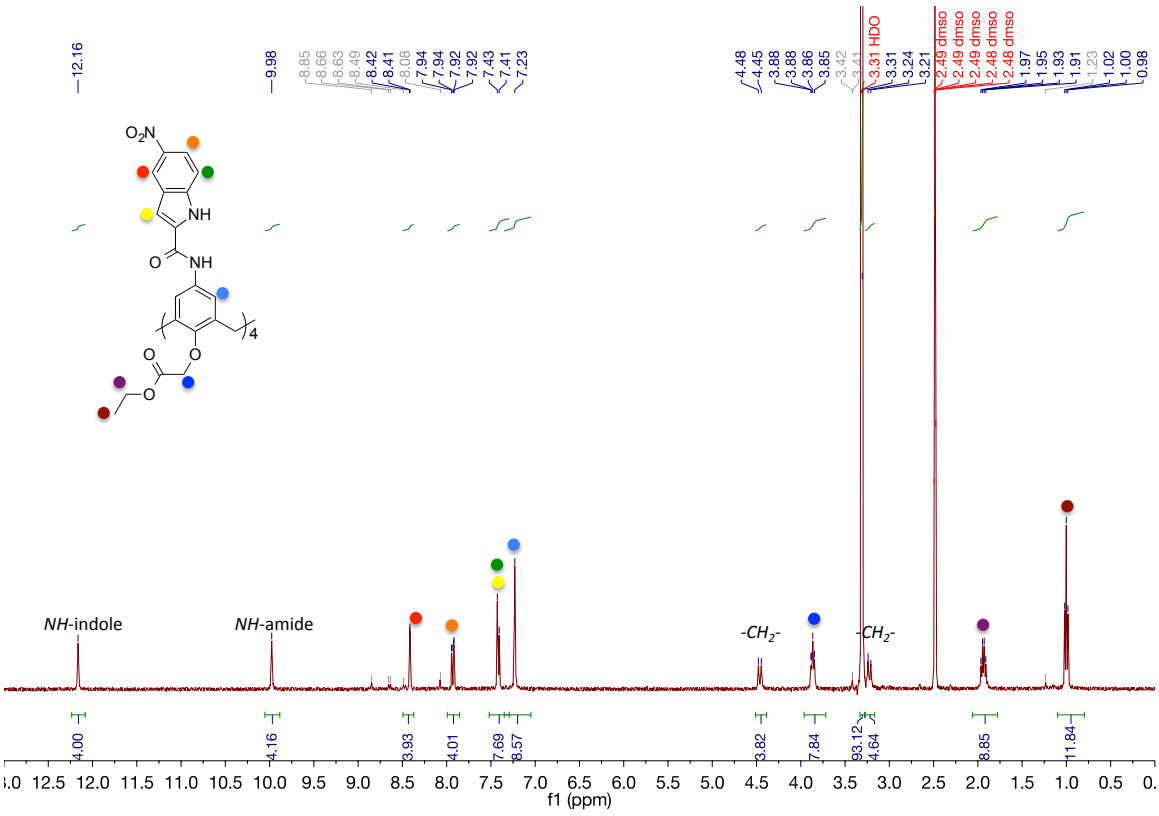

Figure 3.20: ^{1}H NMR spectroscopy of compound **3.7** recorded in DMSO-d_6.

3.4 REFERENCE

1) Sheerder, J.; van Duynhoven, J. P. M.; Engbersen, J. F. J.; Reinhoudt, D. N. *Angew. Chem. Int. Ed.* **1996**, *35*, 1090-1093.

2) Oarkesh, R.; Lee, T. C.; Gunnlaugsson, T. *Org, Biomol. Chem.* **2007**, *5*, 310-317. (b) Callan, J. F.; de Silva, A. P.; Magri, D. C.; *Tetrahedron* **2005**, *35*, 8551-8588. (C) gunnlaugsson, T.; Leonard, J. P.; Murrey, N. S. *Organic. Lett.* **2004**, *6*, 1557-1560. (d) de Silva, A. P.; Gunaratne, H. Q. N.; Gunnlaugsson, T.; Huxley, A. J. M.; McCoy, C. P.; Rademacher, J. T.; Rice, T. E. *Chem. Rev.* **1997**, *97*, 1515-1566.

3) García-España, E.; Díaz, P.; Lienaíes, J. M.; Bianchi, A. *Coord. Chem. Rev.* **2006**, *250*, 3094-3117.

4) (a) Sessler, J. L.; Camiolo, S.; Gale, P. A.; *Coord. Chem. Rev.* **2003**, *240*, 17-39. (b) Best, M. D.; Tobey, S. L.; Anslyn, E. V. *Coord. Chem. Rev.* **2003**, *240*, 3-15. (c) Choi, K.; Hamilton, A. D.; *Coord. Chem. Rev.* **2003**, *240*, 101-110.

5) (a) Chrisstoffels, L. A. J.; de Jong, F.; Reinhoudt, D. N.; Sivelli, S.; Gazzola, L.; Casnati.; Ungaro, R. *J. Am. Chem. Soc.* **1999**, *121*, 10142-10151. (b) Bohmer, V. *Angew. Chem. Int. Ed.* **1995**, *34*, 713-745. (c) Tuntulani, T.; Thavornyutikarn, P.; Poompradub, S.; Jaiboon, N.; Ruangpornvisuti, V.; Chaiohit, N.; Asfani, Z.; Vicens, J. *Tetrahedron*, **2002**, *58*, 10277-10292.

6) (a) Gale, P. A. *Coord. Chem. Rev.* **2000**, *199*, 181-233. (b) Gale, P. A. *Coord. Chem. Rev.* **2001**, *213*, 79-128.

7) Scheerder, J.; Fochi, M.; Engbersen, J. F. E.; Reinhoudt, D. N. *J. Org. Chem.* **1994**, *59*, 7815-7820.

8) Dudie, M.; Colombo, A.; Sansone, F.; Casnati, A.; Donofrio, G.; Ungaro, R. *Tetrahedron* **2004**, *60*, 11613-11618.

9) Wang, F.; Zhang, J.; Ding, X.; Dong, S.; Liu, M.; Zheng, B.; Shijun, W.; Ling, Y.; Yu, Y.; Gibson, H. W.; Huang, F. *Angew. Chem. Int. Ed.* **2010**, *49*, 1090-1094.

10) (a) Vysotsky, M. O.; Bolt, M.; Thondorf, I.; Böhmer, V. *Chem. Eur. J.* **2003**, *9*, 3375-3382. (b) Vysotsky, M. O.; Thondorf, I.; Böhmer, V. *Org. Lett.* **2000**, *2*, 3571-3574. (c) Mogck, O.; Böhmer, V.; Vogt, W. *Tetrahedron* **1996**, *52*, 8489-8496.

11) Scheerder, J.; van Duynhoven, J. P. M.; Engbersen, J. F. J.; Reinhoudt, D. N. *Angew. Chem. Int. Ed.* **1996**, *35*, 1090-1093.

Chapter 4: Crown-6-ether Strapped Calix[4]arene Bearing Pyrenyl Moieties Towards the Detection of the Cs^+ Ion Using Graphene Field-Effect Transistors

4.1 INTRODUCTION

The detection of metal cations is of great interest to chemists, biologists, clinical biochemists, and environmentalists. Among the cations of analytical importance is $^{137}Cs^+$. This radioactive species has draw enormous attention as the result of the Daiichi nuclear power plant explosion in Japan in March of 2011. This accident provoked renewed efforts to develop small molecules capable of detecting cesium, particularly those that could function on in aqueous environments where other salts are present in large excess.

Ether-based macrocycles have a strong affinity for alkali metal cations because of chelation and macrocyclic preorganization effects. Calix[4]arenes, cyclic tetramers with phenolic and methylene moieties, are capable of chelating various ions. Moreover, they can be modified to tone their affinities and thus target particular analysis. Such characteristics have made calixarenes attractive for use in a number of fields.[2] Among other applications, calix[4]arene derivatives have been used to produce chemical sensors for heavy metal and alkali metal cations.[3] Crown-ether linked calix[4]arenes have for instance, high affinities been developed that alkali and alkaline-earth metal ions.[4] Additionally, 1,3-alternate crown-6-ether strapped calix[4]arene has been reported that exhibits high selectivity towards the Cs^+ cations in both acidic and alkaline media. This system is an effective extractant displaying ratios for Cs^+/Na^+ and Cs^+/K^+ exceeding 10^4 and 10^2 in this case of the nitrate salts under conditions of aqueous-organic two phase extraction.[5] For sensing, ^1H NMR spectroscopic, atomic absorption spectrometry, and ion sensitive electrodes have all been exploited as the analytical methods. Optical sensors are

also of interest, as noted in Chapter 2.[6] However, the synthesis of optical sensors for Cs^+ remains challenging. Therefore, as an alternative to other Cs^+ sensors we have sought to use an electronic ion sensing approach. This chapter details progress made in pursuit of this objective using modified graphene.

Graphene exhibits remarkably high carrier mobility, high carrier density, and low intrinsic noise. These characteristics promise a high signal-to-noise ratio in detection when graphene is incorporated into an electronic sensor system.[7] As a general rule, the conductance of graphene is highly sensitive to local electrical and chemical perturbations. This reflects the fact that every atom of a graphene film is exposed to the environment. In addition, the Fermi level of zero-bandgap graphene can be modulated by the gate voltage. As a consequence, the charge carriers can be either holes or electrons depending on the gate voltage.[8] Such ambipolar properties allow the desired working point to be set. When detection is based on a field-effect, a large bandgap is desired. The bandgap of graphene can be increased by reducing atomistic or chemical dopants. Using these purified forms the electronic fluctuation can be read using graphene-bound field-effect transistors.[9] In this work, a new approach to detecting the Cs^+ cation based on crown-ether strapped calix[4]arene modified graphene field-effect transistors (GFETs) is prepared.

This approach relies on compound **4.1**, a crown-ether linked calix[4]arene. This derivative bears pyrene moieties to facilitate interaction with the graphene via π–π donor-acceptor interactions. The idea is then that this cesium receptor **4.1** will alter the electronic behavior of the GFETs and this modulation will be perturbed upon complexation of the Cs^+ ion. If the design works as desired the response will depend on the concentration and characteristics of the Cs^+ ions, thus enabling quantitative and selective detection of this critical species.

4.2 RESULTS AND DISCUSSIONS

4.2.1 Synthesis and Spectroscopic Studies of Receptor 4.1

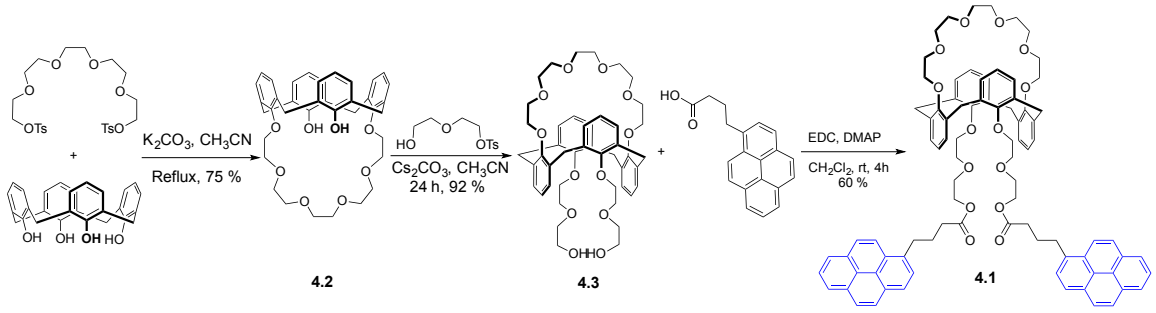

Scheme 4.1: Synthesis of the pyrene-fuctionalized crown-6-ether strapped calix[4]arene receptor **4.1**.

Compound **4.3**, key precursor for **4.1** was prepared by reported literature.[10] Esterification with 1-pyrenebutyric acid was carried out in the presence of EDC (1-ethyl-3-(3-dimethylaminopropyl)carbodiimide) and DMAP (4-dimethylaminopyridine) over the course of 4 hours at room temperature. This gave compound **4.1** in 49% yield. The interaction of compound **4.1** with the cesium ion (as the picrate salt) was studied via ^{1}H NMR spectroscopy. Cesium binding was monitored by change in the proton resonances. As can be seen from Figure **4.1**, in the absence of the cesium salt, the Ar-CH_2-Ar protons appear at 3.7 ppm, the corresponding proton signals shifted to 3.5 ppm in the presence of excess of Cs^+ ion. Unlike what was true for the cesium cation, in adding K^+ and Na^+, led to little distinguishable change in the proton resonances, although a broadening of the spectral regions corresponding to the crown-6-ether subunit and di-ethylene glycol moieties near 3.2-3.7 ppm was observed. This broadening is characteristic of weak

interactions with the crown ether cavity and faster exchange. This is considered reasonable in light of the fact that the K^+ and Na^+ cations are smaller than the Cs^+ cation.

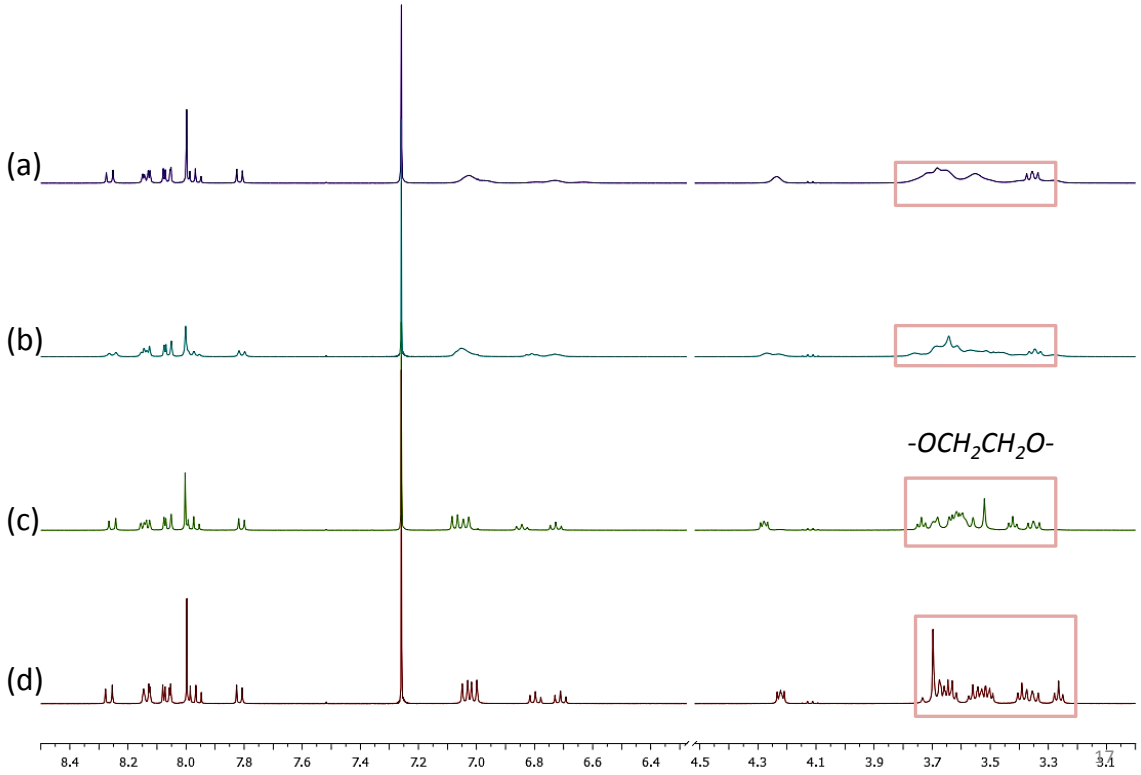

Figure 4.1: Partial ^1H NMR spectra of **4.1**, (a) **4.1** with 10 equiv of Na^+, (b) **4.1** with 10 equiv of K^+ (c) **4.1** with 10 equiv of Cs^+ and (d) **4.1** only in $CDCl_3$. The Picrate (2,4,6-trinitrophenolate) anion was used as the counterion.

Fluorescence spectroscopic studies were also performed to investigate ability of receptor **4.1** to act as a fluorescence-based chemosensor. No significant changes in the emission spectrum were observed after introducing Na^+, K^+, and Cs^+ salts to compound **4.1**. These finding lead us to that in spite of the presence of the fluorogenic pyrene

moiety, the binding properties of compound **4.1** could not be studied by fluorescence spectroscopy (Figure 4.2).

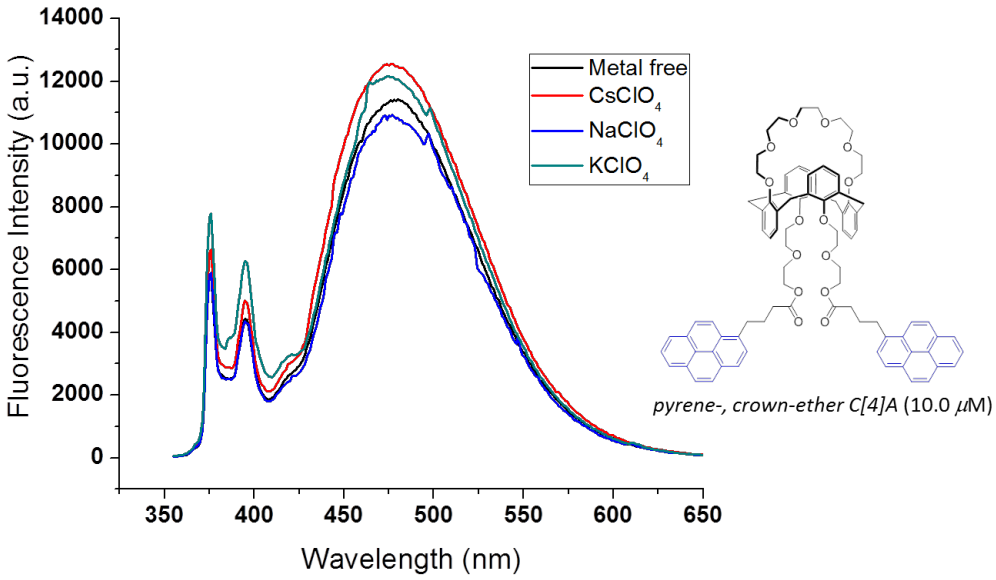

Figure 4.2: Fluorescence spectra of receptor **4.1** (10.0 μM) recorded before and after the addition of excess of Cs^+, K^+, and Na^+ (all as their perchlorate) in chloroform with excitation at 344 nm.

4.2.2 Preparation of Graphene Field-Effect Transistors

In order to fabricate graphene FETs, large-area monolayer graphene was synthesized. This was done via chemical vapor deposition (CVD) on copper foils. The resulting monolayer graphene was transferred onto a silicon oxide substrate. Source and drain electrodes were then fabricated through thermal evaporation of Au using a shadow mask, as described in Figure 4.3. The graphene FETs obtained in this way were functionalized by dipping into a 0.5 mM solution of receptor **4.1** in chloroform for 24 hr. Unbound molecules were removed by rinsing the FETs with fresh chloroform. To test the sensing performance of the graphene FETs, they were immersed in a 100 μM cesium picrate solution and dried with N_2. Then, the electrical properties of the graphene FETs were studied in order to prove the extent of interaction between the Cs^+ ion and receptor **4.1** bound on the graphene surface.

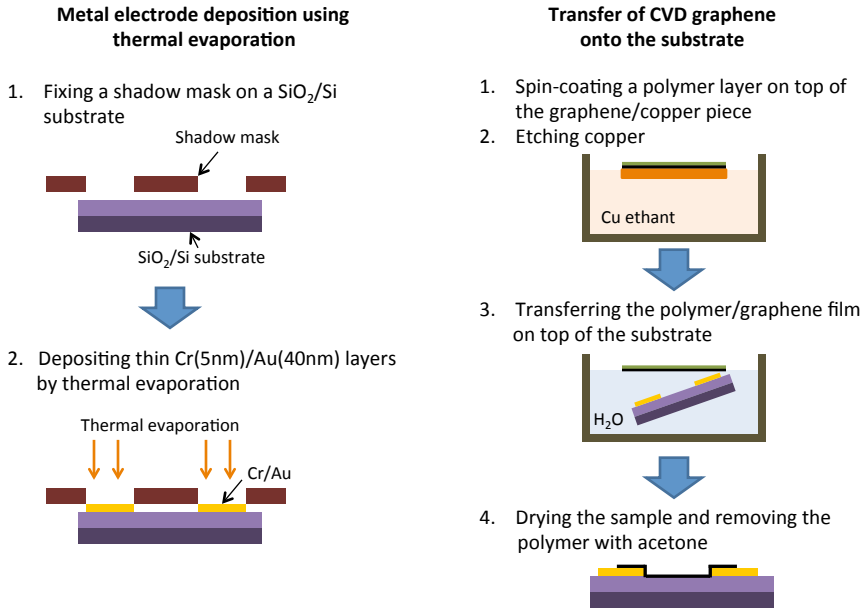

Figure 4.3: Fabrication of graphene field-effect transistors (GFETs).

4.2.3 Raman Spectroscopy and I-V Measurements

An effort was made to prove the GFETs bound on **4.1**,.Raman spectroscopy is extremely sensitive to changes in the geometric structure and surface properties of graphene. In principle, this could allow the so-called layer number, structural quality, and doping status of the modified graphene to be determined. In fact, the graphene FETs bould on **4.1** showed typical Raman signatures with a G band at 1578 cm^{-1} and a 2D band at 2665 cm^{-1}.[11] The intensity ratio of the 2D band to the G band (I_{2D}/I_G) was > 2, while the full width at half maximum (FWHM) of the 2D band was < 35 cm^{-1}. Such finding are consistent monolayer of graphene being present in the FETs.[12] Furthermore, a minimal D peak at 1350 cm^{-1} indication was seen that this was taken as high quality of the graphene was being used in this work.

After immobilizing compound **4.1** on the graphene FET (Step B in Figure 4.4), the G and 2D bands shifted to 1583 and 1678 cm^{-1}, respectively. Exposing the graphene FET in the cesium picrate solution (Step C in Figure 4.4) led to modest shifts in the G and 2D bands, the Raman peaks became broader after each step. This is consistent with increased doping.

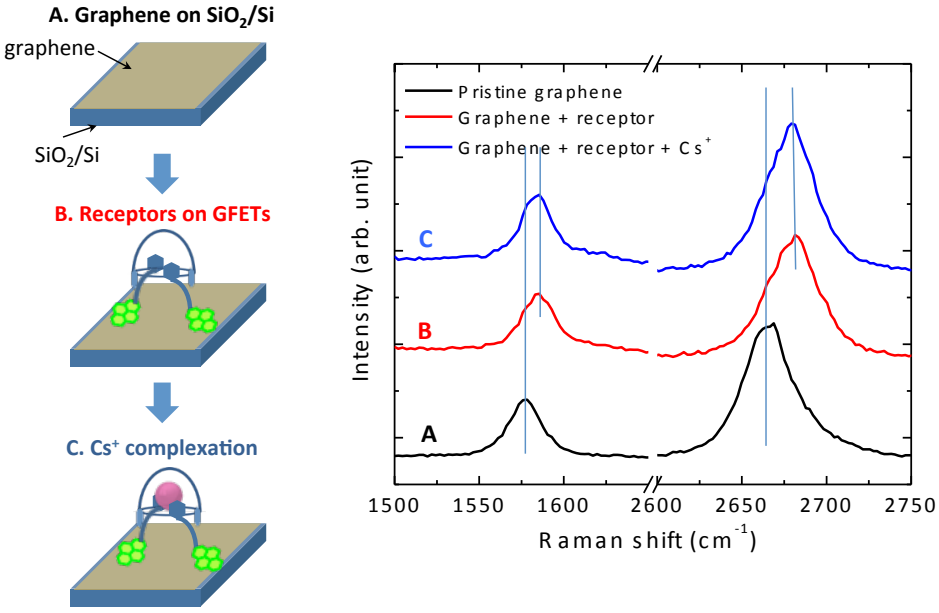

Figure 4.4: Raman spectra of GFETs: A) pristine graphene, B) GFETs functionalized with receptor **4.1** (0.5 mM), C) after exposure of the system in B) to Cs^+ picrate salt (100 μM) in acetonitrile.

Electrical measurements revealed an alteration of the conductance of the graphene FETs due to the introduction of the organic molecule and ion onto the graphene surface. Figure 4.5 shows current-voltage (I_D-V_G, I_D is the drain current, V_G is the gate voltage) characteristics of the graphene FET before and after functionalization with **4.1**. The pristine graphene FET is characterized by a typical I-V curve with a large positive shift in the Dirac point as would be expected for a graphene that is highly p-doped. Immobilization of the receptor, **4.1** on the graphene FET caused a shift in the Dirac point toward 0 V. The shift of the Dirac point toward zero gate voltage implies that the graphene FET was becoming n-doped. Exposure to CsPic in acetonitrile, the Dirac point shifted closer toward 0 V. However the shift was not large.

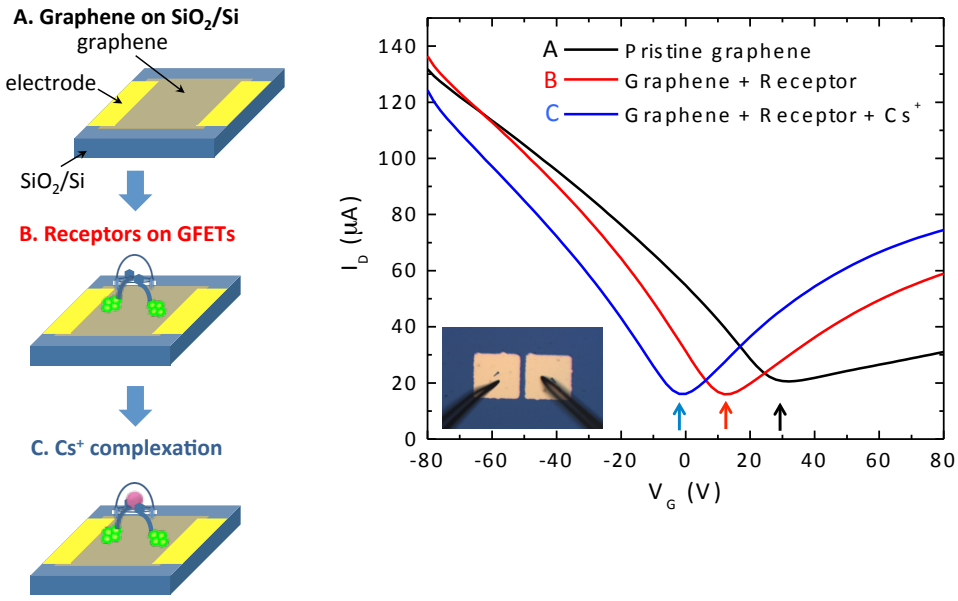

Figure 4.5: Current *versus* voltage (I-V) traces for graphene on gold electrodes; A) pristine graphene, B) GFETs functionalized with receptor **4.1** (0.5 mM), C) after exposure of the system in B) to Cs^+ picrate salt (100 μM) in acetonitrile).

The response determinants graphene FETs is not completely understood. However, based on the Raman spectroscopic observations and the electrical analyses, the following hypothesis can be developed: Graphene is highly sensitive to changes in the surface properties. As a consequence, its electrical properties can be easily altered by surface modulations. When receptor **4.1** is immobilized onto a graphene surface and if the gate voltage is negative, the flow of positively charged carriers is facile. However, upon Cs^+ cation complexation, a positive potential can be developed near the graphene surfaces. This hinders hole conduction at negative gate voltages. To the extent this true, conduction at negative gate voltages should be decreased (cf. Figure 4.6). In fact, however, relatively response to Cs^+ was seen. Further studies, including control experiments studying various factors, such as solvent, incubation time, and graphene

surface contamination will be necessary if this approach is to be developed further. Better receptors may also be required. All Raman spectroscopic studies and I-V measurements were performed by Dr. Ji Won Suk.

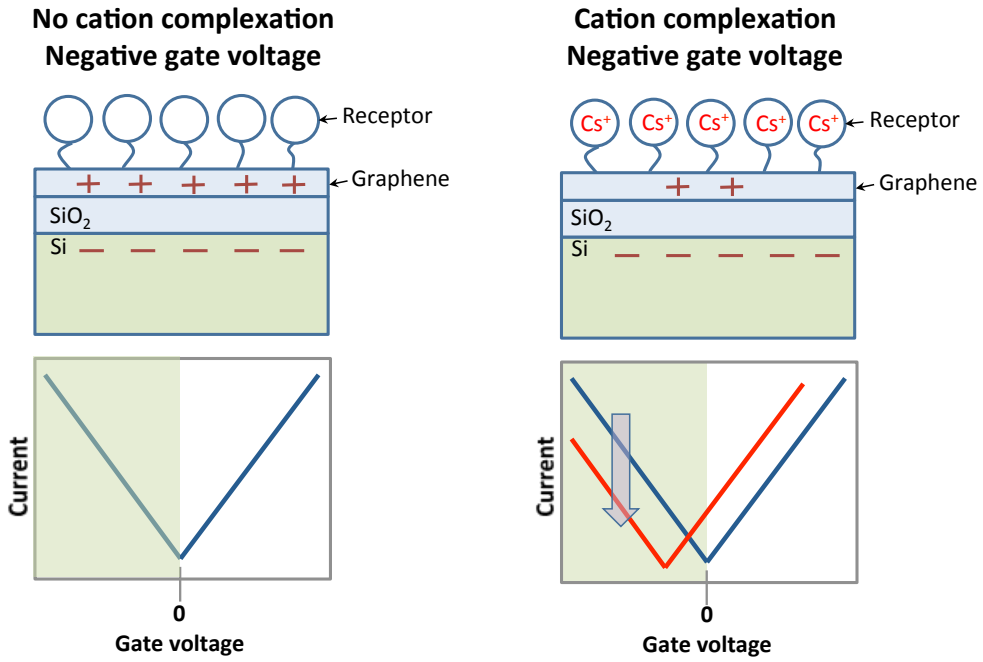

Figure 4.6: I-V response expected before and after complexation of the cesium ion for GFETs functionalized with receptor **4.1**

4.3 CONCLUSION

A Cesium cation selective receptor for using in a GFET electronic sensor was designed and synthesized. This system was based on a crown-6-ether linked calix[4]arene motif bearning pyrene groups. Its interactions with alkali metal ions (Cs^+, K^+ and Na^+; picrate anion salts) were investigated. The system was then used to construct a graphene field-effect (GFETs) device. Alternations of the GFETs before and after exposure to Cs Picrate salt in acetonitrile were studied using Raman spectroscopy and current *versus* gate

voltage (I-V) measurements. The results of these studies revealed little, if any response to Cs^+.

4.4 FUTURE DIRECTIONS

The Raman spectral shifts and Dirac point changes as the graphene FETs were functionalized with a receptor **4.1** were more dramatic than those produced by exposure to the cesium cation. These may be a modest Cs^+ dependent effect. However, it is necessary to confirm that the electronic changes come from a) the immobilization of receptor **4.1** and b) its interaction with the Cs^+ ion. Other alkali metal salts should be investigated. In addition, the sensitivity of graphene FETs should be compared to optical methods over various concentration ranges. The relationship between the electronical perturbation induced by attachment of organic receptor and, possibly, Cs^+ cation complexation has to be confirmed and then explained. Counter ion effects also should be investigated. It is hoped that the initial effects descrived in this chapter will set the stage for the eventual development of GFET-based methods for the detection of various ions, including the Cs^+ cation. This goal is presently for from being realized.

4.5 REFERENCE

1) Ludwig, R.; Nguyen, T. K. D. *Sensors*, **2002**, *2*, 397-416.

2) Solov'ev, V. P.; Strakhova, N. N.; Raevsky, O. A.; Diger, V. R.; Schneider, H.-J. *J. Org. Chem*, **1996**, *61*, 5221-5226.

3) Forster, R. J.; Caddgan, A.; Diaz, M. T.; Diamond, D *Sensors and Actuators B,* **1991**, *4*, 325-331.

4) Ramachandran, B. R.; Baker, S. D.; Suravajhula, G.; Derosa, P. A. *J. Incl. Phenom. Macrocycl. Chem.,* **2013**, *75*, 185–195.

5) (a) Casnati, A.; Pochini, A.; Ungaro. R.; Ugozzoli, F.; Arnaud, F.; Fanni, S.;Schwing, M. J.; Egbering, R. J. M., de Jong, F.; Reinhoudi, D. N. *J. Am. Chem. Soc*. **1995**, *117*, 2767-2777 (b) Sachleben, R. A.; Urvoas, A.; Bryan, J. C.; Haverlock, T. J.; Hay, B. P.; Moyer, B. A. *Chem. Commun*. **1999**, 1751-1752.

6) Bühlmann, P.; Pretsch, E.; Bakker, E. *Chem. Rev*. **1998**, *98*, 1593–1687

7) (a) Avouris, P. *Nano Lett*. **2010**, *10*, 4285-4294. (b) Novoselov, K. S.; Geim,; A. K.; Morozov, S. V.; Jiang, D.; Zhang, Y.; Dubonos, S. V.; Grigorieva, I. V.; Firsov, A. A. *Science*, **2004**, *306*, 666-669.

8) Barone, V.; Hod, O.; Scuseria, G. E. *Nano Lett*., **2006**, *6*, 2748-2754.

9) Han, M.; Ozyilmaz, B.; Zhang, Y.; Jarillo-Herero, P.; Kim. *P. Phys. Status Solidi B*, **2007**, *244*, 4134-4137.

10) Kim, J. S.; Thuéry, P.; Nierlich, M.; Rim, J. A.; Yang, J. K.; Lee. J. K.; Cho, K. H.; Lee, J. H.; Vinces, J. *Bull. Korean Chem. Soc*. **2001**, *22*, 321–324.

11) (a) Pisana, S.; Lazzeri, M.; Casiraghi, C.; Novoselov, K. S.; Geim, A. K.; Ferrari, A. C.; Mauri, F. *Nat. Mater*. **2007**, *6*, 198-201. (b) Das, B.; Voggu, R.; Rout, C. S.; Rao, C. N. R. *Chem. Commun*. **2008**, 5155-5157.

12) Malard, L. M.; Pimenta, M. A.; Dresselhaus, G.; Dresselhaus, M. S. *Physics Reports*, **2009**, *473*, 51-87.

Chapter 5: Experimental Procedures

5.1 General procedures

Unless otherwise indicated, all reagents and solvents were purchased from commercial suppliers (Aldrich, TCI and Acros) and used without further purification. NMR spectra were recorded on a Varian Innova instruments. All deuterated solvents were purchased from Cambridge Laboratories, Inc. Chemical shifts were recorded in unit of δ (ppm) and referenced to the residual solvent. High-resolution electrospray ionization (ESI) mass spectra were recorded on a Varian QF ESI 9.4 Tesla Instrument with Internal Calibration. Column chromatography was performed on Sorbent silica gel (40-63 μm). Analytical thin layer chromatography (TLC) analyses were carried on glass-backed silica gel slides (250 μm, Sorbent Technologies). UV-Vis spectra were recorded using a Varian Cary 5000 spectrophotometer at room temperature. A cell length of 10 mm was used for all UV-Vis spectral studies.

5.2 Experimental details for chapter 2

5.2.1 Synthetic Procedures and Characterization Data

Synthesis of **2.2**: Benzoyl chloride (50 μL, 0. 435 mmol) was dropped into to a solution of compound **2.3** (100 mg, 0.087 mmol) in 1 mL of cooled DMF for 12 h under an atmosphere of N_2. The mixture was quenched by addition of 5 mL of a solution of Na_2CO_3 dissolved in 50% aqueous EtOH. The resulting yellowish solution was separated and washed three times with 10 mL of water. The organic layer was then separated off and dried over anhydrous Na_2SO_4. The solvent was then evaporated *in vacuo* to give a yellowish powder. Purification by silica gel column chromatography (solvent: hexanes /ethyl acetate (7/1)) yielded the desired compound as a white solid **2.2**

(49% yield). ^{1}H NMR (400 MHz, $CDCl_3$): δ (ppm) 10.01(s, 1H,), 7.01-7.0 (d, 2H, *J* = 8.78), 6.93-6.99 (m, 9H), 6.86 (broad, 1H), 6.80-6.76 (t, 2H, *J* = 7.47, *J* = 1.97), 6.70 (broad, 1H), 6.68 (s, 4H), 6.66 (s, 1H), 6.61-6.57 (t, 1H, *J* = 14.87, *J* = 7.42), 6.56-6.52 (t, 1H, *J* = 14.44, *J*=7.46), 6.53-6.52 (d, 1H, *J* = 3.03), 6.01-5.99 (t, 1H, *J* = 3.14 Hz, *J* = 6.15 Hz), 5.98-5.97 (t, 2H, *J* = 3.09 Hz, *J* = 5.88 Hz), 5.92-5.91 (t, 1H, *J* = 2.95 Hz, *J* = 6.04 Hz), 5.89-5.88 (t, 1H, *J* = 3.39, Hz, *J* = 6.13), 5.83-5.82 (t, 1H, *J* = 5.97 Hz, *J* = 2.96 Hz), 3.82- 3.75 (m, 12H), 3.68-3.60 (m, 2H), 3.56-3.52 (m, 2H), 3.47-3.41 (m, 2H), 3.30-3.25 (t, 4H, *J* = 6.76Hz, *J* = 15.68Hz), 1.92 (s, 3H), 1.88 (s, 3H), 1.66 (s, 3H), 1.57 (s, 3H), 1.45 (s, 3H), 1.36 (s, 3H,), 1.20-1.11 (sextet, 4H), 0.60-0.56 (t, 6H, *J* = 7.45 Hz, *J* = 14.96 Hz).; ^{13}C NMR (100 MHz, $CDCl_3$) 185.8, 157.5, 157.4, 156.8, 156.8, 155.9, 155.7, 146.0, 138.5, 138.2, 137.2, 137.1, 137.1, 136.3, 135.8, 135.3, 134.3, 134.3, 134.3, 134.2, 134.1, 134.0, 134.0, 133.7, 129.5, 129.5, 129.4, 129.2, 129.1, 129.1, 128.5, 128.0, 122.8, 121.9, 120.9, 113.9, 113.8, 108.7, 106.9, 105.7, 105.4, 104.8, 104.8, 104.7, 71.8, 66.8, 66.7, 65.3, 64.7, 44.5, 43.8, 38.0, 37.5, 35.7, 30.1, 29.7, 29.7, 29.4, 28.8, 28.4, 22.8, 10.4 HRMS (ESI) *m/z* 1195.592 $[M + Na]^+$ calcd for $C_{77}H_{80}N_4O_7$, found 1172.603.

Synthesis of **2.1**: A mixture of compound **2.2** (134 mg, 0.114 mmol) and 3-(dicyanomethylidene)indan-1-one (110 mg, 0.571 mmol) were dissolved in 4 mL of a 1:1 (v/v) mixture consisting of THF and EtOH. After the reaction was completed, a dark red solid was obtained by removal of solvent *in vacu*. Column chromatography over silica gel (eluent: hexanes /ethyl acetate (4/1)), followed by recrystallization from methanol and dichloromethane, gave 154 mg (85% yield) of **2.1** as a red solid. ^{1}H NMR (400 MHz, $CDCl_3$): δ (ppm) 8.86 (s, 1H), 8.66-8.64 (d, 1H, *J* = 7.47Hz), 7.85-7.83 (d, 1H, *J* = 6.88Hz), 7.73-7.65 (m, 1H), 7.67-7.65 (d, 1H, *J* = 2.71), 7.37-7.34 (d, 2H, *J* = 15.99), 7.35-7.29 (d, 2H, *J* = 10.31), 7.14-7.12 (d, 2H, *J* = 8.56), 7.09-7.01 (m, 10H), 6.88-6.78 (m, 7H), 6.64-6.60 (t, 1H, *J* = 14.75, *J* = 7.37), 6.53-6.50 (t, 1H, *J* = 15.02, *J* =

7.59), 6.09-6.06 (t, 1H, J = 6.11, J = 3.16), 6.05-6.03 (t, 1H, J = 6.29, J = 3.18), 6.02-6.01 (t, 1H, J = 6.11, J = 3.20), 6.00-5.98 (t, 1H, J = 5.97, J = 2.92), 5.99-5.97 (t, 1H, J = 6.18, J = 3.05), 5.85-5.83 (t, 1H, J = 5.99, J = 3.01), 3.89-3.84 (m, 4H), 3.80 (s, 8H), 3.74-3.68 (m, 2H), 3.62-3.57 (m, 2H), 3.41-3.37 (m, 4H), 2.04 (s, 3H), 1.98 (s, 3H), 1.82 (s, 3H), 1.75 (s, 3H), 1.56 (s, 3H), 1.44 (s, 3H), 1.37-1.28 (sextet, 4H), 0.73-0.69 (t, 6H, J = 14.87, J = 7.43) ; ^{13}C NMR ($CDCl_3$, 100 MHz) 187.4, 163.7, 157.6, 157.4, 156.7, 156.7, 155.7, 155.6, 152.6, 140.2, 139.4, 130.0, 138.4, 137.9, 137.5, 136.1, 135.2, 134.6, 134.2, 134.2, 134.2, 134.1, 134.0, 133.9, 129.7, 129.6, 129.5, 129.4, 129.3, 128.5, 128.2, 124.9, 123.5, 122.8, 121.8, 117.2, 115.6, 115.2, 114.0, 113.9, 113.1, 106.8, 105.8, 105.2, 105.1, 104.9, 104.2, 77.2, 72.4, 67.7, 67.4, 65.7, 65.2, 44.4, 44.0, 38.3, 37.5, 35.6, 30.2, 30.0, 29.3, 23.0, 10.2 HRMS (ESI) m/z 1371.629 $[M + Na]^+$ calcd for $C_{89}H_{84}N_6O_7$, found 1348.640.

5.2.2 Single Crystal X-ray Crystallographic Data

All crystal structures were solved by Dr. Vincent M. Lynch of this department. X-ray crystallographic data for **2.1** were collected at -140 °C on a Nonius Kappa CCD diffractometer using a Bruker AXS Apex II detector and a graphite monochromator with MoKα radiation (λ = 0.71075 Å). Reduced temperatures were maintained by use of an Oxford Cryosystems 600 low-temperature device. A total of 776 frames of data were collected using ω-scans with a scan range of 1.0° and a counting time of 93 seconds per frame. Details of crystal data, data collection and structure refinement are listed in Table 1. Data reduction was performed using SAINT V8.27B.[1] The structure was solved by direct methods using SIR97[2] and refined by full-matrix least-squares on F^2 with anisotropic displacement parameters for the non-H atoms using SHELXL-97.[3] Structure analysis was aided by use of the programs PLATON98[4] and WinGX.[5]

A molecule of chloroform was badly disordered around a crystallographic inversion center at 0, 0, ½. Attempts to model the disorder were unsatisfactory. The contributions to the scattering factors due to the solvent molecule were removed by use of the utility SQUEEZE[6] in PLATON98.

The function, $\Sigma w(|F_o|^2 - |F_c|^2)^2$, was minimized, where $w = 1/[(\sigma(F_o))^2 + (0.0803*P)^2 + (3.9869*P)]$ and $P = (|F_o|^2 + 2|F_c|^2)/3$. $R_w(F^2)$ refined to 0.183, with R(F) equal to 0.0624 and a goodness of fit, S, = 1.02. Definitions used for calculating R(F),$R_w(F^2)$ and the goodness of fit, S, are given below.[7] The data were checked for secondary extinction but no correction was necessary. Neutral atom scattering factors and values used to calculate the linear absorption coefficient are from the International Tables for X-ray Crystallography (1992).[8] Figure 5.1 was generated using SHELXTL/PC.[9] Tables of positional and thermal parameters, bond lengths and angles, torsion angles and figures, along with additional details of the structure can be obtained from the Cambridge Crystallographic Data Centre by quoting CCDC number 1440484 .

Empirical formula	C_{91} H_{86} Cl_6 N_6 O_7	
Formula weight	1588.35	
Temperature	133(2) K	
Wavelength	0.71073 Å	
Crystal system	triclinic	
Space group	P -1	
Unit cell dimensions	a = 14.8278(10) Å	α= 108.103(3)°.
	b = 15.0838(10) Å	β= 97.486(3)°.
	c = 20.0662(12) Å	γ = 103.078(3)°.
Volume	4056.5(5) $Å^3$	
Z	2	
Density (calculated)	1.300 Mg/m^3	
Absorption coefficient	0.272 mm^{-1}	
F(000)	1664	
Crystal size	0.40 x 0.15 x 0.15 mm^3	
Theta range for data collection	1.992 to 24.999°.	
Index ranges	-17<=h<=17, -17<=k<=17, -23<=l<=23	
Reflections collected	60391	
Independent reflections	14242 [R(int) = 0.0715]	
Completeness to theta = 25.242°	97.0 %	
Absorption correction	Semi-empirical from equivalents	
Max. and min. transmission	1.00 and 0.849	
Refinement method	Full-matrix least-squares on F^2	
Data / restraints / parameters	14242 / 37 / 1014	
Goodness-of-fit on F^2	1.019	
Final R indices [I>2sigma(I)]	R1 = 0.0624, wR2 = 0.1530	
R indices (all data)	R1 = 0.1144, wR2 = 0.1829	
Extinction coefficient	n/a	
Largest diff. peak and hole	0.677 and -1.037 $e.Å^{-3}$	

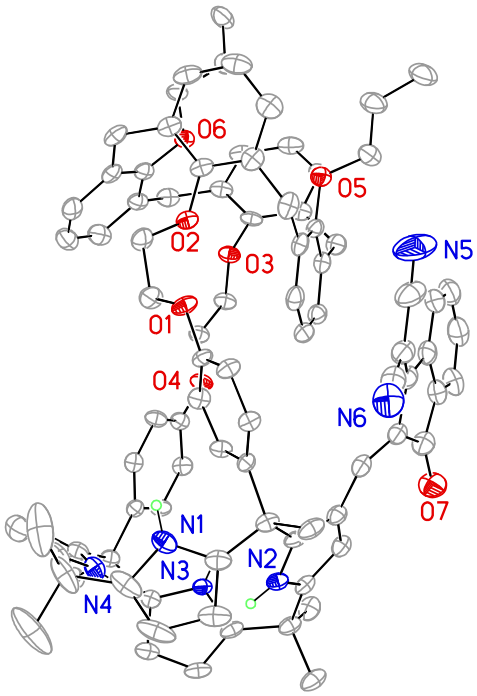

Figure 5.1: View of **2.1**. Displacement ellipsoids are scaled to the 50% probability level. Most hydrogen atoms have been omitted for clarity.

5.2.3 Studies by UV-Vis spectroscopy

All binding affinities reported in Figure 3.7 were carried out in commercially available Across $CHCl_3$ containing amylene as a stabilizer. All anions were studied in the form of their commercially available TBA^+ salts.

A match to a 1:1 theoretical binding curve was sought for titration experiments wherein;

$[receptor]_0 = [receptor] + [receptor\text{-}guest]$

and the following equation was derived and used to determine the binding affinities:

$$\Delta\delta = \frac{1 + aK + xK - \sqrt{-4axK^2 + (-1 - aK - xK)^2}}{2K} \Delta\varepsilon$$

Where,

ΔA (measured change in absorbance relative to the initial solution) is the y variable;

x is the concentration of guest (TBA^+ anion salts) added;

a is the initial concentration of receptor (remains constant over the course of titration);

Δε is the extinction coefficient difference between free receptor and receptor-quest complex ($\Delta\varepsilon = \varepsilon_{complex} - \varepsilon_{receptor}$);

K is the binding affinity (K_a) of the receptor under analysis for the guest in question.

mol/L	Δ Abs. at 587 nm
0	0
0.000005	0.005881921
0.00001	0.01366061
0.000015	0.021076799
0.00002	0.030095682
0.000025	0.037866309
0.00003	0.043787569
0.00004	0.051264018
0.00005	0.061068446
0.00006	0.071439639
0.00007	0.08183296
0.00008	0.09021093
0.00009	0.097539678
0.0001	0.106460318
0.000115	0.118520394
0.00013	0.128625736
0.000145	0.137499675
0.00016	0.144968256
0.000175	0.148851439
0.00019	0.154542551
0.000205	0.155154452
0.00022	0.157949939
0.000235	0.157521501
0.00025	0.156796798
0.000265	0.155104593

Table 5.1: Raw data used to obtain the binding constant of Figure 2.5. This corresponds to the interaction of CsF to the preformed **2.1** as obtained from a UV-Vis spectroscopic titration carried out in $CD_3OD/CDCl_3$ (1/9, v/v).

5.3 EXPERIMENTAL DETAILS FOR CHAPTER 3

5.3.1 Synthetic Procedures and Characterization Data

Synthesis of **3.3**: Under a nitrogen atmosphere, compounds **3.5** (1 g, 1.63 mmol) and **3.6** (1.38 g, 6.68 mmol) were dissolved in 10 mL of DMF in the presence of EDCI (1.56 g, 8.15 mmol) and 1-hydroxybenzotriazole (1.26 g, 8.15 mmol). The mixture was stirred for 6 h at room temperature. After the reaction was deemed complete (TLC), solvents were removed *in vacuo*. To the resulting yellowish solid, CH_2Cl_2 (50 mL) was added and the organic phase was separated off and washed three times with water (3 × 50 mL). The organic layer was dried over anhydrous Na_2SO_4 and evaporated *in vacuo* to give a yellow solid. Crystallization from a mixture of dichloromethane and methanol without column chromatography, gave 0.4 g (40% yield) of a pale yellow solid. ^{1}H NMR (400 MHz, DMSO-d_6) δ 12.13 (br s, 4H, NH), 9.92 (br s, 4H, NH), 8.32 (s, 4H), 7.90-7.87 (d, 4H, *J* = 12Hz), 7.41-7.39 (d, 4H, *J* = 12Hz), 7.36 (s, 4H), 7.18 (s, 8H), 4.43-4.40 (d, 4H, *J* = 12Hz), 3.84-3.80 (t, 8H, *J* = 8Hz &8Hz), 3.20-3.17 (d, 4H, *J* = 12Hz), 1.91-1.85 (m, 8H), 0.99-0.95 (t, 12H, *J* = 8Hz &8Hz); ^{13}C NMR (100 MHz, DMSO- d_6) δ 158.7, 153.2, 141.4, 139.6, 135.4, 134.9, 133.0, 126.5 119.3, 118.8, 113.0, 105.9, 76.9, 31.3, 23.2, 10.6. HR-ESI-MS calc. $C_{76}H_{68}N_{12}O_{16}$ 1404.48762; found 1416. 48590 $[M+Na]^{2+}$.

Synthesis of **3.6**: To a mixture of 5-nitroindole-2-carboxylic acid (2.5 g, 10.67 mmol) in ethanol (50 mL) was added aqueous NaOH (2.56 g, 64 mmol in 60 mL of water) solution. After heating the reaction mixture for 4 h, dilute HCl was added to the mixture until the initial clear yellow mixture became viscous. After filtration by glass filter with water, desired product was obtained as a brown solid in 93% yield. ^{1}H NMR (400 MHz, DMSO-d_6) δ 11.52 (s, 1H), 10.93-10.90 (dd, 1H, *J* = 4Hz & *J* = 12Hz), 10.39

(d, 1H, *J* = 8Hz), 10.19 (s, 1H), 6.18 (br, 1H) ^{13}C NMR (100 MHz, DMSO-d_6) δ 162.6, 141.8, 140.4, 132.5, 126.5, 120.0, 119.6, 113.5, 110.2.

HR-ESI-MS calc. $C_9H_6N_2O_4$ 206.03; found 205.02530 $[M-H]^-$.

Synthesis of **3.4**: Under a nitrogen atmosphere, compound **3.5** (500 mg, 0.815 mmol) and indole-2-carboxylic acid (538 mg, 3.34 mmol) were dissolved in 5 mL of mixture of DCM/THF (2:1) in the presence of EDCI (781 mg, 4.075 mmol) and 4-dimethylaminopyridine (438.1 mg, 3.586 mmol). The reaction mixture was allowed to stir for 4 h at room temperature. After the reaction was deemed complete (TLC), solvents were removed *in vacuo*. To the resulting yellowish solid, CH_2Cl_2 (50 mL) and water (50 mL) were added. Then, organic phase was separated off and washed three times with water (30 mL). The organic layer was dried over anhydrous Na_2SO_4 and evaporated *in vacuo* to give yellow solid. Column chromatography over silica gel (eluent: ethyl acetate/hexane (1:1)), followed by recrystallization from methylene chloride and methanol, gave 0.5 g (39% yield) ^{1}H NMR (400 MHz, DMSO-d_6) δ 11.50 (s, 4H), 9.88 (s, 4H), 7.44-7.42 (d, 4H, *J*=8Hz), 7.36-7.34 (d, 4H, *J*=8Hz), 7.24 (s, 8H), 7.21 (s, 4H), 7.13-7.09 (t, 4H, *J*= 8Hz & *J*=16Hz), 6.96-6.92 (t, 4H, *J*= 8Hz & *J*=16Hz), 4.47-4.44 (d, 4H, *J*=12Hz), 3.88-3.84 (t, 8H, *J*= 8Hz & *J*=16Hz), 3.24-3.21 (d, 4H, *J*=12Hz), 2.02-1.93 (m, 8H), 1.01-0.97 (t, 9H, *J*= 8Hz & *J*=16Hz), ^{13}C NMR (100 MHz, DMSO- d_6) δ 159.80, 152.91, 137.04, 134.72, 133.28, 132.07, 127.47, 123.98, 122.10, 121.65, 120.17 , 112.69, 103.97, 77.16, 23.21, 10.67. HR-ESI-MS calc. $C_{76}H_{72}N_8O_8$ 1224.55; found 1247.54 $(M+Na)^+$.

Synthesis of **3.7**: Compounds **3.8** and **3.9** were synthesized using known procedures, respectively. Then, compounds **3.8** (269.9 mg, 0.326 mmol) and **3.9** (300 mg,

1.335 mmol) were dissolved in 5 mL of THF in the presence of NEt_3 (2 mL). The reaction mixture was heated for 4h under reflux. After cooling, to the resulting yellowish solid, CH_2Cl_2 (50 mL) and water (50 mL) were added. Then, organic phase was separated and washed three times with 10 mL of water. The organic layer was then dried over anhydrous Na_2SO_4 and the solvent was evaporated *in vacuo* to give a yellowish powder. Purification by crystallization gave a pale yellow solid **3.7** (25% yield). ^{1}H NMR (400 MHz, $CDCl_3$): δ (ppm) 12.16 (s, 4H-*indole*), 9.98 (s, 4H-*amide*), 8.42 (s, 4H, *J* = 4Hz), 7.94-7.92 (d, 4H, *J* = 8Hz), 7.43-7.41 (d, 4H, *J* = 8Hz), 7.41 (s, 4H), 7.23 (s, 8H), 4.48-4.45 (d, 4H, *J* = 12Hz), 3.88-3.85 (m, 8H), 3.24-3.21 (d, 4H, *J* = 12Hz), 1.97-1.91 (m, 8H), 1.02-0.98 (t, 12H, *J* = 8Hz & *J* =16Hz),

5.3.2 ^{1}H NMR Spectroscopic Studies

All binding affinities reported in Figure 3.9 and Figure 3.17 were carried out in a solution consisting of 10% DMSO in $CHCl_3$. All cations and anions were studied in the form of their commercially available ClO_4^- and TBA^+ salts. In the case of titrations carried out with the intention of determining binding affinities, the receptor concentration was kept constant throughout the titration study. The following equation was used to determine the presumed 1:1 binding affinities.

$$\Delta\delta = \frac{1 + aK + xK - \sqrt{-4axK^2 + (-1 - aK - xK)^2}}{2K} (\delta_{complex} - \delta_{host})$$

where,

Δδ (measured change in the chemical shift of the hydrogen signal of interest relative to the chemical shift of the same signal in receptor) was taken as the y variable;

x is the concentration of guest added;

a is the initial concentration of receptor (remains constant over the course of titration);

$\delta_{complex}$ is the chemical shift of the hydrogen of interest in receptor-guest complex

δ_{host} is the chemical shift of the same hydrogen of interest in receptor;

K is the binding affinity (K_a) of receptor for the guest in question.

$[TBAH_2PO_4]$	Chemical shift (Δδ)
0.0000	0.00
0.0006	0.35
0.0012	0.83
0.0018	1.13
0.0024	1.43
0.0030	1.67
0.0036	1.76
0.0042	1.86
0.0048	1.91
0.0054	1.97

Table 5.2: Raw data used to obtain the binding constant of Figure 3.9. This corresponds to the interaction of $H_2PO_4^-$ (TBA^+ salt) with the preformed receptor **3.3** as obtained from a ^1H NMR spectroscopic titration carried out in DMSO-d_6/$CDCl_3$ (1/9, v/v).

[TBACl]	Chemical shift (Δδ)
0.0000	0.00
0.0006	0.08
0.0012	0.27
0.0018	0.43
0.0024	0.57
0.0030	0.69
0.0036	0.79
0.0042	0.86
0.0048	0.92
0.0054	0.97
0.0060	1.02
0.0066	1.05
0.0072	1.08
0.0084	1.14
0.0096	1.17

Table 5.3: Raw data of used to obtain the binding constant of Figure 3.17. This corresponds to the interaction of Cl^- (TBA+ salt) with the preformed receptor complex **3.4**•Li^+ as obtained from a ^1H NMR spectroscopic titration carried out in DMSO-d_6/$CDCl_3$ (1/9, v/v).

The stoichiometry of binding was determined using one of two Job plot methods.

Job plot method-1:

$[receptor]_{stock} = [guest]_{stock}$

The total concentration of the receptor and the salt of interest were kept constant by varying the mole fraction of receptor from 0 to 1 (in these experiments, all mixtures were obtained by mixing in different proportions receptor and guest stock solutions, which had have the same numerical concentration values).

[receptor] + [guest] = constant

Job plot method-2:

Data from titration carried out to determine the binding affinities were used. Experimentally,

[receptor] = constant

The data were then manipulated mathematically such that

[receptor] + [guest] = constant

This conversion is formulized in the Excel formula sheet (*cf*. Table 5.4).

	A	B	C	D	E	F	G	H
1		Cons. Receptor 1.00E-05				If Ct	If Ct	If Ct
2				at λ_{max}	at λ_{max}	=$B$1	=$B$1	=$B$1
3	$[anion]_n$	Ct	Mole fraction X_{anion}	A	ΔA	A/Ct × Conc.	ΔA/Ct × Conc.	plot
4	0	=$B$1+A4	=A4/B4	0.66	=D5/$D$5	=D4*$F$2/B4	=$D$4*(1-C4)	=F4-G4

Table 5.4: Job plot method-2: Excel formula sheet used to obtain a binding affinity values from the raw data obtained from UV-Vis spectral titrations.

$[TBAH_2PO_4]$	Ct	Xp	A	DA	A	A	dDA
0	1.00E-05	0.00E+00	0.662685514	0.00E+00	6.63E-01	6.63E-01	0.00E+00
0.000001	1.10E-05	9.09E-02	0.700917363	3.82E-02	6.37E-01	6.02E-01	3.48E-02
0.000002	1.20E-05	1.67E-01	0.739075184	7.64E-02	6.16E-01	5.52E-01	6.37E-02
0.000003	1.30E-05	2.31E-01	0.77702558	1.14E-01	5.98E-01	5.10E-01	8.80E-02
0.000004	1.40E-05	2.86E-01	0.806946755	1.44E-01	5.76E-01	4.73E-01	1.03E-01
0.000005	1.50E-05	3.33E-01	0.839885414	1.77E-01	5.60E-01	4.42E-01	1.18E-01
0.000006	1.60E-05	3.75E-01	0.875616968	2.13E-01	5.47E-01	4.14E-01	1.33E-01
0.000007	1.70E-05	4.12E-01	0.90652293	2.44E-01	5.33E-01	3.90E-01	1.43E-01
0.000008	1.80E-05	4.44E-01	0.929230571	2.67E-01	5.16E-01	3.68E-01	1.48E-01
0.000009	1.90E-05	4.74E-01	0.945428431	2.83E-01	4.98E-01	3.49E-01	1.49E-01
0.00001	2.00E-05	5.00E-01	0.961199462	2.99E-01	4.81E-01	3.31E-01	1.49E-01
0.000011	2.10E-05	5.24E-01	0.970430493	3.08E-01	4.62E-01	3.16E-01	1.47E-01

Table 5.5: Raw data used to create the Job plot shown in Figure 3.10 corresponding to the interaction of compound **3.3** with the TBA^+ salts of $H_2PO_4^-$ as recorded using UV-Vis spectroscopy in DMSO/ $CHCl_3$ (5/95, v/v). These data were treated according to Job Plot method-2 (Table 5.4).

Host / Guest Mole fraction (**3.3** / $H_2P_2O_7^{3-}$)	Mole fraction × Δ abs.	Δ abs. at 353 nm
1	0	0
0.9	0.10892418	0.098031762
0.8	0.193459034	0.154767227
0.7	0.260175049	0.182122535
0.6	0.317930192	0.190758115
0.5	0.333031237	0.166515619
0.4	0.342757195	0.137102878
0.3	0.381717026	0.114515108
0.2	0.362234712	0.072446942
0.1	0.368650735	0.036865073
0	0.330406249	0

Host / Guest Mole fraction (**3.3** / Cl^-)	Mole fraction × Δ abs.	Δ abs. at 390 nm
1	0	0
0.9	0.001769963	0.001966626
0.8	0.014453	0.01806625
0.7	0.02615144	0.0373592
0.6	0.035921811	0.059869684
0.5	0.038038824	0.076077648
0.4	0.032501051	0.081252627
0.3	0.027293142	0.09097714
0.2	0.020535178	0.102675892
0.1	0.011425067	0.114250667
0	0	0.112771831

Table 5.6: Raw data of used to construct the Job plot, show in Figure 3.10. This corresponds to the interaction of compound **3.3** with the TBA^+ salts of $HP_2O_7^{3-}$ and Cl^-, respectively, as obtained from UV-Vis spectral titrations carried out in DMSO/ $CHCl_3$ (5/95, v/v). These plots were constructed using the Job plot method-1.

5.4 EXPERIMENTAL DETAILS FOR CHAPTER 4

Synthesis of **4.1**: Under a nitrogen atmosphere, compound **4.3** (120 mg, 0.149 mmol) and 1-pyrenebutylic acid (128 mg, 0.447 mmol) were dissolved in methylene chloride in the presence of EDCI (85.7 mg, 0.447 mmol) and 4-(dimethylamino)pyridine (54.8 mg, 0.447 mmol). The reaction mixture was then stirred for 12 h at room temperature. After the reaction was deemed complete by TLC analysis, the solvents were removed *in vacuo*. To the resulting yellowish solid, CH_2Cl_2 (10 mL) and water (10 mL) were added and the organic phase was separated off and washed three times with water (3 × 10 mL). The organic layer was dried over anhydrous Na_2SO_4 and evaporated *in vacuo* to give a yellow solid. Then crude product was purified by silica gel column chromatography (100% ethyl acetate, eluent). Yield 49%. ^{1}H NMR (400 MHz, $CDCl_3$) δ 8.32-7.80 (m, 18H, pyrene), 7.10-7.03 (dd, 8H, *J*=18, *J*=12), 6.82 (t, 2H, *J*=12), 6.74 (t, 2H, *J*=12), 4.25 (t, 4H, *J*=8), 3.75-3.50 (m, 24H), 3.41 (t, 4H, *J*=8), 3.36 (t, 4H, *J*=8), 3.29 (t, 4H, *J*=8), 2.51 (t, 4H, *J*=8), 2.20 (m, 4H) ^{13}C NMR (100 MHz, $CDCl_3$) δ 173.5, 156.5, 156.2, 135.7, 133.7,131.4, 130.1, 123.0, 128.7, 128.6, 129.5, 129.4, 126.7, 125.8, 125.1, 124.9, 124.8, 123.3, 122.4, 122.1, 71.3, 71.1, 71.0, 70.1, 70.0, 69.4, 69.0, 6 3.6, 37.4, 33.8, 32.7, 25.8.

HR-ESI-MS calc. $C_{86}H_{86}O_{14}$ 1342.62; found 1365.59 $[M+Na]^+$.

5.5 REFERENCE

1) SAINT V8.27B Bruker AXS Inc, (2012), Madison, WI.
2) Altomare A., Burla M.C., Camalli M., Cascarano G.L., Giacovazzo C., Guagliardi A., Moliterni A.G.G., Polidori G.,Spagna R. SIR97. A program for crystal structure solution. *J. Appl. Cryst.* **1999,** *32*, 115-119.
3) Sheldrick, G. M. SHELXL97. Program for the Refinement of Crystal Structures, Acta Cryst. **2008**, *A64*, 112-122.
4) Spek, A. L. PLATON, A Multipurpose Crystallographic Tool. Utrecht University, The Netherlands, 1998.
5) Farrugia, L. J. WinGX 1.64. An Integrated System of Windows Programs for the Solution, Refinement and Analysis of Single Crystal X-ray Diffraction Data. *J. Appl. Cryst.* **1999**, *32*. 837-838.
6) Sluis, P. v. d.; Spek, A. L. SQUEEZE. *Acta Cryst.* **1990.** *A46*, 194-201.
7) $R_W(F^2) = \{\Sigma w(|F_o|^2 - |F_c|^2)^2/\Sigma w(|F_o|)^4\}^{1/2}$ where w is the weight given each reflection.$R(F) = \Sigma(|F_o| - |F_c|)/\Sigma|F_o|\}$ for reflections with $F_o > 4(\sigma(F_o))$. $S = [\Sigma w(|F_o|^2 - |F_c|^2)^2/(n - p)]^{1/2}$, where n is the number of reflections and p is the number of refined parameters.
8) Wilson, A. J. C. International Tables for X-ray Crystallography. **Vol. C**, Tables 4.2.6.8 and 6.1.1.4, Kluwer Academic Press, Boston, **1992.**
9) Sheldrick, G. M. SHELXTL/PC (Version 5.03). Siemens Analytical X-ray Instruments, Inc., Madison, Wisconsin, **1994**.

Reference

1.6 REFERENCE

1) von Baeyer, A. Ber. Dtsch. Chem. Ges., 1872, 5, 25-26.

2) Iqbal, M.; Mangiafico, T.; Gusche, C. D. *Tetrahedron* **1987**, *43*, 4917-4930.

3) Chawla, H. M.; Singh, S. P.; Upreti, S. *Tetrahedron,* **2006**, *62*, 7854-7865. (b) Kim, J. Y.; Kim, G.; Kim, C. R.; Lee, J. H.; Kim, J. S. *J. Org. Chem.* **2003**, *68*, 1933-1937. (c) Ludwig, R. *Fresenius J. Anal. Chem.* **2000**, *367*, 103-128. (d) Chawla, H. M.; Srinivas, K.; Meena. *Tetrahedron* **1995**, *51*, 2709-2718.

4) McCarrick, M.; Wu, B.; Harris, S. J.; Diamond, D.; Barret, G.; Mckervey, M. A. *J. Chem. Soc. Chem. Commun.* **1992**, 1287-1289.

5) Gutsche, C. D. *Calixarenes*, The Royal Society of Chemistry, Cambridge, UK, **1989**, Vol 1.

6) Kubo, Y.; Hanaguchi, S, -I.; Kotani, K.; Yoshida, K. J. *Tetrahedron Lett.* **1991**, *32*, 7419-7420.

7) Kubo, Y.; Hamaguchi, S. -I.; Niimi, A.; Yoshida, K.; Tokita, S. *J. Chem. Soc. Chem. Commun.* **1993**, 305-307.

8) Chang, K. -C.; Su, I, -H.; Lee, G. -H.; Chung, W. -S. *Tetrahedron Lett.* **2007**, 7274-7278.

9) Kao, T. –L.; Wang, C. –C.; Pan, Y. –T.; Shiao, Y. –J.; Yen, J. –Y.; Shu, C. –M.; Lee, G. –H.; Peng, S. –M.; Chung, W. –S. *J. Org. Chem.* **2005**, *70*, 2912-2920.

10) Ho, I. –T.; Lee, G. –H.; Chung, W. –S. *J. Org. Chem.* **2007**, *27*, 2434-2442.

11) Liang, Z.; Liu, Z.; Gao, Y. *Tetrahedron Lett.* **2007**, *48*, 3587-3590.

12) Kubo, K.; Maeda, S.; Nakamura, M.; Tokita, S. J. *Chem. Soc. Chem. Commun.* **1994**, 1725-1726.

13) Quinlan, E.; Matthews, S. E.; Gunnlaugsson, T. *Tetrahedron Lett.* **2006**, *47*, 9333-9338.

14) Quinlan, E.; Matthews, S. E.; Gunnlaugsson, T. *J. Org. Chem.* **2007**, *72*, 7497-7503.

15) Kubo, E.; Maeda, S.; Tokita, S.; Kubo, Y. *Nature* **1996**, *382*, 522-524.

16) McCarrick, M., Harris, S. J.; Diamond, D. *J. Mat. Chem.* **1994**, *4*, 217-221.

17) (a) Hines, J. H.; Wanigasekara, E.; Rudkevich, D. M.; Rogers, R. D. *J. Mat. Chem.* **2008**, *18*, 4050-4055. (b) Ohira, S. –I.; Wanigasekara, E.; Rudkevich, D. M.; Dasgupta, P. K. *Talanta* **2008**, *77*, 1814-1820.

18) (a) de Silva, A. P.; Gunaratne, H. Q. N.; Gunlaugsson, T.; Huxley, J. M.; Mchoy, C. P.; Rademacher, J. T.; Rice, T. E. *Chem. Rev.* **1997**, *97*, 1515- 1566. (b) Kim, J. S.; Quang, D. T. *Chem. Rev.* **2007**, *107*, 3780-3799.

2.5 REFERENCE

1) Delacroix, D.; Guerre, J. P.; Leblanc, P.; Hickman, C. Radionuclide and Radiation Protection Data Handbook; Nuclear Technology Publishing, **2002**.

2) Relman, A. S. *Yale J. Biol. Med.* **1956**, *29*, 248-262.

3) (a) Kim, S. K.; Sessler, J. L.; Gross, D. E.; Lee, C. –H.; Kim, J. S.; Lynch, V. M.; Delmau, L. H.; Hay, B. P. *J. Am. Chem. Soc.* **2010**, *132*, 5827-5836. (b) Kim, S. K.; Lynch, V. M.; Young, N. J.; Hay, B. P.; Lee, C. H.; Kim, J. S.; Moyer, B. A.; Sessler, J. L. *J. Am. Chem. Soc.* **2012**, *134*, 20837-20843. (c) Kim, S. K.; Hay, B. P.; Kim, J. S.; Moyer, B. A.; Sessler, J. L. *Chem. Commun.* **2013**, *49*, 2112-2114.

4) (a) Custelcean, R.; Delmau, L. H.; Moyer, B. A.; Sessler, J. L.; Cho, W. –S.; Gross, D.; Bates, G. W.; Brooks, S. J.; Light, M. E.; Gale, P. A. *Angew, Chem, Int. Ed.* **2005**, *44*, 2537-2542. (b) Bush, L. C.; Heath, R. B.; Feng, X. U.; Wang, P. A.; Maksimovie, L.; Song, A. L.; Chung, W. –S.; Berinstain, A. B.; Scaiano, J. C.; Berson, J. A. *J. Am. Chem. Soc.* **1997**, *119*, 1406-1415. (c) Sato, W.; Miyaji, H.; Sessler, J. L.; *Tetrahedron Lett.* **2000**, *41*, 6731-6736.

5) (a) Leray, I.; Valeur, B. *Eur. J. Inorg. Chem.* **2009**, 3525-3535. (b) Kim, J. S.; Quang, D. T. *Chem. Rev.* **2007**, *107*, 3780-3799.

6) Reichardt, C. Solvents and solvent effects in organic chemistry. 3rd ed. Weinheim: Wiley-VCH; 2003.

7) (a) Bella, S. D. *Chem. Soc. Rev.* **2001**, *30*, 355-366. (b) Whittall, I. R.; McDonagh, A. M.; Humphrey, M. P.; Samoc, M. *Adv. Organomet. Chem.* **1998**, *42*, 291-362. (c) Planells, M.; Robertson, N. *Eur. J. Org. Chem.* **2012**, 4947-4953.

8) Brinas, R. P.; Bruckner, C. *Tetrahedron* **2002**, *58*, 4375-4381.

9) Kim, S. –H.; Hong, S. –J.; Yoo, J.; Kim, S. K.; Sessler, J. L.; Lee, C. –H. *Org. Lett.* **2009**, *11*, 3626-3629.

10) (a) Nishiyabu, R.; Anzenbacher, Jr., P. *Org. Lett.* **2006**, *8*, 359-362. (b) Nishiyabu, R.; Anzenbacher, Jr., P. *Am. Chem. Soc.* **2005**, *127*, 8270-8271.

3.4 REFERENCE

1) Sheerder, J.; van Duynhoven, J. P. M.; Engbersen, J. F. J.; Reinhoudt, D. N. *Angew. Chem. Int. Ed.* **1996**, *35*, 1090-1093.

2) Oarkesh, R.; Lee, T. C.; Gunnlaugsson, T. *Org, Biomol. Chem.* **2007**, *5*, 310-317. (b) Callan, J. F.; de Silva, A. P.; Magri, D. C.; *Tetrahedron* **2005**, *35*, 8551-8588. (C) gunnlaugsson, T.; Leonard, J. P.; Murrey, N. S. *Organic. Lett.* **2004**, *6*, 1557-1560. (d) de Silva, A. P.; Gunaratne, H. Q. N.; Gunnlaugsson, T.; Huxley, A. J. M.; McCoy, C. P.; Rademacher, J. T.; Rice, T. E. *Chem. Rev.* **1997**, *97*, 1515-1566.

3) García-España, E.; Díaz, P.; Lienaíes, J. M.; Bianchi, A. *Coord. Chem. Rev.* **2006**, *250*, 3094-3117.

4) (a) Sessler, J. L.; Camiolo, S.; Gale, P. A.; *Coord. Chem. Rev.* **2003**, *240*, 17-39. (b) Best, M. D.; Tobey, S. L.; Anslyn, E. V. *Coord. Chem. Rev.* **2003**, *240*, 3-15. (c) Choi, K.; Hamilton, A. D.; *Coord. Chem. Rev.* **2003**, *240*, 101-110.

5) (a) Chrisstoffels, L. A. J.; de Jong, F.; Reinhoudt, D. N.; Sivelli, S.; Gazzola, L.; Casnati.; Ungaro, R. *J. Am. Chem. Soc.* **1999**, *121*, 10142-10151. (b) Bohmer, V. *Angew. Chem. Int. Ed.* **1995**, *34*, 713-745. (c) Tuntulani, T.; Thavornyutikarn, P.; Poompradub, S.; Jaiboon, N.; Ruangpornvisuti, V.; Chaiohit, N.; Asfani, Z.; Vicens, J. *Tetrahedron*, **2002**, *58*, 10277-10292.

6) (a) Gale, P. A. *Coord. Chem. Rev.* **2000**, *199*, 181-233. (b) Gale, P. A. *Coord. Chem. Rev.* **2001**, *213*, 79-128.

7) Scheerder, J.; Fochi, M.; Engbersen, J. F. E.; Reinhoudt, D. N. *J. Org. Chem.* **1994**, *59*, 7815-7820.

8) Dudie, M.; Colombo, A.; Sansone, F.; Casnati, A.; Donofrio, G.; Ungaro, R. *Tetrahedron* **2004**, *60*, 11613-11618.

9) Wang, F.; Zhang, J.; Ding, X.; Dong, S.; Liu, M.; Zheng, B.; Shijun, W.; Ling, Y.; Yu, Y.; Gibson, H. W.; Huang, F. *Angew. Chem. Int. Ed.* **2010**, *49*, 1090-1094.

10) (a) Vysotsky, M. O.; Bolt, M.; Thondorf, I.; Böhmer, V. *Chem. Eur. J.* **2003**, *9*, 3375-3382. (b) Vysotsky, M. O.; Thondorf, I.; Böhmer, V. *Org. Lett.* **2000**, *2*, 3571-3574. (c) Mogck, O.; Böhmer, V.; Vogt, W. *Tetrahedron* **1996**, *52*, 8489-8496.

11) Scheerder, J.; van Duynhoven, J. P. M.; Engbersen, J. F. J.; Reinhoudt, D. N. *Angew. Chem. Int. Ed.* **1996**, *35*, 1090-1093.

4.5 REFERENCE

1) Ludwig, R.; Nguyen, T. K. D. *Sensors*, **2002**, *2*, 397-416.

2) Solov'ev, V. P.; Strakhova, N. N.; Raevsky, O. A.; Diger, V. R.; Schneider, H.-J. *J. Org. Chem*, **1996**, *61*, 5221-5226.

3) Forster, R. J.; Caddgan, A.; Diaz, M. T.; Diamond, D *Sensors and Actuators B,* **1991**, *4*, 325-331.

4) Ramachandran, B. R.; Baker, S. D.; Suravajhula, G.; Derosa, P. A. *J. Incl. Phenom. Macrocycl. Chem.,* **2013**, *75*, 185–195.

5) (a) Casnati, A.; Pochini, A.; Ungaro. R.; Ugozzoli, F.; Arnaud, F.; Fanni, S.;Schwing, M. J.; Egbering, R. J. M., de Jong, F.; Reinhoudi, D. N. *J. Am. Chem. Soc*. **1995**, *117*, 2767-2777 (b) Sachleben, R. A.; Urvoas, A.; Bryan, J. C.; Haverlock, T. J.; Hay, B. P.; Moyer, B. A. *Chem. Commun*. **1999**, 1751-1752.

6) Bühlmann, P.; Pretsch, E.; Bakker, E. *Chem. Rev*. **1998**, *98*, 1593–1687

7) (a) Avouris, P. *Nano Lett*. **2010**, *10*, 4285-4294. (b) Novoselov, K. S.; Geim,; A. K.; Morozov, S. V.; Jiang, D.; Zhang, Y.; Dubonos, S. V.; Grigorieva, I. V.; Firsov, A. A. *Science*, **2004**, *306*, 666-669.

8) Barone, V.; Hod, O.; Scuseria, G. E. *Nano Lett*., **2006**, *6*, 2748-2754.

9) Han, M.; Ozyilmaz, B.; Zhang, Y.; Jarillo-Herero, P.; Kim. *P. Phys. Status Solidi B*, **2007**, *244*, 4134-4137.

10) Kim, J. S.; Thuéry, P.; Nierlich, M.; Rim, J. A.; Yang, J. K.; Lee. J. K.; Cho, K. H.; Lee, J. H.; Vinces, J. *Bull. Korean Chem. Soc*. **2001**, *22*, 321–324.

11) (a) Pisana, S.; Lazzeri, M.; Casiraghi, C.; Novoselov, K. S.; Geim, A. K.; Ferrari, A. C.; Mauri, F. *Nat. Mater*. **2007**, *6*, 198-201. (b) Das, B.; Voggu, R.; Rout, C. S.; Rao, C. N. R. *Chem. Commun*. **2008**, 5155-5157.

12) Malard, L. M.; Pimenta, M. A.; Dresselhaus, G.; Dresselhaus, M. S. *Physics Reports*, **2009**, *473*, 51-87.

5.5 REFERENCE

1) SAINT V8.27B Bruker AXS Inc, (2012), Madison, WI.
2) Altomare A., Burla M.C., Camalli M., Cascarano G.L., Giacovazzo C., Guagliardi A., Moliterni A.G.G., Polidori G.,Spagna R. SIR97. A program for crystal structure solution. *J. Appl. Cryst.* **1999,** *32*, 115-119.
3) Sheldrick, G. M. SHELXL97. Program for the Refinement of Crystal Structures, Acta Cryst. **2008**, *A64*, 112-122.
4) Spek, A. L. PLATON, A Multipurpose Crystallographic Tool. Utrecht University, The Netherlands, 1998.
5) Farrugia, L. J. WinGX 1.64. An Integrated System of Windows Programs for the Solution, Refinement and Analysis of Single Crystal X-ray Diffraction Data. *J. Appl. Cryst.* **1999**, *32*. 837-838.
6) Sluis, P. v. d.; Spek, A. L. SQUEEZE. *Acta Cryst.* **1990.** *A46*, 194-201.
7) $R_W(F^2) = \{\Sigma w(|F_o|^2 - |F_c|^2)^2/\Sigma w(|F_o|)^4\}^{1/2}$ where w is the weight given each reflection.$R(F) = \Sigma(|F_o| - |F_c|)/\Sigma|F_o|\}$ for reflections with $F_o > 4(\sigma(F_o))$. $S = [\Sigma w(|F_o|^2 - |F_c|^2)^2/(n - p)]^{1/2}$, where n is the number of reflections and p is the number of refined parameters.
8) Wilson, A. J. C. International Tables for X-ray Crystallography. **Vol. C**, Tables 4.2.6.8 and 6.1.1.4, Kluwer Academic Press, Boston, **1992.**
9) Sheldrick, G. M. SHELXTL/PC (Version 5.03). Siemens Analytical X-ray Instruments, Inc., Madison, Wisconsin, **1994**.

Vita

Yerim Yeon was born in Chung-Ju, South Korea. She received her bachelor's degree in chemistry at Chungbuk National University and master's degree in organic chemistry in 2003-2005 at Yonsei University, respectively. Her research during her M.S. degree involved glass surface modification method development through covalent bonding interaction. Following college, she pursued a career in the R&D center of LG Chemicals as a research scientist for 2.5 years, where her research focused on suspension polymerization of polymer particles having positive and negative charges for toner type of E-paper and development of electrically conductive LCD adhesion film synthesized by polymerization of oligomer. After these experiences in industry, in the fall of 2010 she joined the Sessler group at The University of Texas at Austin to pursue her PhD in chemistry. Her research was focus primarily on the development of calix[4]arene-based ion or ion-pair receptors.

Permanent address (or email): yerimyeon@gmail.com

This dissertation was typed by Yerim Yeon.